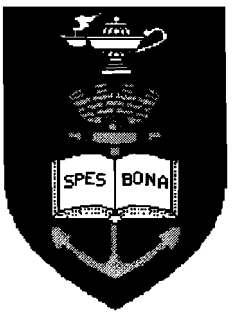

UNIVERSITY OF CAPE TOWN

EFFECTS OF GEOMAGNETICALLY INDUCED CURRENTS ON POWER TRANSFORMERS AND REACTORS

L A T Amuanyena

THESIS SUBMITTED IN FULFILMENT OF THE REQUIREMENT FOR A MASTER OF SCIENCE DEGREE IN ELECTRICAL ENGINEERING

AUGUST 2003

SUPERVISOR

Prof C T Gaunt
Department of Electrical Engineering
University of Cape Town

DECLARATION

I, Lameka Amuanyena, hereby declare that unless properly referenced and acknowledged, the work contained in this thesis is my own work.

Signed by candidate
Signature removed

Date: 28 AUGUST 2003

ACKNOWLEDGEMENTS

Firstly and most importantly, I would like to thank God Almighty for courage, strength and grace during the course of this MSc project.

My sincere gratitude goes out to my supervisor Prof. C. T. Gaunt for the supervision, support and guidance before and during the course of the project.

Special thanks to Prof. G. McLaren, Dr. J. Koen, Messrs C. Wozniak, J. De Bruto, A. Khan, A. Wellard, R. Cormack and J. Oaks. Very special thanks go to the directors of Bicon Namibia Consulting Engineers for allowing me to freeze my contract to pursue the MSc full-time.

Heartful thanks to my parents, colleagues: Sicelo Mabuza, Sengiphile Simelane, Benjamin Sebitosi, Khayakazi Mngxuma (that's it), David Kutelama and Lerato Lerato (yo what is up man, what is up man) and friends: Phillip Butkis, Renathe Kapuka, Aili Amupolo, Martha Nyambali and Tuli Titus.

SYNOPSIS

Approximately every eleven years, the sun undergoes solar disturbances whose interference with the earth's main magnetic field result in the induction of geomagnetic earth surface potentials. These potentials produce quasi-dc currents called geomagnetically induced currents (GICs) when flowing through man-made systems.

GICs entering electric power systems via grounded neutrals of star-transformers could drive the magnetic core of these transformers and associated transformers or reactors into saturation. Depending on the construction of the transformer/reactor, saturation can result in concealed and physical effects. The concealed effects are: production of harmonics and unusual swings in real and reactive power flow while physical effects are: intense stray flux, temperature rise and gas formation.

Some of the GICs effects such as gas formation have been experienced on the Eskom transmission network. There had been more reported incidents on reactors than on transformers and hence the effects were simulated on reactors. Two types of reactors were used in the simulation and were: three matched single-phase reactor units and a three-phase reactor unit, both non-gapped and air-gapped.

The simulation involved simultaneous ac and dc energisation of the reactors. The ac energisation was done by applying constant ac fluxes close to saturation to the reactor's models. The dc energisation was done by applying small amounts of varying dc fluxes relative to ac fluxes over a whole range of the reactor's magnetisation curve.

Magnetisation curve of the reactors' magnetic core was modelled with trigonometric equations presented by Takács. Relationships between excitation current and flux and between reactive power, excitation current and flux were defined using the models' magnetic circuits. The impacts of incrementing dc fluxes on excitation current and reactive power were analysed and the excitation current was Fourier-transformed for various harmonic contents. It was found out that incrementing dc flux does only have impacts on the excitation current of the single-phase reactor units and not on the excitation current of the three-phase reactor units.

Analysis of the excitation current for the single-phase reactor units revealed that as applied dc flux gradually increased, the excitation current increased in the phases and in the neutral. Without dc flux, the excitation current rarely consisted of harmonics but with gradual dc flux increment, the excitation current began to consist of both even and odd harmonics. The harmonics could have easily been above recommended compatibility levels for harmonics as injected dc flux increased. Simultaneously reactive power increased exponentially as dc flux injection increased. The harmonics for single-phase units with smaller gaps were more in terms of magnitudes than units with larger gaps at a particular ac flux and dc flux.

The validity of the mathematical modelling was tested in the laboratory on the single-phase and three-phase reactor units with the same dimensions. The ac energisation was done by applying constant ac voltages equivalent to ac fluxes used in the simulation. The dc energisation was done by injecting dc currents obtained from the model.

Analysis of the laboratory excitation current for the single-phase reactors revealed that as injected dc current gradually increased, the excitation current increased in the phases and in the neutral. The excitation current began to consist of both even and odd harmonics easily above recommended compatibility levels for harmonics. Reactive power increased exponentially, while the increase in temperature remained constant. The harmonics for single-phase units with smaller gaps were more in terms of magnitudes than units with larger gaps at a particular ac voltage and dc current determined from the model.

Next, comparisons were carried out between measured and modelled results, which consisted of phase and neutral fundamental currents, phase and neutral harmonics (from second to tenth), phase and neutral reactive power. Plotting the measured results on the x-axis and the modelled results on the y-axis, both axis scaled the same for every type of results i.e. fundamental current, second harmonics, etc; the two methods (measured and modelled) were correlated. The methods depicted almost diagonally linear relationships between them for single-phase units. There were differences in magnitudes between measured and modelled harmonics for three-phase units but the order of increase in magnitudes among harmonics remained similar between the two methods. Errors that did not lead to perfect correlations were identified to be measuring equipment errors at low currents and neglect of hysteresis loops in the modelling of the magnetisation curve of the reactor's magnetic cores.

Next, Eskom field-collected measurements during both major and minor storm activities for Hydra and Grassridge transformers in 2001 were analysed in the light of measured and modelled results. In the measurements, both substations' transformers contained dc currents in the neutrals with or without much storm activities but increasing as the storm activities increase. Third and sixth harmonics were measured in the neutral of the transformers with or without much storm activities fluctuating alongside dc currents' fluctuations. Phase current harmonics on the HV side, which were very similar those on the LV side remained unaffected by the presence of dc currents in the neutrals.

Grassridge transformer measurements were compared to modelled and measured quantities since its transformer's magnetisation properties were known and it was three-phase three-limb like the three-phase reactors (previously simulated and tested). The lack of detailed design information such as core yoke lengths makes comparison difficult if not possible. Grassridge measurements appeared to look similar to both measured and modelled measurements with a slight injection of dc flux density between 0 and 0.1 Teslas since it's only then when fifth harmonics is predominantly higher followed by second, then third, fourth and fifth lastly.

In conclusions, it was found out that saturation in transformers and reactors are accompanied with concealed and physical effects. Concealed effects, which occur in the initial stages of saturation, were mostly observed in this research. They included the production of odd and even harmonics and increase in reactive power flow while physical effects that occur in extreme saturation involve intense stray flux, heating and gas evolution.

Based on the findings in the research, it was therefore recommended that single-phase units should be disconnected from the power network prior to reported major magnetic events. For new reactor units, it was recommended to use three-phase three limb transformer/reactors units since it is the only least type susceptible to GICs impacts. It was also recommended to be more strict on the specifications of conditions that could cause imbalance among transformer/reactor phases such as number of turns and gap sizes and ensure that they are equal in all phases at all times after installation.

CONTENTS

CHAPTER 1

INTRODUCTION

1.1 BACKGROUND

The sun causes solar disturbances by hurling fierce dense waves of charged particles on its surface and emitting them into space nearly after every eleven years. Such a plasma stream flow is called solar wind of which a portion may reach the earth several days later. When it reaches the earth, it interacts with and fluctuates the earth's magnetic field, resulting in a process known as a geomagnetic storm [30].

Geomagnetic storms produce quasi-dc currents called geomagnetically induced currents (GICs) when flowing through man-made systems including power systems. In power systems, they may cause half cycle saturation of power transformer and shunt reactors. The saturation may result in large harmonics, unusual swing in real and reactive power flow and intense stray flux, which may cause malfunction of power transformers, shunt reactors, relays and circuit breakers [3, 28].

GICs occur worse at high latitudinal or near auroral zones. In these zones, the magnetic field is more concentrated and fluctuations in the magnetic field could result in large amounts of induced GICs making countries such as Canada or Scandinavia countries more vulnerable than mid-latitude countries such South Africa [13, 26].

Since the late 1980's Eskom was aware of the possible detrimental effects of GICs. At that stage it was believed that power networks at mid-latitude such as in Southern Africa were immune to GICs' impacts. A research project was initiated to investigate the

validity of such a belief [30]. It was found that GICs do indeed constitute a threat to the Eskom Main Transmission System.

Meanwhile in South Africa, there had been several reported incidents of transformers' and reactors' failure with more incidents on reactors at the height of storm activities of the previous two cycles [29, 30]. It was for this reason that this project was initiated to determine the effect of dc current on reactors.

1.2 OBJECTIVES OF RESEARCH

This research investigates and reviews the response of transformers and reactors to GICs. The investigation includes both mathematical modelling and laboratory testing of small-scale models of both single-phase and three-phase reactor units due to a relatively large occurrence of reactor failures than that of transformers in South Africa. The objectives are to match the mathematical models to the measurements under various conditions of loading, paying particular attention to the saturation of their magnetic cores, and deduce extrapolation to large-scale transformers and reactors using field data.

1.3 RESEARCH METHODOLOGY

The following procedure was followed to conduct the research:

- A literature review was carried out to establish the effects of GICs on large transformers and reactors and on the modelling of transformers and reactors. Work reported in the literature indicated that GICs' effects were associated with the saturation of transformer's or reactor's magnetic core and hence particular attention was paid to the saturation of their magnetic core.

- Single-phase and three-phase reactor units were mathematically modelled allowing for a non-linear magnetization curve in order to conceive the alleged effects of GICs.

- Laboratory testing was carried out on laboratory-sized units due to the difficulty of injecting currents in an operational system. Work reported in the literature indicated that laboratory tests had only been carried out using separate ac and dc excitation of the transformer. In this research simultaneous energisation was carried out, as the method devised appears to be suitable since it mimics reality. A varying dc current was injected into the neutral using a dc source. Its effects and reactor types on harmonics and reactive power were investigated. The transformers and reactors were monitored for acoustic noise, vibration, temperature and any other indicator, which could be used for transformer protection or condition monitoring.

- Field results collected at the Hydra and Grassridge Substation during low and high GICs' activities were extensively analysed in the light of mathematical modelling and laboratory test results.

- The results of the mathematical modelling, laboratory tests and field measurements were correlated.

- Finally based on the research, conclusions were drawn and recommendations were proposed.

1.4 CHAPTER OUTLINE

This report consists of seven chapters including the introduction.

Chapter 2 reviews literature into the effects of GICs on large transformers and reactors. It also reviews the mathematical modelling methods of transformers and reactors paying particular attention to the saturation of their magnetic core. The literature alleged this condition to be associated with the saturation of their magnetic core.

Chapter 3 covers the mathematical modelling of non-gapped and air-gapped reactors for both single-phase and three-phase units. Simultaneous ac and dc excitation of the reactor was carried out keeping ac excitation constant while varying dc excitation. Ac excitation was chosen close to the saturation of the reactors' magnetic cores.

In **Chapter 4**, reactors are tested in the laboratory under similar dc and ac excitation conditions to those of the mathematical modelling in Chapter 4. Next, effects of simultaneous dc and ac excitation were observed.

Chapter 5 compares mathematical modelling and laboratory testing results for a possible correlation while **Chapter 6** correlates the two with field results.

Chapter 7, which is the last chapter, evaluates the findings of the research and proposes recommendations based on the research.

CHAPTER 2

LITERATURE REVIEW

Approximately every eleven years, solar disturbances interrupt the earth's magnetic field in a process that leads to the induction of geomagnetically induced currents (GICs). GICs entering electric power systems via earthed neutral of transformers and reactors can have detrimental effects on power system equipment.

This chapter reviews literature describing the effects of GICs on large transformers and reactors. It also covers the mathematical modelling methods of transformers and reactors and, in particular, the saturation of the magnetic core.

2.1 GEOMAGNETIC STORMS

2.1.1 SUNSPOTS AND CORONAL MASS EJECTIONS

In 1610, shortly after viewing the sun with his new telescope, Galileo Galilei made the first European observations of dark spots on the sun called sunspots. Continuous observations of sunspots were later on made [19].

According to NASA [19], sunspots increase and decrease in number approximately every eleven years in a cyclic manner as depicted in Figure 2. 1. Sunspots produce dense waves of protons and electrons and emit them as coronal mass ejections (CMEs) into space, expanding as they rise. The more the sunspots are, the larger the CMEs tend to be.

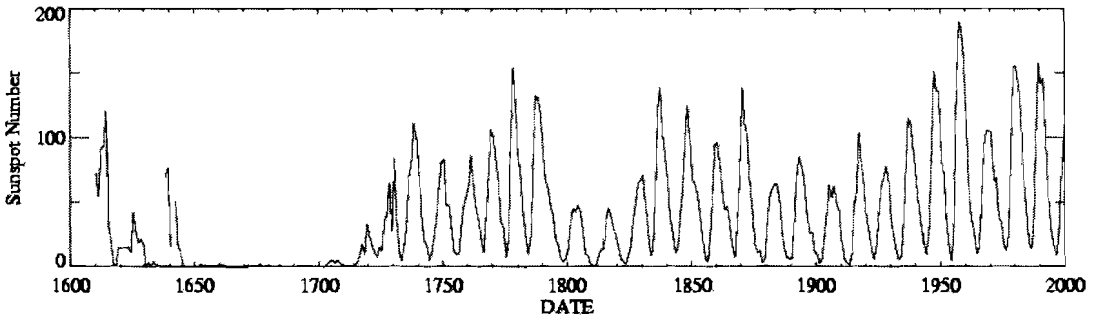

Figure 2. 1 Monthly averages of sunspot numbers from 1610 -2000 [19].

A portion of CMEs would normally only reach the earth several days later; the rest would be dispersed in space [30].

Scientists have been numbering the solar cycles since 1755. The cycle peaking during 2000 and 2001 is Solar Cycle 23. The next would be Solar Cycle 24. The starting and ending dates for the cycles are given in Appendix A [24].

2.1.2 GEOMAGNETIC INDUCED CURRENTS (GICs)

On reaching the earth, CMEs interferes with its magnetic field resulting in an electric potential difference on its surface [3, 26, 28, 30, 31, 33, 53]. This electric potential difference is accompanied with low frequency currents commonly known as geomagnetically induced current (GICs) when flowing through man-made systems. Although sunspots were discovered in 1610, GICs were only first reported in the late 1840s in the wires of the electric telegraph in North America. Subsequently, GIC effects on telegraph lines were reported on two separate occasions in North America in 1859 and 1866. Impacts on power systems were first noticed in 1940 and have occurred during every cycle ever since [3].

Lu, Liu and De La Ree [35] noted the low frequency of GICs to be in the range of 0.001 to 0.1 Hz making them to be somewhat equivalent to dc currents. They also noted that GICs could reach peak values as high as 200 A at the extremes of the three sets of factors that determine them. The three sets are:

- Extent and strength of the electric field in the power system [7].

- Electric system characteristics such as power system orientation, lengths of transmission lines, electrical resistance, transformer/reactor type and connection and station ground [7].
- Geology since power systems located at high latitudes, near auroral zones or at rocky zones are most vulnerable because of their high relative resistance allowing more current to flow in alternative paths, such as power lines located above them [30].

2.1.3 GICs INTERACTION WITH POWER SYSTEMS

GICs interact with electric power systems via grounded neutral of wye-transformers as shown in Figure 2. 2. After entering the transformer through the neutral, the current splits equally among the three phases of the transformer and into the transmission line. From there, it terminates at the star point of the next transformer except in case of an autotransformer where it may not necessarily terminate at the earth point but flow via the series winding to the next transformer [30].

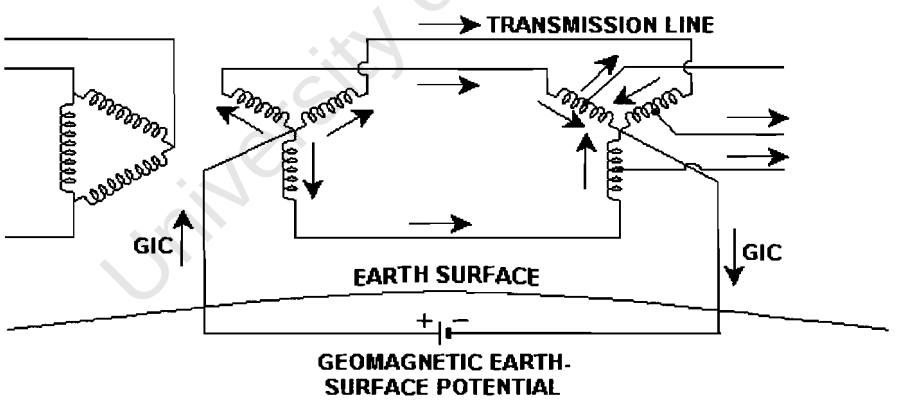

Figure 2. 2 Induced voltages drive GIC through the neutral grounding points of power transformers [30].

2.2 HALF-CYCLE SATURATION AND ITS EFFECTS

Under normal operation, magnetising current flows through magnetic core windings and most of the magnetic flux confines itself within the core. In such a case, an almost linear

relationship defined by the ratio of flux density to magnetic intensity, *u*, exists between the magnetisation current and the magnetic flux (origin to about point A in Figure 2. 3) [38].

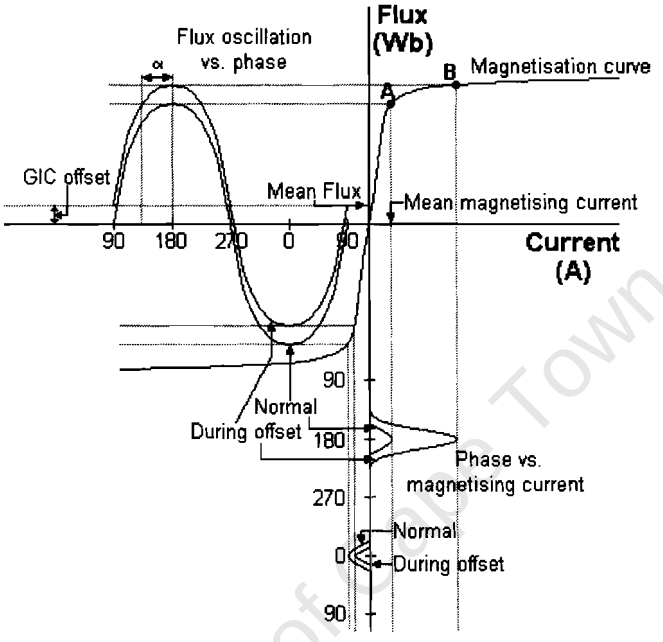

Figure 2. 3 Typical presentation of magnetisation curve of a ferromagnetic material [38].

As the magnetic flux increases, a point is reached where the magnetic core domains saturate and the almost linear relationship magnetisation current and magnetic flux does not exist anymore in which case the core undergoes saturation [38, 53]. In an attempt to cut down production costs, magnetic cores of transformers and reactors in practical applications are usually designed to function slightly below this point. Decades of design engineering have increased efficiencies and capabilities of these devices to such an extent that it would take low levels of AC excitation current to provide the magnetic flux needed. Low levels of GICs may drive these devices into half-cycle saturation [28]. GICs have been measured up to 10 A in South Africa [30] and up to 200 A in North America [35]. These may cause half-cycle saturation of power transformers and reactors.

According to Tattersfield [51], magnetic core domains become reluctant to the magnetic flux as saturation progresses. This results in leakage flux and higher levels of excitation current drawn.

Magnetic core saturation of power transformers and reactors results in the following: production of harmonics [55], unusual swing in real and reactive power flow [28] and intense stray flux, temperature rise and gas formation [3]. Of these three effects, the first two may be considered concealed since it cannot be sensed by any of the five senses; the last set may be considered physical.

The degree and extent of effects in transformer and reactor differ due to their different constructions and configurations.

2.2.1 HARMONICS

Walling and Khan [55] describes that the exciting current of transformers saturated by dc currents has both even and odd-order harmonic components, with the overall trend for magnitude to decrease with increasing order at a given current magnitude.

Excitation current waveform may still contain a small percentage of harmonics without having necessarily saturated because as long as the relationship between flux density and flux intensity is not purely linear, the purely fundamental voltage waveform would never produce an excitation current waveform purely composed of fundamental current. The small percentage of harmonics due to non-linearity would however rarely be hazardous to distribution systems.

The South African Bureau of Standards drew up minimum standards to be applied as measures of power quality at the point of supply to end customers of electricity utilities. In these minimum standards, they gave the compatibility levels on LV and MV networks for voltage harmonics. Voltage harmonics' requirements are not similar those of currents' but could give an indication of what to be expected of current harmonics (the author

could not find compatibility levels current harmonics). Voltage harmonics' levels are displayed in Table 2. 1 [40].

Table 2. 1 Compatibility levels for harmonic voltages expressed as a percentage of the declared voltage of LV and MV power systems [40].

1	2	3	4	5	6
Odd harmonics non-multiple of 3		**Odd harmonics multiple of 3**		**Even harmonics**	
Order	**Harmonic voltage**	**Order**	**Harmonic voltage**	**Order**	**Harmonic voltage**
H	%	h	%	h	%
5	6	3	5	2	2
7	5	9	1.5	4	1
11	3.5	15	0.3	6	0.5
13	3	21	0.2	8	0.5
17	2	>21	0.2	10	0.5
19	1.5			12	0.2
23	1.5			>12	0.2
25	1.5				
>25	0.2 + 1.3 x 25/h				

These compatibility levels can be applied on HV systems as well since from LV or MV systems to HV systems, voltage harmonics' magnitudes are transformed in equal proportions to those of fundamental voltages.

If compatibility levels for harmonic voltages are not adhered to, they may result in the following undesirable effects in a distribution system:

- Increase in I^2R losses in reactors/transformers [5]
- Equipment heating [5]
- Equipment malfunction and failure [5]
- Fuse and breaker mis-operation [23]
- Process problems [23]
- Conductor heating [5]

2.2.2 INCREASE IN REACTIVE POWER FLOW

Magnetic coils used in transformers are mainly inductive devices. With their exciting current lagging the system voltage by 90 degrees, they create reactive power loss in the transformer according to Kappenman and Albertson [28]. Kappenman and Albertson stated that under normal conditions, this reactive power is very small. However at half-cycle saturation with extreme abnormal increase in exciting current, they stated that large amounts of reactive power losses could result within the transformer.

During solar cycle 17 in 1940, five incidences of large increases in reactive power were reported by Davidson [11] on 10 electric systems across the United States and Canada. Unusual shifts in MVA and MVAR flow in transformers and reactors were reported during solar cycle 19 in 1972 across North America. None of these incidences caused physical damage to transformers and reactors.

2.2.3 INTENSE STRAY FLUX, HEATING AND GAS EVOLUTION

Albertson, Thorson and Miske [3] stated that during the half-cycle saturation, there might be leakage flux spilling outside the normal flux paths within the core. They further stated this leakage flux could cause rapid, excessive heating of the structural members giving rise to two concerns.

The first concern is that winding insulation adjacent to the structural member may be heated severely, resulting in thermal degradation of the insulation as Figure 2. 4 depicts. Minnesota Power Electric [21] identified that damage to this extent requires a considerable amount of heating.

Figure 2. 4 Transformer heating caused by GICs as a result of insulation damage on large current carrying windings [21].

The second concern is that an intense, local heat source might rapidly decompose adjacent insulation and generate a free gas bubble in the oil. The existence and mobility of a gas bubble could cause or contribute to a dielectric breakdown.

Several gases could result from hot spots. The presence of such gases usually indicates possible internal problems of transformers and reactors. Table 2. 2 displays the gases and their possible causes, which could be GICs triggered.

Table 2. 2 Possible gas formation due to GICs saturation [30].

Gas / Cause	Ethane (C2H6)	Ethylene (C2H4)	Methane (CH4)
Overheated oil / Thermal hotspots	X	X	X
Low energy electrical discharges			X

Some large transformers and reactors are fitted with gas-monitoring units. Once these units detect gas presence, a dissolved gas-in-oil analysis (DGA) test can be carried out to determine the content amount of each individual gas [30].

Reactor 4 (765 kV, single-phase unit) on the white phase at the Alpha substation was one of the reactor units fitted with a gas-monitoring unit. Following the major magnetic storm of 06 November 2001, the reactor tripped on Buchholz the following day. The DGA test on this unit revealed signs of degradation as the storm activity increased as shown in Figure 2. 5. GICs might have caused the degradation but other factors might be attributed to it [30].

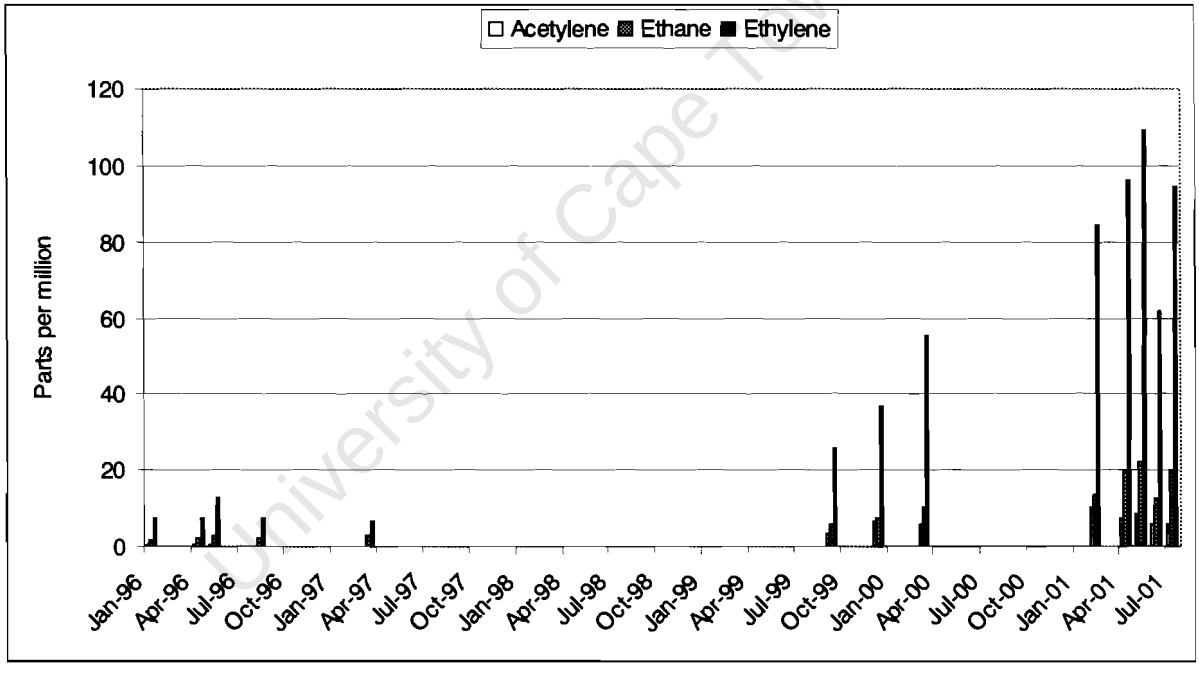

Figure 2. 5 DGA results for Alpha Reactor 4 (White phase) before and after the major storm that occurred on 31March 2001 [30].

In a separate incident, the DGA test was done for a reactor at the Droërivier substation shortly before and after the storm. According to the laboratory report following the sample taken on 28 September 2001, the amount of acetylene was considered to be insignificant. However, the sample of the same unit only six weeks later read, "The gas analysis on sample 200257913 contains acetylene gas, indicating discharges of high

energy". Due to this sudden increase another sample was taken on 14 November, which showed a slight decrease of the concentration of acetylene gas indicating that the condition stabilized. Figure 2. 6 shows the increase in gasses due to the 06 November storm event [8, 30].

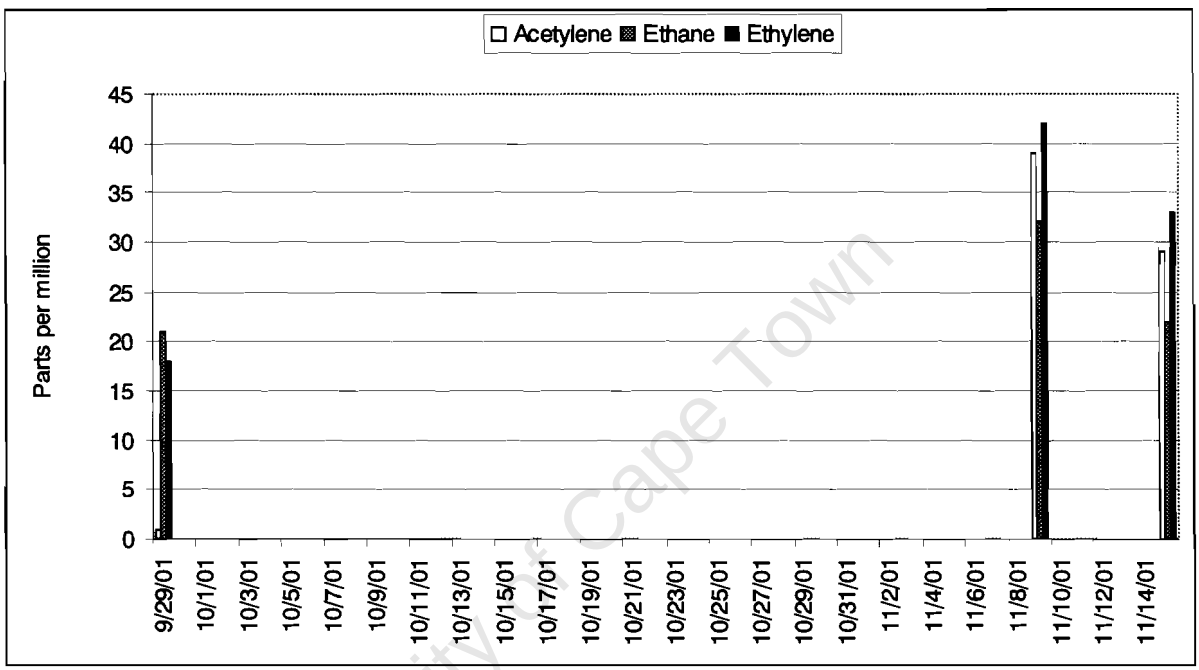

Figure 2. 6 DGA results for a Droërivier substation reactor during before and after the major storm that occurred on 06 November 2001 [30].

At the Droërivier substation there are three transformers and five reactors. The reactor for which results in Figure 2. 6 are shown is the only unit supplied by its specific manufacturer. A possible reason why it was the only one affected by GICs could be attributed to its internal design arrangement (see section 2.4) [30].

2.3 INCREASING POWER SYSTEMS SUSCEPTIBILIY TO GICs

Power systems are more susceptible today mainly because of the two following reasons [7, 28, 45]:

- Huge recent power networks' transformations
- Increasing geomagnetic storm trend

Power networks went through huge transformations in the twentieth century. Transmission grid lines had expanded over longer distances with neutral ground points spanning long distances and hence linking large cumulative earth surface potentials. Also, increased high-voltage interconnections brought in a large number of power system equipment and hence exposing a large number of equipment. Furthermore, many of modern extra high-voltage power transformers are constructed as single-phase units than three-phase units due to physical size limitations [28]. As we shall see later on, single-phase unit tends to saturate more quickly than comparable three-phase units.

2.4 SINGLE-PHASE AND THREE-PHASE REACTOR DESIGNS

Saturation causes in reactors would be similar to those of transformers since saturation begins in the magnetic core. The degree and extent of causes would however differ due to their different constructions and configurations. Nepsi [22] drew Figure 2. 7 to show a basic reactor configuration for both single-phase and three-phases.

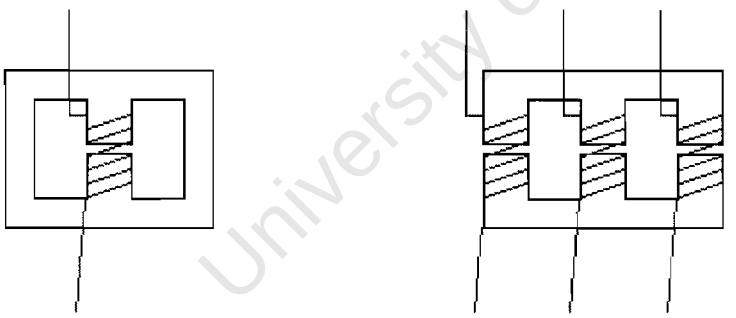

a) Single-phase core b) Three-phase core

Figure 2. 7 Typical iron-core reactor design [22].

Both single-phase and three-phase reactors contain an air gap kept apart by a non-magnetic medium such as wood (without oil insulation). Roters [46] stated that the air gap brings in an additional magneto motive force in a circuit consisting a reactor.

Roters further stated that precise mathematical calculation of the permeance of flux paths through air is rarely a practical possibility. This is apparently because the flux does not

usually confine itself to any particular path, which has a simple mathematical law and hence the computations are usually carried out by simplifying assumptions regarding the flux paths or by an entirely graphical method usually referred to as *field mapping*.

The method of field mapping consists essentially in sketching the distribution of flux lines and equipotential lines in such a manner that the total volume of the field is broken up into smaller unit volumes each having the same permeance. The permeance of the entire field is then obtained by adding the permeances of the unit volumes in series and parallel until the entire volume of the field is covered [46].

2.5 HYSTERESIS CURVES OF POWER TRANSFORMERS AND REACTORS

Takács [49] stated that ferromagnetic substances are characterised by two important properties: the Curie point and large atomic dipole moments. When an external magnetic field is applied, their domains align and spread themselves out in the magnetic field direction. When the applied field gets removed, not all domains move back to their original state. The material would in fact trace path *abcd* rather than *aod* as shown in Figure 2. 8 when the applied field gets reversed.

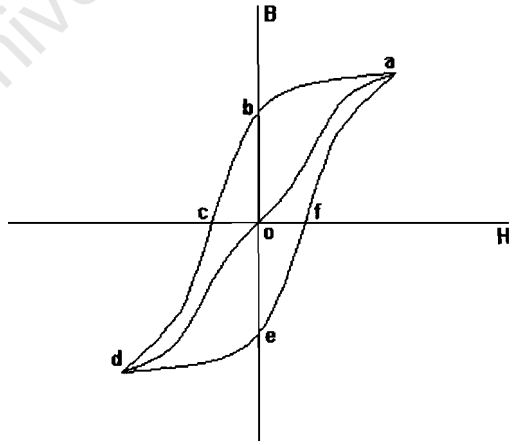

Figure 2. 8 Typical hysteresis loop of a ferromagnetic material [49, 51].

If the field gets reversed again, the material would trace path defa. The whole loop *abcdefa* is called a hysteresis loop. The loop area also represents energy dissipated per unit volume. Magnetic materials with narrow hysteresis are termed "soft" and are of great use in electromagnets, transformers, reactors and motors because their energy loss is minimal. "Hard" termed magnetic materials have broad hysteresis loops and are used to make permanent magnets [51].

2.6 SATURATION AND HYSTERESIS CURVE MATHEMATICAL MODELS

There are mathematical models reported in literature, which could be applied to the modelling of saturation and hysteresis in transformers and reactors. Of these, Takács [49] found the Langevin, Brillouin and T(x) functions to be of great interest. They are respectively formulated as follows:

$$L(x) = \coth(x) - 1/x \tag{2. 1}$$

$$B(x) = C_1 \coth(C_1 x) - C_2 \coth(C_2 x) \tag{2. 2}$$

$$T(x) = A_0 x + B_0 \tanh(C_0 x) \tag{2. 3}$$

where A_0, B_0, C_0, C_1 and C_2 are constants.

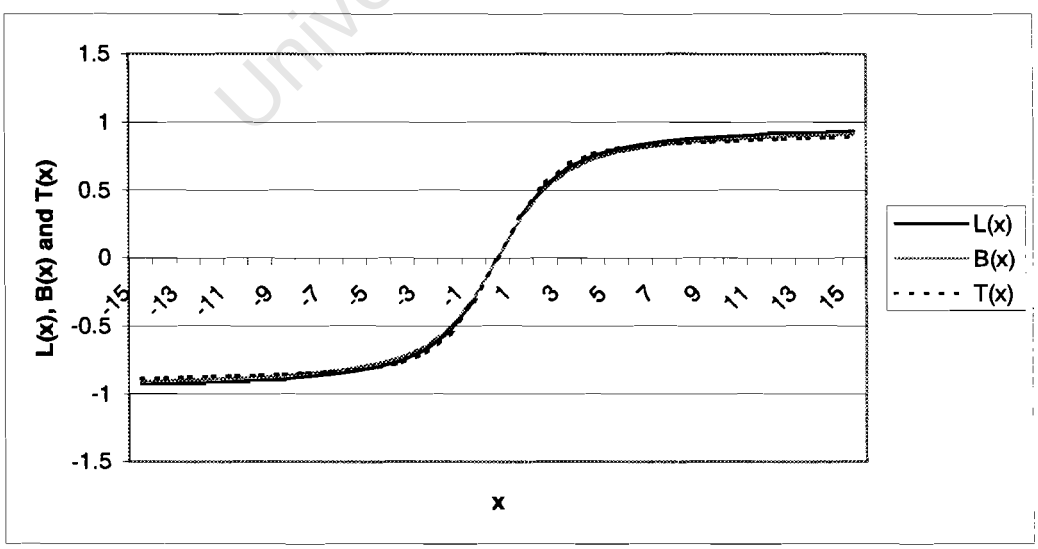

Figure 2. 9 The Langevin, the Brillouin and the T(x) function [49]

The three functions are illustrated in Figure 2. 9 for $A_0 = 0.006$, $B_0 = 0.8$, $C_0 = 0.41667$, $C_1 = 0.975$, $C_2 = 0.005$ [49].

Takács [49] stated that Langevin [32] had brought one of the earliest theories, the Langevin function. Although originally meant for paramagnetic materials, Takács [49] stated further stated that Weiss [57, 56] modified it to equation (2.1) for ferromagnetic materials. Takács [49] however revealed that this function gives best results for gaseous substances only.

Takács [49] stated Brillouin (1927) had modified the Langevin function further making it applicable to solid materials hence getting equation (2.2).

Takács [49] warned that both the Langevin and the Brillouin functions should be handled carefully because of their possible discontinuity when $x = 0$, which is untrue for real magnetisation curve and hysteresis loop.

The most recent model of them all, currently dominating the literature according to Takács [49] is the popular Preisach model. Preisach [43] originally found the Preisach model according to Takács [49]. Mayergoyz [37] and Della Tore [12] modified the original further to give equation (2.3). Unlike the previous two models, the Preisach model is not only applicable to magnetising curves alone but could be slightly modified to represent hysteresis loop as well despite its many other application in other fields of science. Takács [49] reported that when a material doesn't get driven deep into saturation the linear term could be neglected.

Takács [49] also wrote of other two models, which seemingly weren't appealing to him. The first one was Bauer's model based on power series and the second one was by Trutt, Erdelyi and Hopkins [54] and Widger [45] based on rational polynomials and functions.

2.7 SUMMARY

Quasi-dc currents are induced in power networks by the magnetic disturbances caused by solar ejections interacting with the earth's magnetic field. When flowing through man-made systems, the quasi-dc currents are called Geomagnetically Induced Currents (GICs).

GICs could enter power system via earthed neutrals of transformers and reactors and could bias the magnetisation of the core, causing half-cycle saturation. Half-cycle saturation is characterised by the production of harmonics, increase in reactive power flow and intense stray flux, heating and gas formation.

The extent of saturation in various transformers and reactors is determined by the dimensions and arrangement of the core.

Saturation and hysteresis loop of the magnetisation of the core can be modelled with several equations presented by Takács. These equations could be applied to the modelling of saturation in reactors.

CHAPTER 3

MATHEMATICAL MODELLING OF REACTORS

Reported incidents of failures possibly caused by GICs had been reported more on reactors than on transformers in South Africa [30]. For this reason, this Chapter shall simulate two types reactors for the effects of GICs. The types are: three matched single-phase unit reactors and a three-phase unit reactor. For both types, the modelling shall be carried out on non-gapped and air-gapped reactors.

GICs can be modelled with dc currents. DC current in the modelling results from injecting DC flux in the model. Relationships between excitation current (which may consist of a dc component) and various magnetic quantities including dc flux and physical dimensions shall be deduced. Fourier analysis shall be then carried out on the excitation current for various harmonic contents. The impact of incrementing dc flux while maintaining ac flux on harmonics and on reactive power shall be analysed.

3.1 SUSPICIOUS REACTOR FAILURES

Koen [29] conducted an investigation into correlation between past power system equipment failures (in South Africa) and geomagnetic storms for the peak period of activity during solar cycle 22 (1989 – 1994). He concluded that the findings showed circumstantial evidence of transformer and reactor failure and trips at the same time, or shortly following geomagnetic storms. Table 3. 2 shows some of these incidents that could be GIC related.

Table 3. 1 Results of investigation between past system events and solar cycle 22 geomagnetic storms locally [30].

Date	Substation	Equipment	Description
15 Mar 1989	Poseidon - Neptune	Reactor	Permanent fault on the reactor interwinding fault
28 Jul 1990	Beta	Reactor 4	Internal fault; reactor removed on 08 Sep 1990
26 Mar 1991	Hydra	Transformer 21	Permanent fault; reason unknown
18 Apr 1991	Beta	Reactor 2	Internal fault
18 Apr 1991	Beta	Reactor 4	Neutral earthing reactor faulted
19 Jun 1991	Hydra	Reactor 2	Permanent fault; reactor removed
14 Aug 1991	Beta	Reactor 4	Neutral earthing reactor faulted and disconnected
19 Aug 1991	Hydra	Transformer 21	Permanent fault; transformer removed
25 May 1992	Hydra	Transformer 3	Tripping on Buchholz protection
06 May 1993	Hydra	Rector 1	Internal fault and to be replaced
14 Dec 1993	Beta Alpha 2	Reactor	Red phase winding faulted
21 Mar 1994	Hydra Poseidon 1	Reactor	Fault; reactor replaced

More reactor failures continued to be reported during solar cycle 23. On 31 March 2001, the red phase of a 765 kV reactor (single-phase unit) on the Beta substation busbar, linked to the line feeding the Alpha substation went faulty. The explosion vent opened indicating an internal winding fault [30]. The two incidents at the Alpha substation and the Droërivier substation in sub-section 2.2.3 involved reactors.

It is therefore evident there had been more reported failures on reactors than on transformers in South Africa.

3.2 MAGNETIZATION CURVE MODELLING

Flux density and corresponding magnetization force are very crucial for effective modelling. Unfortunately all that was available from the core manufacturer was the magnetization curve graph shown in Figure 3. 1, which covers a satisfactory range beyond the knee of the curve.

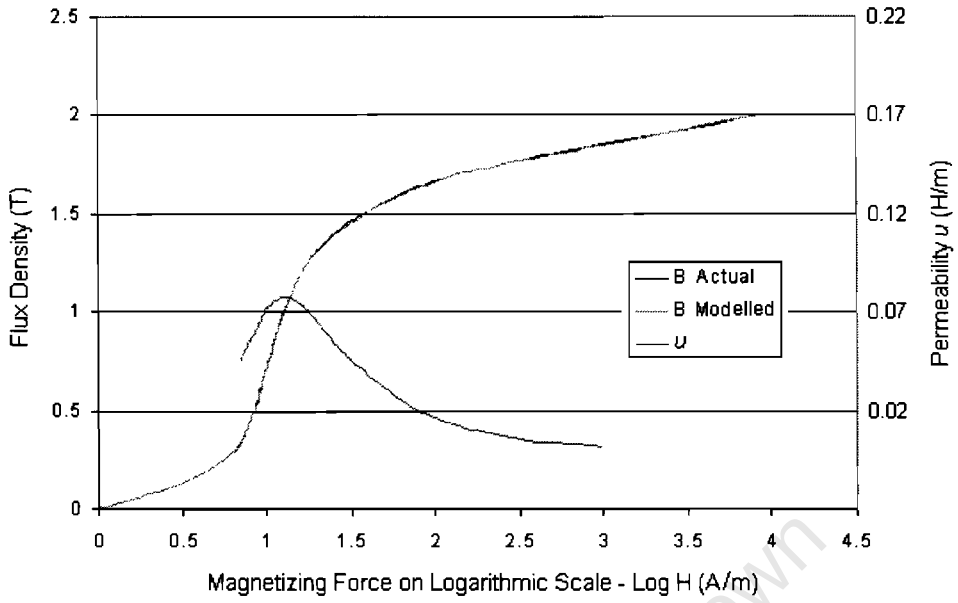

Figure 3. 1 Magnetization and permeability curve for a grain oriented silicon steel (GOSS) magnetic core [4].

Given any flux density level, one needed to give the corresponding magnetization force at any time. This could be obtained by reading off corresponding magnetization force from the graph, which becomes cumbersome for thousands of values as would be needed. It was hence for this reason that an attempt was made to mathematically represent the relationship between flux density (B) and magnetization force or flux intensity (H) using $\tan^{-1}$ functions as investigated by Takács [49] in Chapter 2. Such representation is supposedly an art and could not be done using a single equation. It resulted in five different equations as shown in Table 3. 2 and hence the term 'model equation'. These equations involves constants, which are not easily obtained [49]. One would almost suggest that perhaps a good working knowledge of trigonometric functions was needed, which a trigonometric mathematician would have. This left us with no choice but to find them by trial and error ensuring correlations closer to unity for all flux intensity values between modelled flux density values and manufacturer's flux density values referred to as actual flux density in Table 3. 2. A plot of manufacturer's flux density values can also be seen in Figure 3. 1.

Table 3. 2 Magnetic flux intensity and corresponding magnetic flux density and permeability values.

H (Am)	Log10(H)	Permeability *u*	B (Tesla) Actual	B (Tesla) Model	B (Tesla) Model Equation
0	0			0	$1.29\tanh(\log H)[1-0.8\sec h(\log H)^2]$
1.1	0.0413927			0.0106733	
2	0.30103			0.0766359	
3	0.4771213			0.1261552	
4	0.60206			0.1735487	
5	0.69897			0.2233734	
6	0.7781513			0.2750211	
6.5	0.8129134		0.3	0.2959445	$1.29\tanh(\frac{H}{7.2})[1-0.8\sec h(\frac{H}{8.5})^2]$
7	0.845098	0.046	0.345	0.3426204	
7.1	0.8512583	0.0468	0.35	0.3526589	
7.45	0.8721563	0.05	0.39	0.3895522	
7.55	0.877947	0.051	0.4	0.4005735	
7.95	0.9003671	0.0548	0.445	0.4465974	
8	0.90309	0.0552	0.45	0.4525514	
8.35	0.9216865	0.0585	0.5	0.4953032	
8.5	0.9294189	0.06	0.52	0.5141283	
8.7	0.9395193	0.0615	0.55	0.5396067	
9.05	0.9566486	0.0642	0.6	0.5849687	
9.1	0.9590414	0.0647	0.605	0.5915053	
9.45	0.9754318	0.0676	0.65	0.6374438	
9.75	0.9890046	0.07	0.685	0.6768008	
9.85	0.9934362	0.0706	0.7	0.6898578	
10.1	1.0043214	0.0719	0.73	0.7222602	
10.25	1.0107239	0.0726	0.75	0.7414847	
10.68	1.0285713	0.0741	0.8	0.7953638	
10.74	1.0310043	0.0743	0.807	0.8027095	
11.1	1.045323	0.0753	0.85	0.845734	
11.57	1.0633334	0.0761	0.9	0.8988423	
11.7	1.0681859	0.0763	0.915	0.912857	
12.1	1.0827854	0.0768	0.95	0.9540188	
12.7	1.1038037	0.077	1	1.0099874	

Table 3. 1 Continued

H (Am)	Log10(H)	Permeability u	B (Tesla) Actual	B (Tesla) Model	B (Tesla) Model Equation
13.45	1.1287223	0.0769	1.05	1.0491098	$0.266 + 1.21\tanh(\frac{H}{15})[1 - 0.8\sec h(\frac{H}{8})^2]$
14.2	1.1522883	0.0764	1.1	1.0982092	
14.4	1.1583625	0.0762	1.11	1.1102294	
15.1	1.1789769	0.0753	1.15	1.14896	
15.7	1.1958997	0.0742	1.18	1.1783182	
16.1	1.2068259	0.0735	1.2	1.1961054	
16.7	1.2227165	0.0725	1.22	1.2203732	
17.6	1.2455127	0.0705	1.25	1.2520252	
17.8	1.25042	0.07	1.257	1.2583778	
19.6	1.2922561	0.0658	1.3	1.3066166	
19.7	1.2944662	0.0654	1.304	1.3088963	
22.2	1.346353	0.06	1.35	1.3559865	
25	1.39794	0.055	1.39	1.3925392	
25.8	1.4116197	0.0535	1.4	1.3941281	$0.53 + (\log H)^{0.25\tanh(\log H)}[1 - 0.4\sec h(\log H)^2]$
28.2	1.4502491	0.05	1.428	1.4183991	
30.5	1.4842998	0.0473	1.45	1.4389619	
32.3	1.5092025	0.0448	1.463	1.453497	
38	1.5797836	0.04	1.5	1.4923606	
44.1	1.6444386	0.035	1.529	1.5249619	
48	1.6812412	0.0325	1.55	1.5422743	
52.8	1.7226339	0.0295	1.566	1.5607076	
63	1.7993405	0.025	1.6	1.5921152	
80	1.90309	0.02	1.636	1.6294295	
90	1.9542425	0.018	1.65	1.6458846	
110	2.0413927	0.015	1.67	1.6713527	
138	2.1398791	0.012	1.7	1.7022199	$1.347 + 0.166\log H$
175	2.243038	0.01	1.719	1.7193443	
250	2.39794	0.0073	1.75	1.745058	
355	2.5502284	0.005	1.775	1.7703379	
500	2.69897	0.0035	1.8	1.795029	
1000	3	0.002	1.85	1.845	
2100	3.3222193		1.9	1.8984884	
4500	3.6532125		1.95	1.9534333	
8600	3.9344985		2	2.0001267	

The mathematical representation does not cater for hysteresis. GOSS core materials have some of the narrowest hysteresis loops available and hence ignoring hysteresis would have minimal effects on modelling.

3.3 REACTOR CONFIGURATION

Magnetic cores for single-phase and three-phase reactor units to be modelled in this project were chosen to consist of two E-cores. Figure 3. 2 shows the dimensions (in mm) of the core.

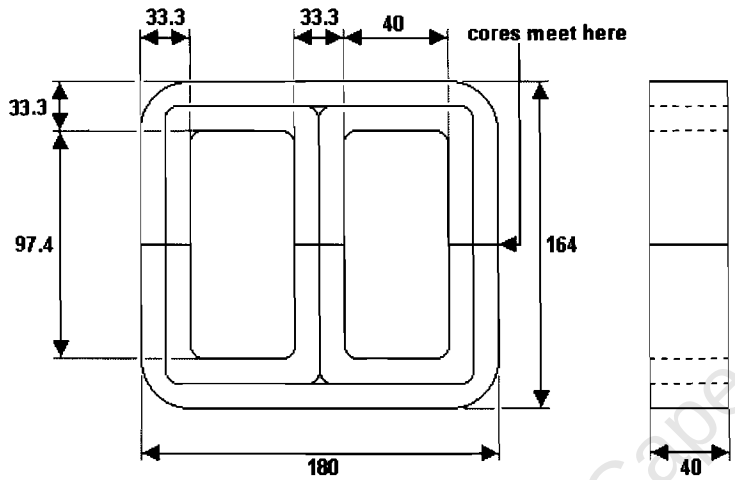

Figure 3. 2 Two magnetic E-cores that formed the basic magnetic core structure of a reactor [4].

Three types of gap thickness were chosen for modelling. These were 0, 250 and 450 micrometres as dictated by the maximum current that could flow in the circuit and by the size availability of gap material. Wiring and most equipment used in these laboratory testing would only allow a maximum of 20 A to flow. These constraints were used to limit the scope of the mathematical modelling.

3.4 EXCITATION CURRENT AND REACTIVE POWER OF A SINGLE-PHASE REACTOR

Figure 3. 3 shows an equivalent magnetic circuit for a single-phase reactor [47]. From this circuit, an attempt to relate excitation current and magnetization flux was made.

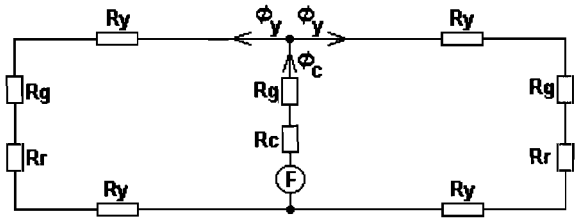

Figure 3. 3 Equivalent magnetic circuit for a single-phase reactor unit.

From the circuit, the following can be deduced:

$$F - \Phi_c R_c - \Phi_c R_g - \Phi_y R_y - \Phi_y R_g - \Phi_y R_r - \Phi_y R_y = 0 \qquad (3.1)$$

where F is magneto-motive force, Φ is flux, R is reluctance and the following subscripts: c, g, y and r are middle core leg, air gap, yoke and side leg respectively. These elements could further be expanded to $F = NI$, $\Phi_c = 2\Phi_y$, $A_c = A_r = A_y$, $L_r = L_c$ and $R = \frac{L}{\mu A}$

where N, I, L, u and A are number of turns, excitation current, segment length, medium permeability and segment cross-sectional area respectively.

The modifications lead equation (3.1) to:

$$NI - B_c A_c \left(\frac{L_c}{\mu_c A_c} + \frac{L_g}{\mu_0 A_c} + \frac{1}{2}\frac{L_g}{\mu_0 A_c} + \frac{L_y}{\mu_y A_c} + \frac{1}{2}\frac{L_c}{\mu_y A_c}\right) = 0$$

$$\Leftrightarrow NI - B_c \left(\frac{L_c}{\mu_c} + \frac{3}{2}\frac{L_g}{\mu_0} + \frac{L_y}{\mu_y} + \frac{1}{2}\frac{L_c}{\mu_y}\right) = 0$$

$$\therefore I = \frac{B_c}{N}\left(\frac{L_c}{\mu_c} + \frac{3}{2}\frac{L_g}{\mu_0} + \frac{L_y}{\mu_y} + \frac{1}{2}\frac{L_c}{\mu_y}\right) \qquad (3.2)$$

Most of the quantities in equation (3.2) are fixed for this particular laboratory model: N = 200 turns, L_c = 0.1307m, L_y = 0.0733m and u_0 = 1.26E-06. There would be three independent values for the gap thickness as dictated by the availability of gap material thickness. The range was dictated by the maximum current that could flow in the circuit as wiring and most equipment used in these laboratory testing would only allow a maximum of 20 A to flow. Hence L_g values were 0, 250 and 450 micrometres.

Reactive power losses can be written as $Q = I^2 \cdot X_L$ with $X_L = \omega \cdot L$ and $L = N \cdot \Phi / I$ and hence $Q = 2 \cdot I \cdot \pi \cdot f \cdot N \cdot B \cdot A$. In these equations, I is excitation current, X_L is reactance, ω is angular frequency, L is inductance, N is number of turns, Φ is flux, f is frequency, B is flux density and A is core cross-sectional area [47].

From equation (3.2), excitation current has flux intensity and permeability (the gradient of the magnetization curve) as variables. Permeability is not readily available and can always be obtained from both flux density and intensity. This hence leaves flux density and flux intensity as potential input variables.

From model formulae in Table 3. 2, flux density is the subject of the formulae and yet it would be the modelling input variable, which implies that to find flux intensity, one would have to make intensity the subject of the formulae. This is however extremely difficult if not impossible. For this reason, it was decided to generate a wider range of a set of values of flux density (ranging from 0 to about 2 Tesla) and corresponding flux intensity (ranging from 0 to about 10^4) and permeability values using model formulae and a spreadsheet. This resulted in 4422 different flux density values and their corresponding flux intensity and permeability values. These values look similar to those in Table 3. 3. 4422 readings fit on 111 Excel pages and are too numerous to be included in the Appendix.

Table 3. 3 First 10 flux density and corresponding flux intensity and permeability values.

H (Am)	Log10(H)	B (Hip)	*u* actual
0	0	0	0.041108
0.006276	0.001	0.000258	0.041108
0.012552	0.002	0.000516	0.041108
0.018828	0.003	0.000774	0.041108
0.025105	0.004	0.001032	0.041108
0.031381	0.005	0.00129	0.041108
0.037657	0.006	0.001548	0.041108
0.043933	0.007	0.001806	0.041107
0.050209	0.008	0.002064	0.041107
0.056485	0.009	0.002322	0.041107
0.062762	0.01	0.00258	0.041107

In the literature it was studied that under dc current excitation, equation (3.2) would contain both odd and even harmonics. For effective harmonic analysis, a wide range of current values during a period would need to be known. It was hence decided that time spacing between any two flux density values (and hence excitation current) generated in one 50Hz period (20 milliseconds) would be 167 microseconds giving 120 readings in one period. This amount of readings was another main motivation to choose 4422 flux density values.

3.4.1 FLUX INJECTION AND RESULTING EXCITATION CURRENT

The permeability for GOSS material in Figure 3. 1 reaches its maximum value at 1 Tesla; the core begins to saturate thereafter. For this reason, the two sets of constant ac flux density to be applied were chosen closer to 1 Tesla. These were 0.9 Tesla root-means-square and 0.95 Tesla root-means-square in Figure 3. 4 and Figure 3. 5 respectively. Variable dc flux was added to both sets in steps of 0.1 Tesla from 0.1 to 0.7 Tesla and 0.65 Tesla to the first and the second set respectively, covering the whole possible range as given in Figure 3. 1. Corresponding excitation current waveforms for the second set can be seen from **Error! Reference source not found.** to Figure 3. 8. The second set excitation currents are more distorted and saturated than the first set and for this reason, the first set excitation current waveforms were plotted in Appendix B.

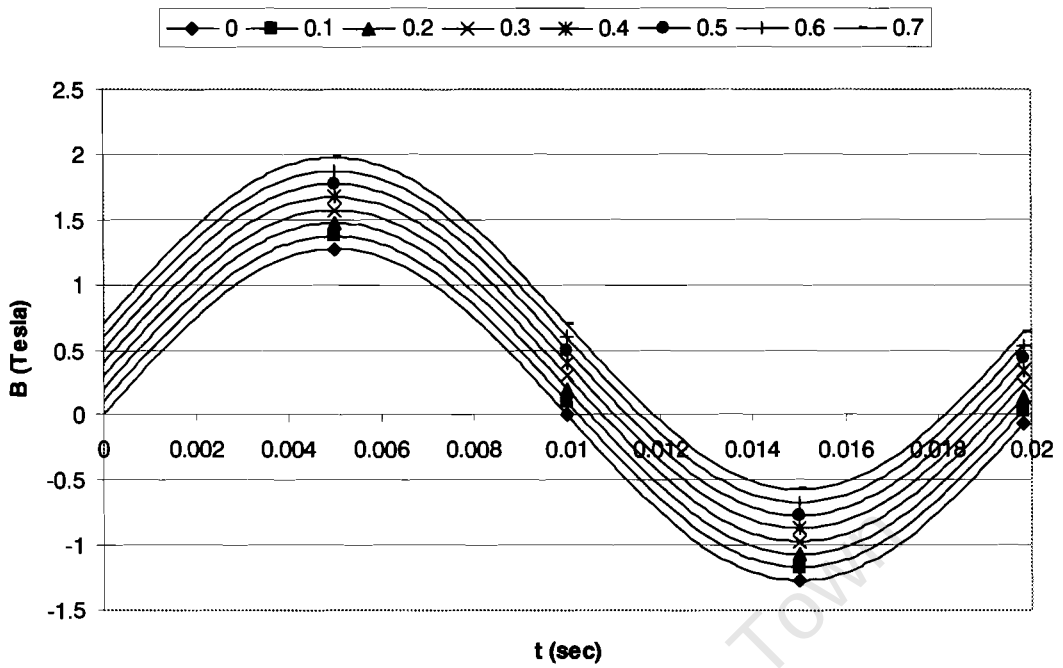

Figure 3. 4 Flux intensity waveforms at ac flux of 0.9 Teslas plus a range of dc flux offset of 0.1 to 0.7 Teslas.

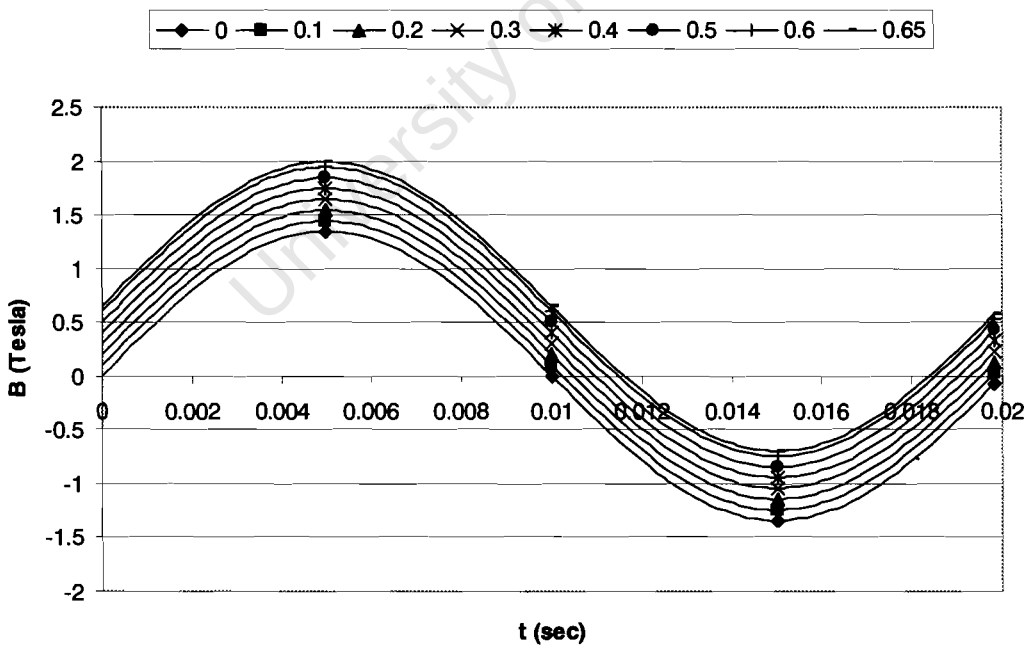

Figure 3. 5 Flux intensity waveforms at ac flux of 0.95 Teslas plus a range of dc flux offset of 0.1 to 0.65 Teslas.

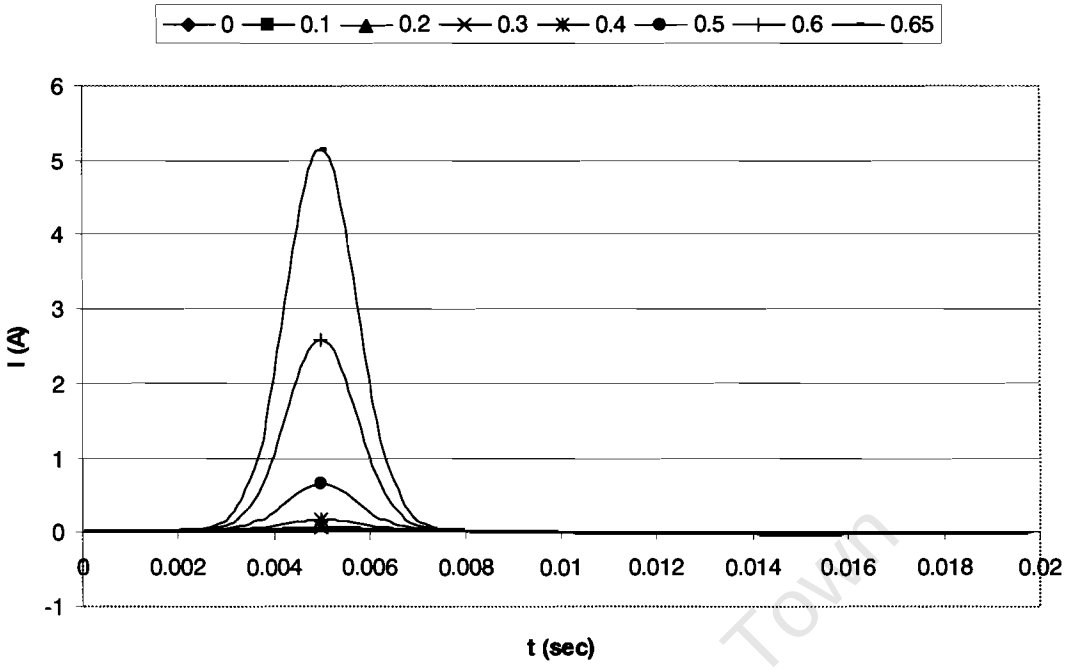

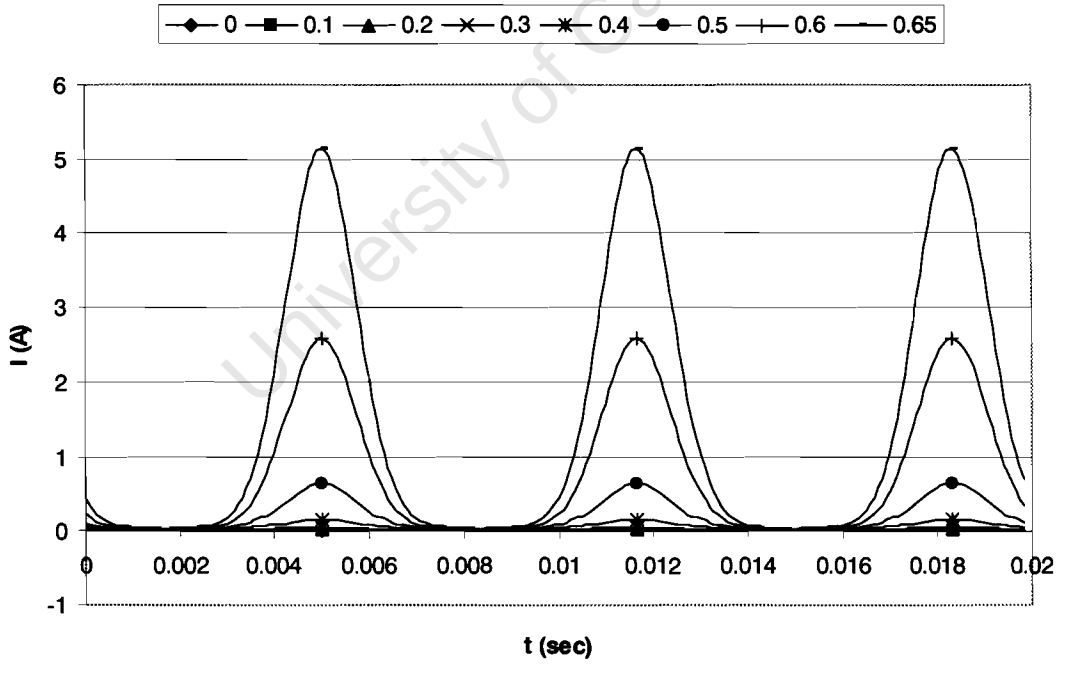

Figure 3. 6 Current waveforms resulting from ac flux of 0.95 Teslas plus a range of dc flux offset of 0.1 to 0.65 Teslas for the non-gapped single-phase reactor.

a. One phase

b. Neutral

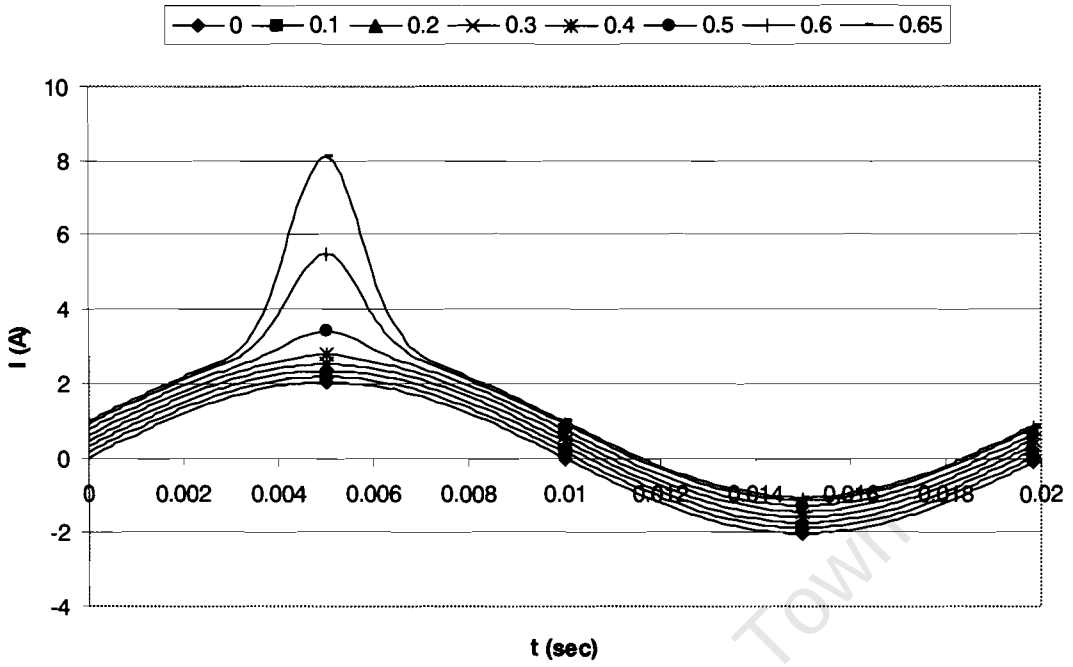

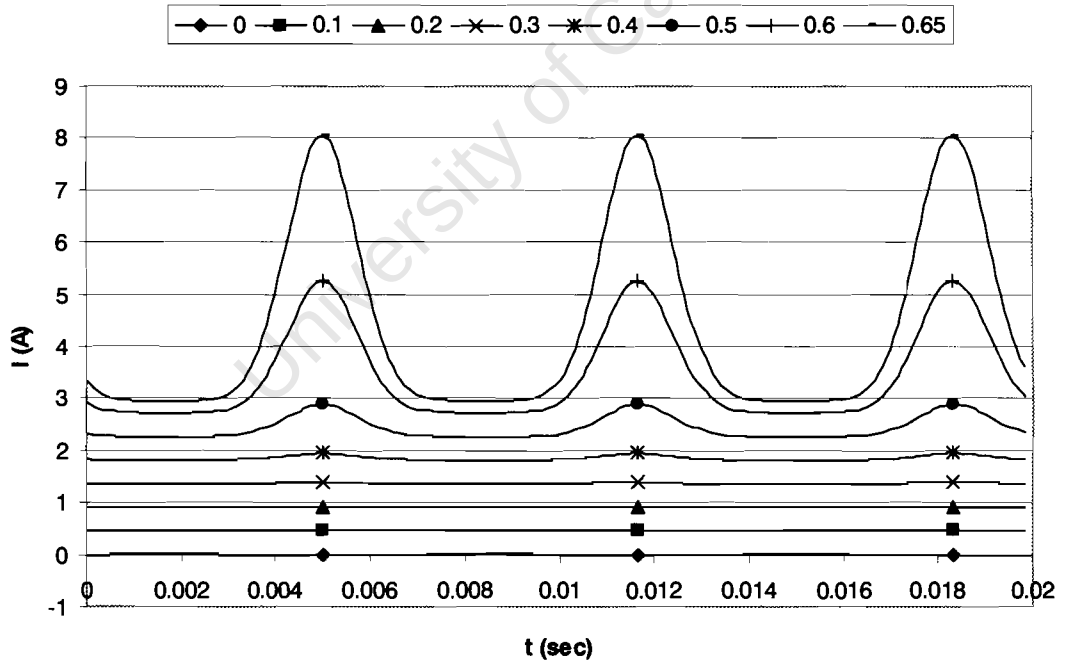

Figure 3. 7 Flux intensity waveforms at ac flux of 0.95 Teslas plus a range of dc flux offset of 0.1 to 0.65 Teslas for the 250 micrometre gapped single-phase reactor.

a. One phase

b. Neutral

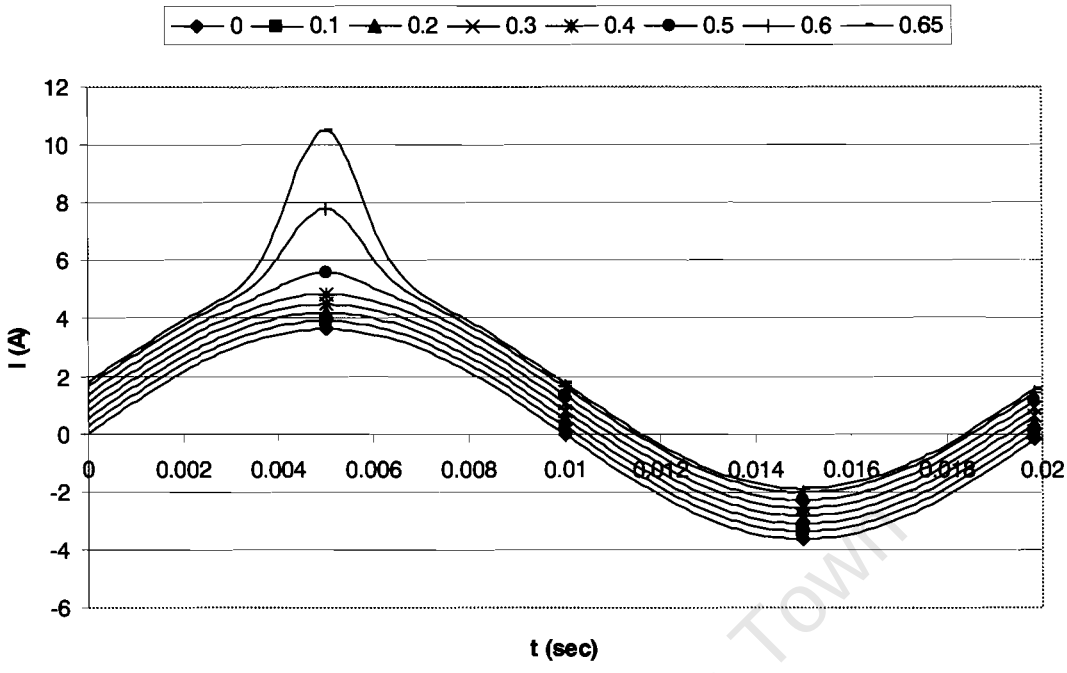

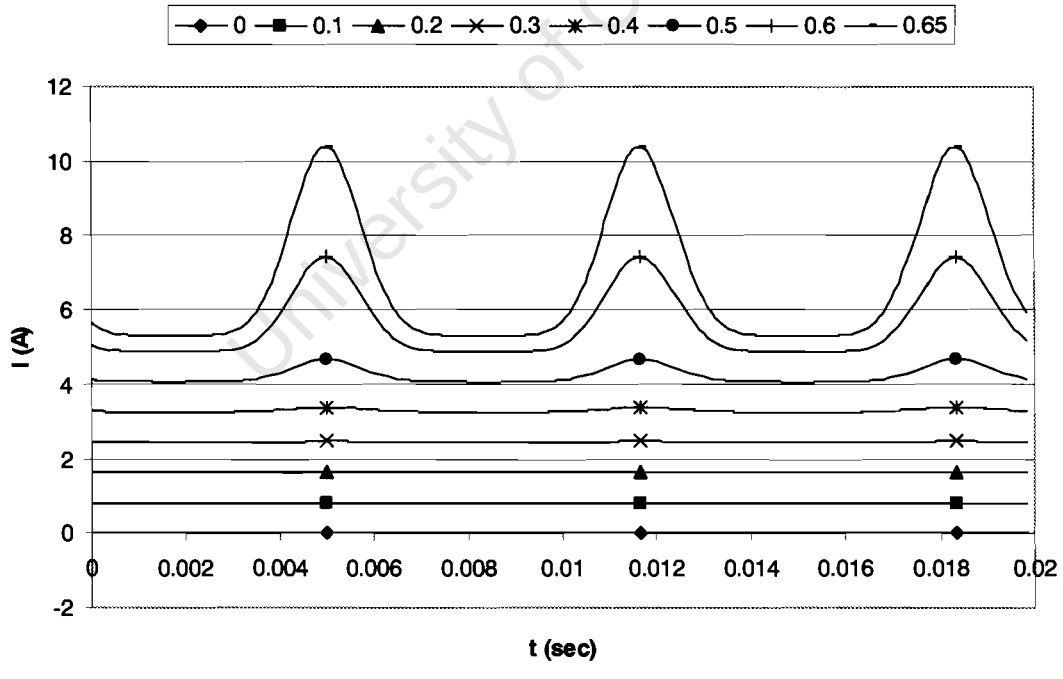

Figure 3. 8 Flux intensity waveforms at ac flux of 0.95 Teslas plus a range of dc flux offset of 0.1 to 0.65 Teslas for the 450 micrometre gapped single-phase reactor.

a. One phase

b. Neutral

3.4.2 CURRENT HARMONIC AND REACTIVE POWER ANALYSIS

From Fourier analysis, a current waveform can be expressed as [39]:

$$f_p(t) = \sum_{-\infty}^{\infty} F(n) \text{ for all } n \text{ integers.} \tag{3. 3}$$

where the Fourier coefficient $F(n)$ can be expressed as:

$$\begin{aligned} F(n) &= \frac{1}{T_0}\int_0^{T_0} f_p(t)e^{-jn\omega_0 t}\partial t \\ &\approx \frac{1}{T_0}\sum_0^{T_0} f_p(t)e^{-jn\omega_0 t}\Delta t = \frac{1}{T_0}\sum_0^{T_0} f_p(t)[\cos(n\omega_0 t) - j\sin(n\omega_0 t)]\Delta t \end{aligned} \tag{3. 4}$$

Harmonic current content for n^{th} harmonic expect for n equal to 0, can be written as [39]:

$$h(n) = F(n)e^{jn\omega_0 t} + F(-n)e^{-jn\omega_0 t} \tag{3. 5}$$

Harmonic current content for the 0^{th} harmonic would only be $F(n)e^{jn\omega_0 t}$.

Results for current harmonics and expected reactive power losses are displayed in Table 3. 4 for single-phase non-gapped reactor units reactor units for the second set of modelling. All results for first set of modelling can be found in Appendix B.

Table 3. 4 Harmonic current contents of current waveform and reactive power for single-phase non-gapped reactors in one phase.

ac Flux	dc Flux	Current (A)			Current harmonics (% of fundamental current)									Reactive power
(T)	(T)	dc	total	1st	2nd	3rd	4th	5th	6th	7th	8th	9th	10th	(VAR)
0.95	0	-0	0.02	0.02	0.0	5.7	0.0	6.3	0.0	0.7	0.0	0.5	0.0	1.45
0.95	0.1	0	0.02	0.02	2.9	3.4	5.0	6.9	0.3	0.0	0.8	0.8	0.0	1.48
0.95	0.2	0.01	0.02	0.02	8.5	2.9	10.8	7.9	1.2	0.9	1.2	0.4	0.2	1.60
0.95	0.3	0.01	0.03	0.03	19.5	14.3	18.1	10.7	3.8	3.0	2.2	0.9	0.4	1.90
0.95	0.4	0.02	0.05	0.04	42.3	35.9	32.7	21.9	14.2	11.1	8.1	5.6	4.2	2.85
0.95	0.5	0.07	0.17	0.10	72.4	63.4	53.3	40.4	30.0	22.0	15.2	10.0	6.4	7.36
0.95	0.6	0.25	0.66	0.34	86.5	75.9	63.2	49.4	37.0	26.5	17.9	11.4	6.8	25.62
0.95	0.65	0.49	1.32	0.67	89.2	78.1	64.7	50.6	37.8	26.8	17.9	11.3	6.7	50.10

Harmonic currents exceed 5% already with or without the injection of dc flux. Table 2.1 gave compatibility levels for voltage harmonics, which although not similar to those of currents', could give an indication of what to be expected of current harmonics. In this table, third and fifth harmonics should not exceed harmonic orders of 5% and 6%

respectively. Lowering ac flux density to ac flux of 0.9 Teslas (without the injection of dc flux) to reduce harmonics' levels makes matter worse (Appendix B – Table 1). These higher levels of harmonics' content could be mostly attributed to the non-purely linear relationship that exists between flux density and flux intensity. However as dc flux gets added on, dc currents produced increases resulting in the increasing of total current and fundamental current increasing and the production of both odd and even harmonics as graphically illustrated in Figure 3. 9 and Figure 3. 10. Resulting total current, fundamental current, harmonics and reactive power are linearly proportional to dc current.

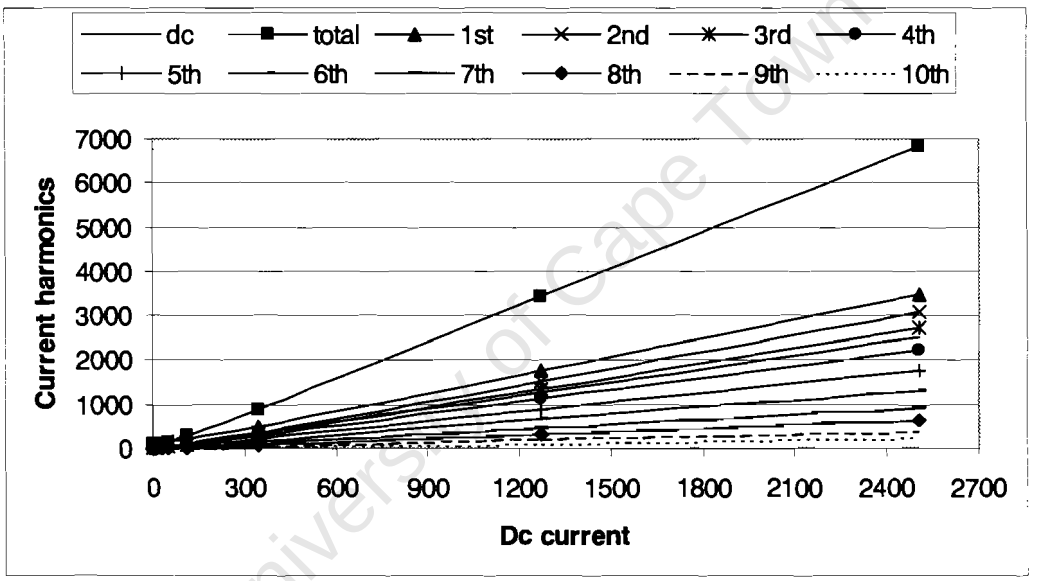

Figure 3. 9 Modelled current harmonics versus dc current both taken as a percentage of fundamental current (both at 0 dc flux offset) at ac flux of 0.95 Teslas for single-phase non-gapped units in one phase.

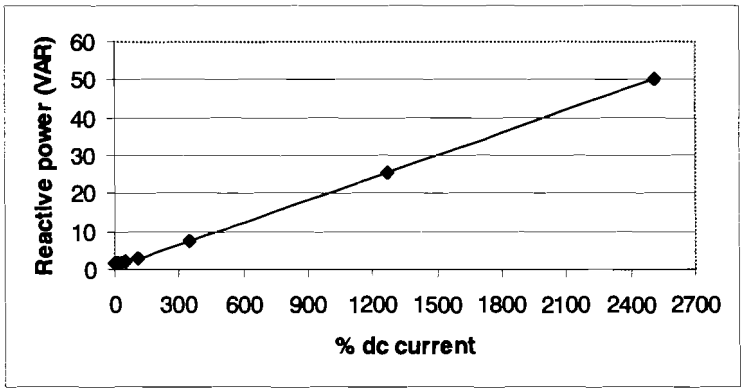

Figure 3. 10 Reactive power versus dc current as a percentage of fundamental current (at 0 dc flux offset) at ac flux of 0.95 Teslas for single-phase non-gapped units.

Table 3. 5 Harmonic current contents of current waveform and reactive power for single-phase non-gapped reactors in the neutral.

ac Flux	dc Flux	Current (A)			Current harmonics (% of fundamental current)								
(T)	(T)	dc	total	1st	2nd	3rd	4^{th}	5th	6th	7th	8th	9th	10th
0.95	0	0	0	0.00	650	∞	1249	451	727	103	146	∞	270
0.95	0.1	0.01	0.01	0.00	100	∞	85.5	45.5	∞	29.0	36.5	∞	38
0.95	0.2	0.02	0.02	0.00	45.6	∞	24.2	17.4	∞	31.7	13.2	∞	13
0.95	0.3	0.03	0.03	0.00	13.4	∞	96.3	7.9	∞	47.0	13.0	∞	18
0.95	0.4	0.06	0.08	0.00	43.5	∞	182	33.8	∞	119	36.8	∞	71
0.95	0.5	0.2	0.29	0.00	86.9	∞	256	70.6	∞	199	36.0	∞	107
0.95	0.6	0.74	1.15	0.00	111	∞	311	92.2	∞	258	33.5	∞	126
0.95	0.65	1.46	2.29	0.00	120	∞	314	91.7	∞	257	31.8	∞	121

As dc current increased, there was a notable increase total currents and a strong presence of the third, sixth and ninth harmonic contents in the neutral. The rest of the harmonics seemed to remain somewhat randomly distributed.

Next, results for current harmonics and expected reactive power losses are displayed in Table 3. 6 for single-phase 250 micrometre gapped reactor units reactor units for the second set of measurements.

Table 3. 6 Harmonic current contents of current waveform and reactive power for single-phase 250 micrometre gapped reactors in one phase.

ac Flux	dc Flux	Current (A)			Current harmonics (% of fundamental current)									Reactive power
(T)	(T)	dc	total	1st	2nd	3rd	4th	5th	6th	7th	8th	9th	10th	(VAR)
0.95	0	0	1.44	1.44	0.0	0.1	0.0	0.1	0.0	0.0	0.0	0.0	0.0	107.21
0.95	0.1	0.15	1.45	1.44	0.0	0.0	0.1	0.1	0.0	0.0	0.0	0.0	0.0	107.24
0.95	0.2	0.3	1.47	1.44	0.1	0.0	0.2	0.1	0.0	0.0	0.0	0.0	0.0	107.37
0.95	0.3	0.46	1.51	1.44	0.3	0.3	0.3	0.2	0.1	0.1	0.0	0.0	0.0	107.66
0.95	0.4	0.62	1.58	1.46	1.1	0.9	0.9	0.6	0.4	0.3	0.2	0.1	0.1	108.62
0.95	0.5	0.81	1.72	1.52	4.7	4.1	3.5	2.6	2.0	1.4	1.0	0.7	0.4	113.13
0.95	0.6	1.14	2.16	1.76	16.9	14.8	12.3	9.6	7.2	5.2	3.5	2.2	1.3	131.38
0.95	0.65	1.46	2.75	2.09	28.7	25.1	20.8	16.3	12.1	8.6	5.8	3.6	2.2	155.86

Harmonic currents are well within compatibility levels in Table 2.1 without the injection of dc flux. As dc flux increases up until 0.5 Tesla, they stay within the range. Meanwhile dc currents produced increases resulting in the increasing of total current and fundamental current and the production of both odd and even harmonics as graphically illustrated in Figure 3. 11 and Figure 3. 12. Resulting total current, fundamental current, harmonics and reactive power are exponentially increasing as dc current constantly increases.

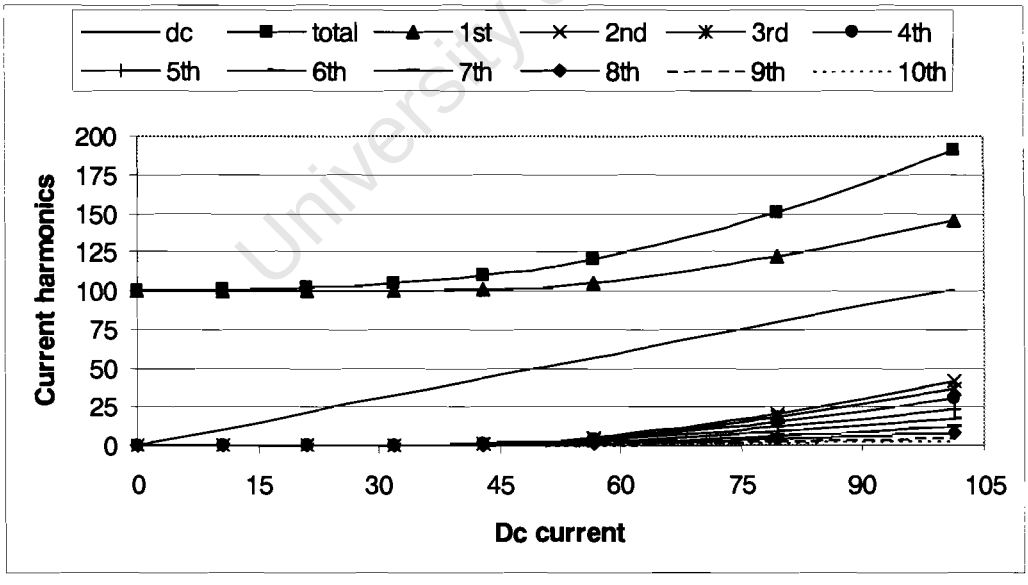

Figure 3. 11 Current harmonics versus dc current both taken as a percentage of fundamental current (both at 0 dc current offset) at ac flux of 0.95 Teslas for single-phase 250 micrometre gapped units in one phase.

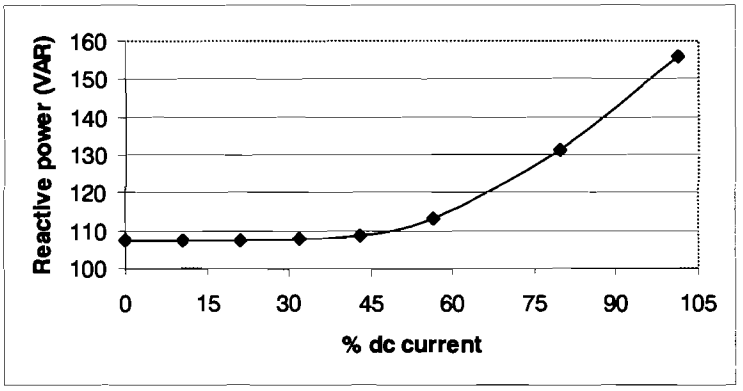

Figure 3. 12 Reactive power versus dc current as a percentage of fundamental current (at 0 dc current offset) at ac flux of 0.95 Teslas for single-phase 250 micrometre gapped units.

Table 3. 7 Harmonic current contents of current waveform and reactive power for single-phase 250 micrometre gapped reactors in the neutral.

ac Flux	dc Flux	Current (A)			Current harmonics (% of fundamental current)								
(T)	(T)	dc	total	1st	2nd	3rd	4th	5th	6th	7th	8th	9th	10th
0.95	0	0	0	0.00	169	∞	286	96.2	∞	71.5	40.9	∞	43.3
0.95	0.1	0.46	0.46	0.00	59.2	∞	14.4	12.4	∞	21.6	10.5	∞	0.4
0.95	0.2	0.91	0.91	0.00	59.5	∞	11.9	12.2	∞	21.7	10.7	∞	0.3
0.95	0.3	1.37	1.37	0.00	59.6	∞	11.8	12.0	∞	20.6	9.2	∞	1.3
0.95	0.4	1.85	1.85	0.00	57.1	∞	9.0	11.7	∞	21.3	10.8	∞	2.5
0.95	0.5	2.44	2.45	0.00	51.9	∞	13.6	17.6	∞	27.5	12.4	∞	8.1
0.95	0.6	3.43	3.54	0.00	35.8	∞	52.7	27.4	∞	54.6	15.2	∞	23.4
0.95	0.65	4.37	4.71	0.00	10.3	∞	88.7	33.9	∞	82.5	17.9	∞	36.5

As dc current increased, there was a notable increase total currents and a strong presence of the third, sixth and ninth harmonic contents in the neutral. The rest of the harmonics seemed to remain somewhat randomly distributed.

Finally, results for current harmonics and expected reactive power losses are displayed in Table 3. 8 for single-phase 250 micrometre gapped reactor units reactor units for the second set of measurements.

Table 3. 8 Harmonic current contents of current waveform and reactive power for single -phase 450 micrometre gapped reactors in one phase.

ac Flux	dc Flux	Current (A)			Current harmonics (% of fundamental current)									Reactive power
(T)	(T)	dc	total	1st	2nd	3rd	4th	5th	6th	7th	8th	9th	10th	(VAR)
0.95	0	0	2.57	2.57	0.0	0.0	0.0	0.0	0.0	0.0	0.0	0.0	0.0	191.82
0.95	0.1	0.27	2.59	2.57	0.0	0.0	0.0	0.1	0.0	0.0	0.0	0.0	0.0	191.85
0.95	0.2	0.54	2.63	2.57	0.1	0.0	0.1	0.1	0.0	0.0	0.0	0.0	0.0	191.98
0.95	0.3	0.82	2.7	2.58	0.2	0.1	0.2	0.1	0.0	0.0	0.0	0.0	0.0	192.27
0.95	0.4	1.1	2.81	2.59	0.6	0.5	0.5	0.3	0.2	0.2	0.1	0.1	0.1	193.22
0.95	0.5	1.41	3	2.65	2.7	2.4	2.0	1.5	1.1	0.8	0.6	0.4	0.2	197.74
0.95	0.6	1.86	3.48	2.89	10.3	9.0	7.5	5.9	4.4	3.1	2.1	1.3	0.8	215.99
0.95	0.65	2.23	4.05	3.22	18.6	16.3	13.5	10.5	7.9	5.6	3.7	2.4	1.4	240.47

Harmonic currents are well within compatibility levels in Table 2.1 without the injection of dc flux. As dc flux increases up until 0.5 Tesla, they stay within the range. Meanwhile dc currents produced increases resulting in the increasing of total current and fundamental current and the production of both odd and even harmonics as graphically illustrated in Figure 3. 13 and Figure 3. 14. Resulting total current, fundamental current, harmonics and reactive power are exponentially increasing as dc current constantly increases.

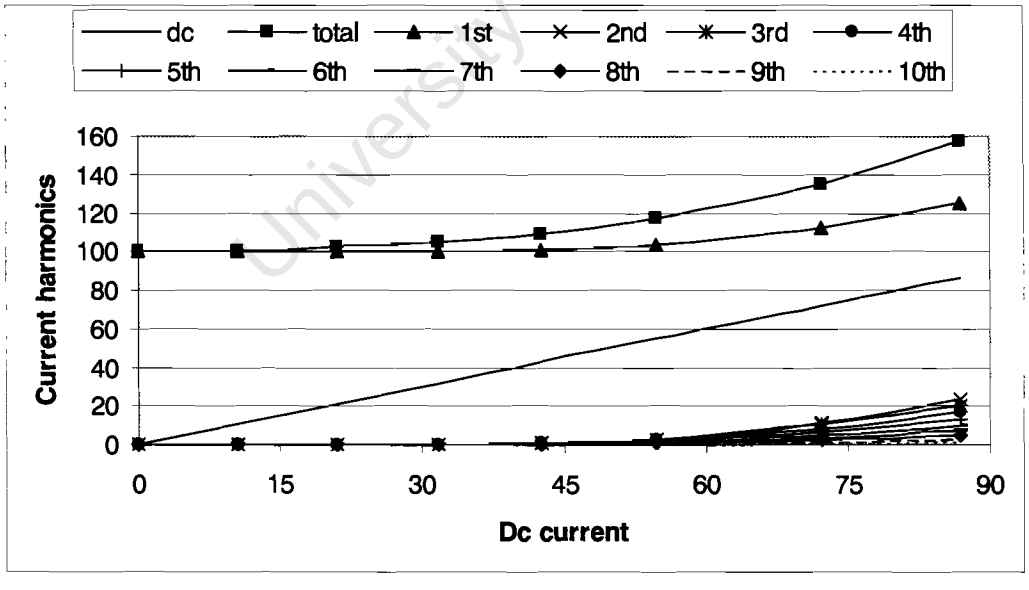

Figure 3. 13 Current harmonics versus dc current both taken as a percentage of fundamental current (both at 0 dc current offset) at ac flux of 0.95 Teslas for single -phase 450 micrometre gapped units in one phase.

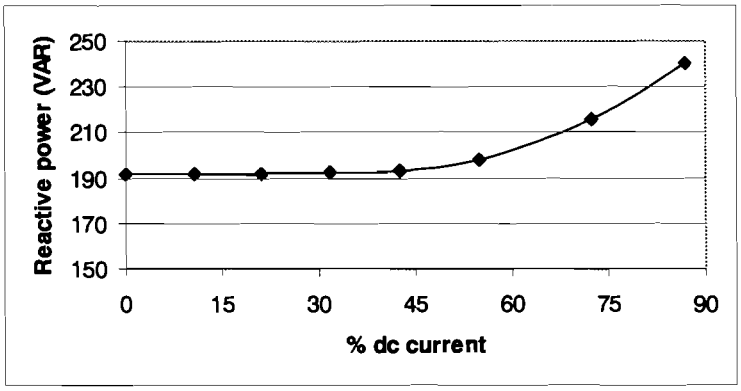

Figure 3. 14 Reactive power versus dc current as a percentage of fundamental current (at 0 dc current offset) at ac flux of 0.95 Teslas for single -phase 450 micrometre gapped units.

Table 3. 9 Harmonic current contents of current waveform and reactive power for single -phase 450 micrometre gapped reactors in the neutral.

ac Flux	dc Flux	Current (A)			Current harmonics (% of fundamental current)								
(T)	(T)	dc	total	1st	2nd	3rd	4th	5th	6th	7th	8th	9th	10th
0.95	0	0	0	0.00	852	∞	1028	485	∞	104	472	∞	95.3
0.95	0.1	0.81	0.81	0.00	57.4	∞	12.1	13.4	∞	22.1	10.5	∞	0.7
0.95	0.2	1.63	1.63	0.00	60.0	∞	12.8	13.1	∞	21.2	11.8	∞	1.4
0.95	0.3	2.45	2.45	0.00	57.6	∞	12.2	11.7	∞	22.2	11.4	∞	0.4
0.95	0.4	3.29	3.29	0.00	55.1	∞	8.1	13.3	∞	20.1	10.7	∞	1.5
0.95	0.5	4.23	4.23	0.00	54.6	∞	10.2	14.2	∞	22.1	10.5	∞	4.8
0.95	0.6	5.57	5.64	0.00	44.5	∞	28.4	21.9	∞	38.2	14.1	∞	15.3
0.95	0.65	6.7	6.92	0.00	22.2	∞	52.7	27.1	∞	53.9	15.3	∞	22.3

As dc current increased, there was a notable increase total currents and a strong presence of the third, sixth and ninth harmonic contents in the neutral. The rest of the harmonics seemed to remain somewhat randomly distributed.

3.5 EXCITATION CURRENT ANALYSIS AND REACTIVE POWER ANALYSIS OF A THREE-PHASE REACTOR

The similar cores that made up single-phase reactors were used to construct a three-phase reactor.

Analysis of an equivalent magnetic circuit for a three-phase reactor leads to equations (3.6) and (3.7).

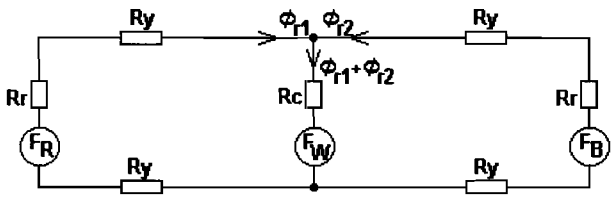

Figure 3. 15 Equivalent magnetic circuit for a gapped three-phase reactor unit.

From the circuit, the following can be deduced:

$$F_R - \Phi_{y1}(R_r + R_g + 2R_y) + \Phi_c(R_g + R_c) - F_W = 0 \qquad (3.6)$$

$$F_B - \Phi_{y2}(R_r + R_g + 2R_y) + \Phi_c(R_g + R_c) - F_W = 0 \qquad (3.7)$$

Equations (3.6) becomes $N(I_W - I_R) - B_c(\frac{L_c}{\mu_c} + \frac{L_g}{\mu_0}) + B_{y1}(\frac{2L_y}{\mu_{y1}} + \frac{L_g}{\mu_0} + \frac{L_c}{\mu_{y1}}) = 0$

and leads to

$$I_W - I_R = \frac{B_c}{N}(\frac{L_c}{\mu_c} + \frac{L_g}{\mu_0}) - \frac{B_{y1}}{N}(\frac{2L_y}{\mu_{y1}} + \frac{L_g}{\mu_0} + \frac{L_c}{\mu_{y1}}) \qquad (3.8)$$

Similarly $I_W - I_B = \frac{B_c}{N}(\frac{L_c}{\mu_c} + \frac{L_g}{\mu_0}) - \frac{B_{y2}}{N}(\frac{2L_y}{\mu_{y2}} + \frac{L_g}{\mu_0} + \frac{L_c}{\mu_{y2}})$ (3. 9)

Also $F_R - \Phi_{y1}(R_r + R_g + 2R_y) + \Phi_{y2}(R_r + R_g + 2R_y) - F_B = 0$

$$I_R - I_B = \frac{B_{y1}}{N}(\frac{2L_y}{\mu_{y1}} + \frac{L_g}{\mu_0} + \frac{L_c}{\mu_{y1}}) - \frac{B_{y2}}{N}(\frac{2L_y}{\mu_{y2}} + \frac{L_g}{\mu_0} + \frac{L_c}{\mu_{y2}}) \qquad (3.10)$$

It is also known that $\Phi_c + \Phi_{y1} + \Phi_{y2} = 0$.

Therefore $B_c + B_{y1} + B_{y2} = 0$ (3. 11)

Talking of flux, a closer look at Figure 3. 15 would reveal that injecting equal dc fluxes in each phase of the circuit (as it should happen) should not make a difference to the circuit. For gapped reactors, source-injecting dc flux into the red phase limb in the

positive direction would more or less split up in two halves; injecting one half into the white phase limb in the negative direction and the other half into the blue phase limb in the negative direction taking the direction of the arrows in the picture as positive. The similar process would be true for source-injected dc fluxes into limb W and limb B. As a result, each of the limbs would consist of the full source-injected dc flux flowing in its positive direction and the two source-injected dc flux halves flowing in its negative direction resulting in an overall dc flux of zero.

Getting back to equations (3.6) – (3.11), they would lead to:

$$I_R = \frac{B_{y1}}{N}\left(\frac{2L_y}{\mu_{y1}} + \frac{L_g}{\mu_0} + \frac{L_c}{\mu_{y1}}\right) \tag{3. 12}$$

$$I_W = \frac{B_c}{N}\left(\frac{L_c}{\mu_c} + \frac{L_g}{\mu_0}\right) \tag{3. 13}$$

$$I_B = \frac{B_{y2}}{N}\left(\frac{2L_y}{\mu_{y2}} + \frac{L_g}{\mu_0} + \frac{L_c}{\mu_{y2}}\right) \tag{3. 14}$$

Definitions of most of the quantities in equation (3.6) – (3.14) are similar to those of single-phase units. The additional subscripts y1 and y2 refer to yoke quantities of the red phase and the blue phase respectively. There are only two gap thickness situations for three-phase units. These 250 and 450 micrometres; the no gap situation doesn't exist for three-phase units as it is impractical and would create serious imbalance currents in the neutrals.

Despite the fact that our three-phase circuit is not affected by dc flux injection, current harmonic analysis (using Fourier theory) and reactive power analysis would still be carried out under similar and equivalent single-phase units' conditions. Flux density generated, frequency and spacing between readings remain the same.

Table 3. 10 Harmonic current contents of current waveform and reactive power for three-phase gapped reactors.

a. **Red and blue phases (outer limb phases)**
b. **White phase (middle limb phase)**

Gap	ac Flux	Current (A)			Current harmonics (% of fundamental current)									Reactive power
(*um*)	(T)	dc	total	fund.	2nd	3rd	4th	5th	6th	7th	8th	9th	10th	(VAR)
250	0.9	0	0.91	0.91	0.00	0.05	0.00	0.16	0.00	0.03	0.00	0.03	0.00	64.49
250	0.95	0	0.96	0.96	0.00	0.04	0.00	0.19	0.00	0.02	0.00	0.03	0.00	71.91
450	0.9	0	1.63	1.63	0.00	0.03	0.00	0.09	0.00	0.02	0.00	0.02	0.00	115.11
450	0.95	0	1.72	1.72	0.00	0.02	0.00	0.11	0.00	0.01	0.00	0.02	0.00	128.32

Gap	ac Flux	Current (A)			Current harmonics (% of fundamental current)									Reactive power
(*um*)	(T)	dc	total	fund.	2nd	3rd	4th	5th	6th	7th	8th	9th	10th	(VAR)
250	0.9	0	0.9	0.9	0.00	0.02	0.00	0.08	0.00	0.01	0.00	0.01	0.00	63.85
250	0.95	0	0.95	0.95	0.00	0.02	0.00	0.09	0.00	0.01	0.00	0.01	0.00	71.17
450	0.9	0	1.62	1.62	0.00	0.01	0.00	0.04	0.00	0.01	0.00	0.01	0.00	114.47
450	0.95	0	1.71	1.71	0.00	0.01	0.00	0.05	0.00	0.01	0.00	0.01	0.00	127.58

Table 3. 11 Harmonic current contents of current waveform for three-phase gapped reactors in the neutrals.

Gap	ac Flux	Current (A)			Current harmonics (% of fundamental current)								
(*um*)	(T)	dc	total	fund.	2nd	3rd	4th	5th	6th	7th	8th	9th	10th
250	0.9	0	0.01	0.01	0	11.8	0	8.6	0	1.6	0	7	0
250	0.95	-0	0.01	0.01	0	11.8	0	8.6	0	1.6	0	7	0
450	0.9	0	0.01	0.01	0	9.65	0	9.83	0	1.23	0	6.7	0
450	0.95	0	0.01	0.01	0	9.65	0	9.83	0	1.23	0	6.7	0

The results are plotted in Figure 3. 16.

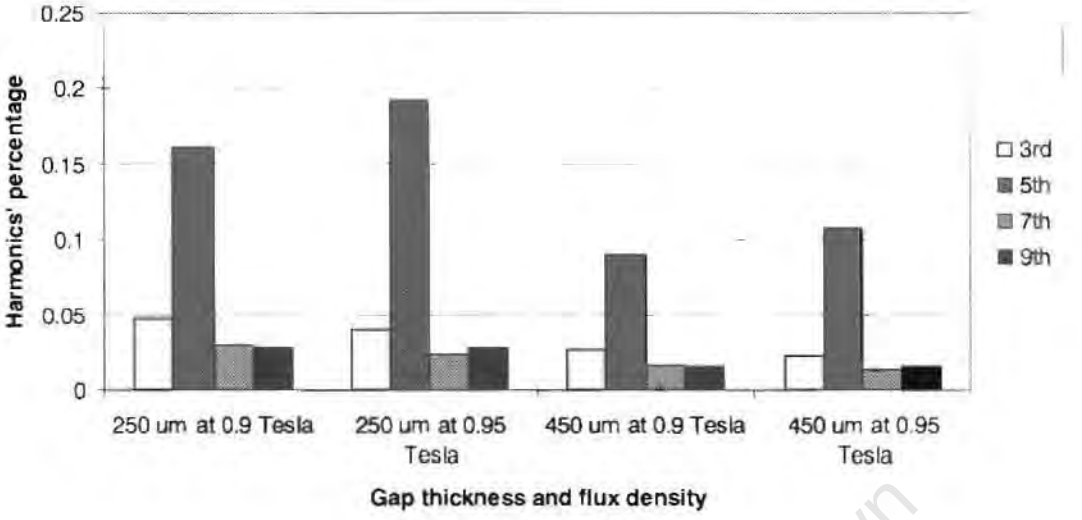

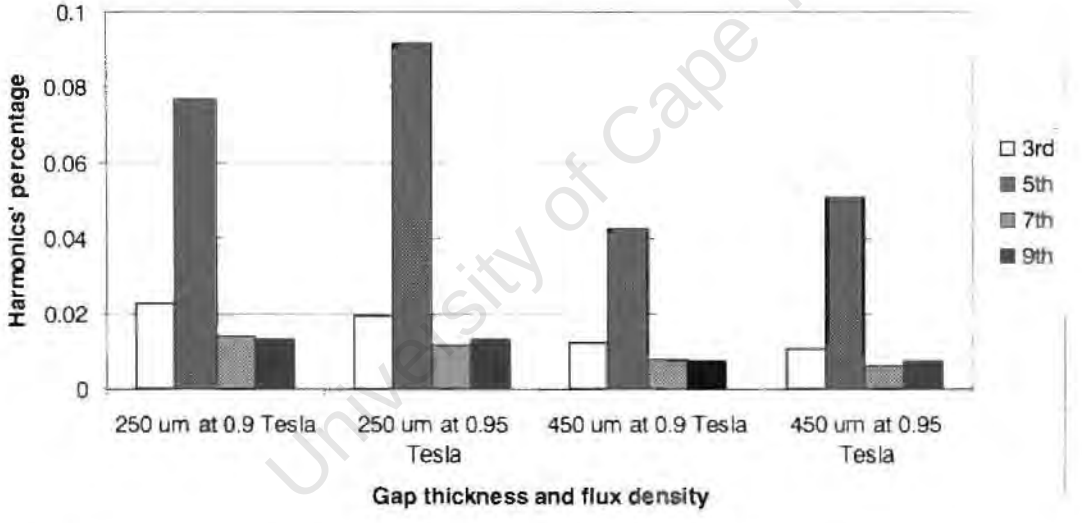

Figure 3. 16 Harmonic current contents of current waveform for three-phase gapped reactors.

a. **Red and blue phases (outer limb phases)**
b. **White phase (middle limb phase)**
c. **Neutral**

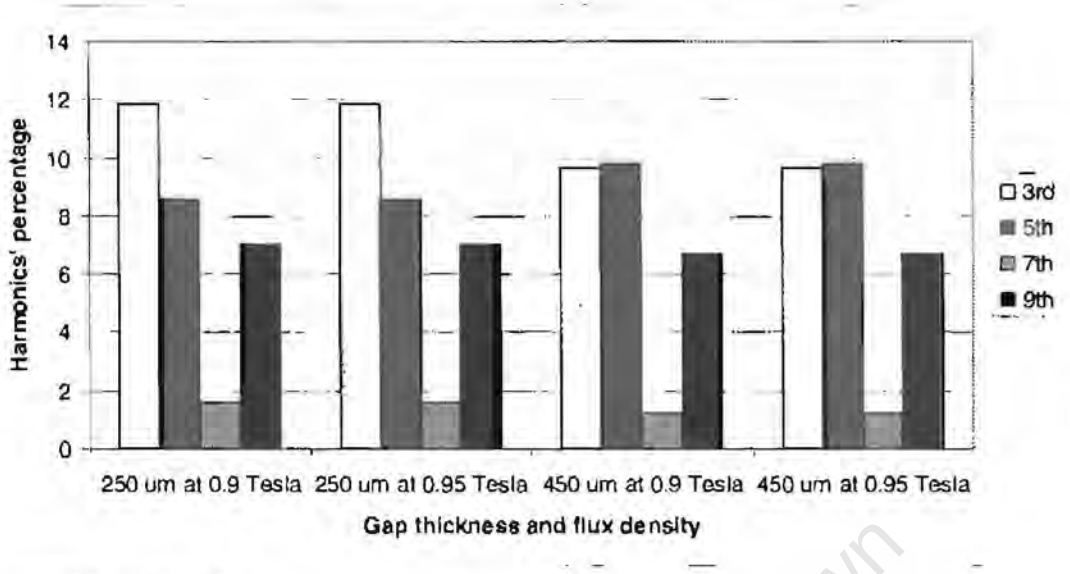

Figure 3.16 (continued)

Harmonic currents are well within compatibility levels for all three-phase reactor situations. While 250 micrometre-gapped reactors are not of the same magnitude as 450 micrometre gapped reactors, the two usually follow a similar pattern. Fifth harmonic present is usually higher followed by third, then ninth predominantly and lastly seventh in the phases. This pattern is only true with 450 micrometre-gapped reactors as third and fifth harmonics swap places with 250 micrometre-gapped reactors.

3.6 SUMMARY

Two types of reactors were used in the modelling: three matched single-phase unit reactors and a three-phase unit reactor. For both types, mathematical relationships between various quantities such as excitation current, flux density, physical dimensions, permeability and reactive power were defined in a magnetic circuit set-up for air-gapped and non-gapped reactor units. Excitation currents were Fourier-transformed for various harmonic contents.

Next, two constant ac flux density values close to saturation were chosen to excite gapped and non-gapped reactors. Varying dc flux density at a constant rate was injected into the model. The dc flux density was distorting the resulting excitation currents for single-phase units while the dc flux density contributions from the three-phases were

cancelling out for three-phase units leaving their resulting excitation currents and reactive power in all phases unchanged. The resulting excitation currents and reactive power were analysed for both single-phase and three-phase units.

Analysis of resulting excitation currents revealed that without dc flux density injection, modelling indicated very low harmonic contents. As injected dc flux density increased, single-phase units began to consist of both even and odd harmonics, which may have exceeded recommended compatibility levels for harmonics. The harmonics were decreasing in magnitudes as the harmonic number increased for a particular dc current. Non-gapped single-phase units harmonic content was higher than gapped units.

Reactive power increased exponentially as dc flux injection increased. The rate of increase in reactive power was higher for non-gapped single-phase units than gapped units

The mathematical modelling gives a basis to carry out laboratory tests.

CHAPTER 4

LABORATORY TESTING

This chapter shall cover laboratory tests on reactors modelled mathematically in the previous Chapter. The laboratory test and mathematical modelling results of these same reactors would ideally be similar, which would indicate the completeness of the model.

4.1 TEST PROTOCOL

In the mathematical modelling, two constant ac flux density values of 0.9 and 0.95 Teslas were independently chosen for modelling and independently applied across gapped and non-gapped reactors that were expected to saturate at 1 Tesla. Eight dc flux values varying from zero in steps of 0.1 Teslas to the uppermost possible flux density (0.7 Teslas) from the manufacturer's flux density curve were separately added on ac flux densities. Reactive power was increasing and excitation current waveforms were getting more distorted (hence consisting both even and odd harmonics) as varying dc flux density increased. At a particular dc flux density, the degree of distortion was inversely proportional to the size of the gap thickness. The overall trend of harmonics was decreasing with increasing order for a particular dc flux and gap size.

In the laboratory, testing would be done on three-phase reactors comprised of single-phase units and three-phase units thereafter, both with and without gaps in them in order to test mathematical modelling results under equivalent conditions and constraints. Modelling ac flux density values of 0.9 and 0.95 Teslas would be converted to laboratory equivalents of 70.7 and 74.6 Volts respectively. One at a time, these voltages would be injected across the reactors and kept constant while varying eight dc current values injected in the phases as determined from the modelling. Maximum dc currents were the

most extreme values that could be determined from the modelling for a particular gap situation. Temperature, current, current harmonics and reactive power in each phase would be recorded.

4.2 EXPERIMENT EQUIPMENT

In order to carry out the tests described in the previous section, a specific circuit whose objective is to test the authenticity of the mathematical results was built. Minimum input dc current determined from the mathematical modelling were 20mA per phase but the availability of variable resistors in the laboratory could only allow a minimum current of 110mA per phase.

The circuit consisted of the following equipment [36].

- Ac generator supply to feed the circuit since its voltage contains lesser harmonics than Municipal mains supply
- Three-phase variac to vary ac voltage
- Three matched reactors (single-phase units and a three-phase unit) whose basic structure is shown in Figure 4. 1.
- 10 V dc battery to act as a dc source in the neutral
- Variable resistors to vary dc current in the circuit
- AC and DC ammeters to measure dc and total current
- Power fluke to measure applied line voltage, current harmonics and reactive power across phases and neutral
- Thermocouple sensor to measure temperature of reactor units

The variac supply was tested for a possibility of introducing harmonics into the circuit by injecting the constant voltages (70.7 and 74.6 Volts) and varying dc current from 0 to 5 Amps by replacing the reactors with three balanced variable resistors. Each phase and the neutral were measured for harmonic currents as dc current increased and no change in harmonic content was observed.

A circuit diagram and a photograph of the equipment are shown in Figure 4. 2 and Figure 4. 3 respectively.

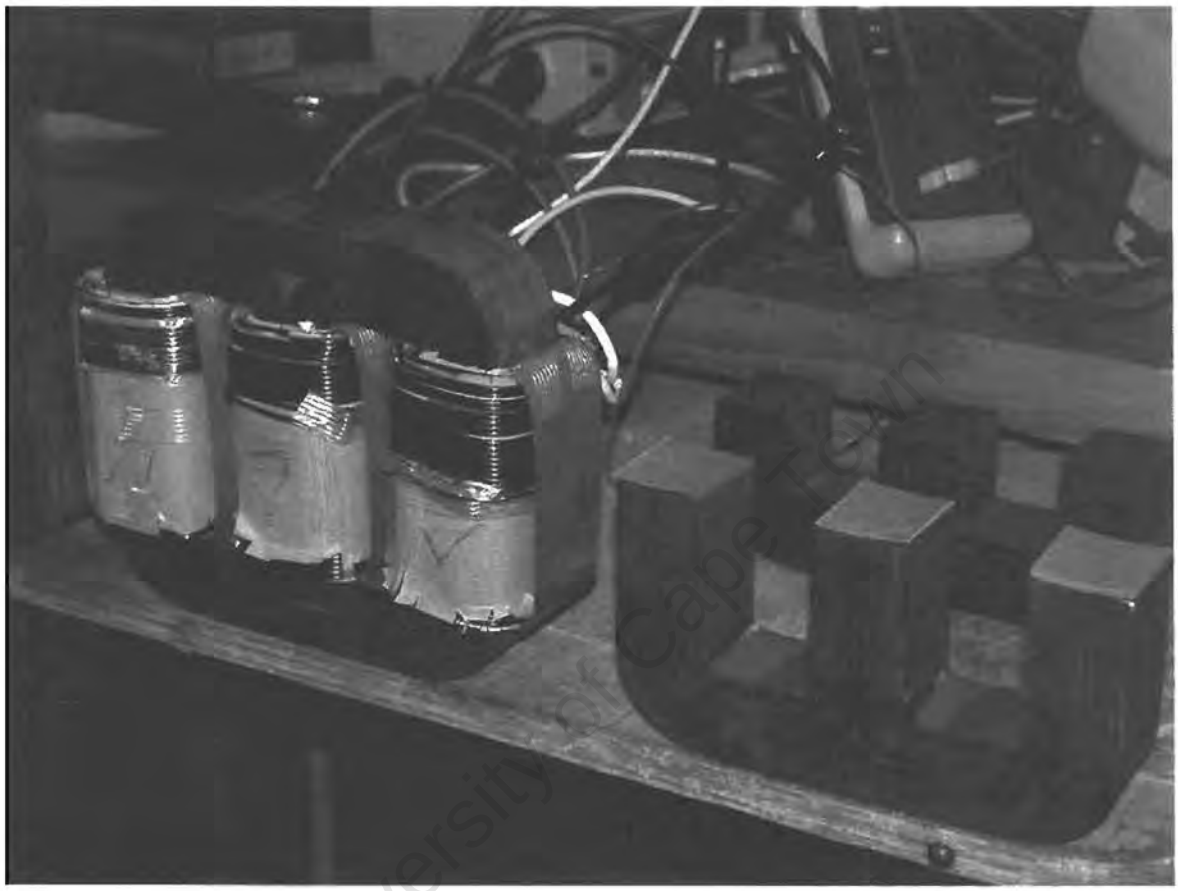

Figure 4. 1 Two magnetic E-cores on the right that make up the basic magnetic core structure of a reactor

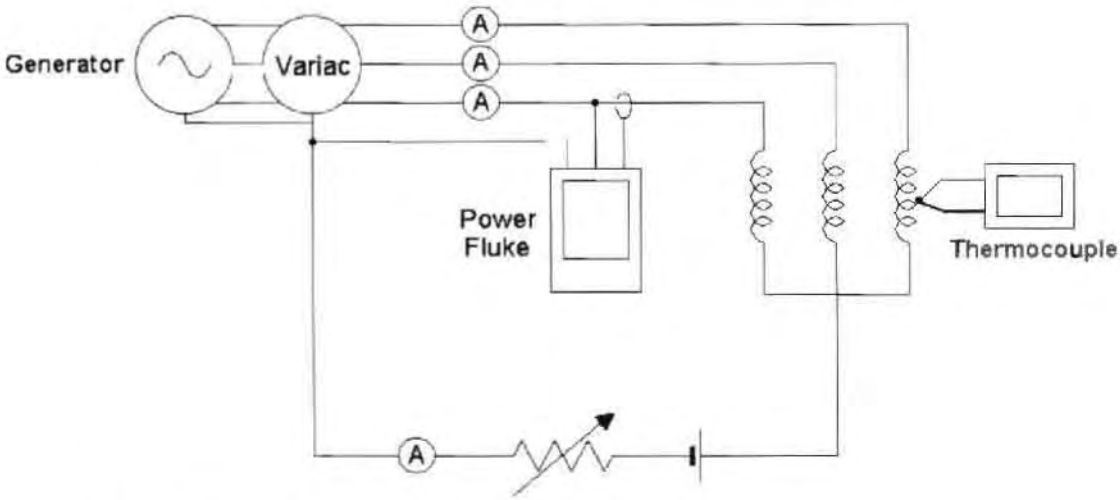

Figure 4. 2 Basic laboratory test circuit [36]

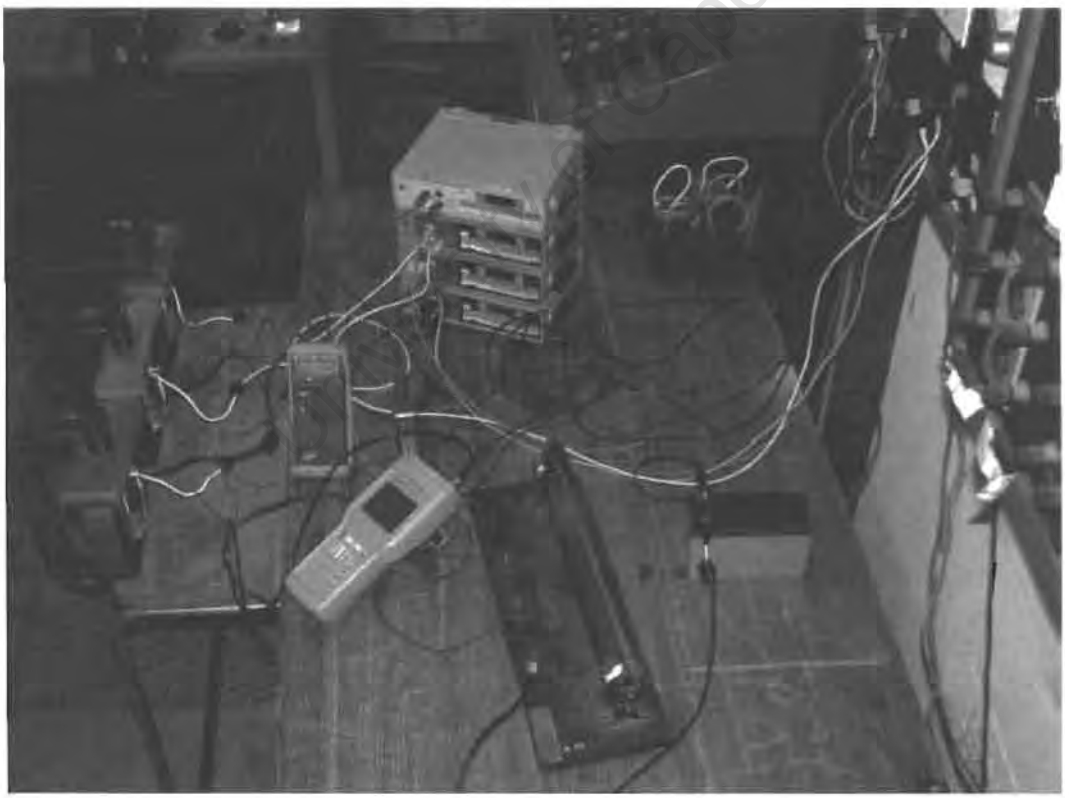

Figure 4. 3 Photograph of the laboratory test circuit

4.3 CONVERSION OF MAGNETIC QUANTITIES

Input variables in the previous Chapter were flux density. Yet in the laboratory, there is only equipment that could measure voltages and currents. Flux density is analogous to voltage and the two are related by:

$$V = 2 \cdot \pi \cdot N \cdot f \cdot B \cdot A \qquad (4.1)$$

where N is 200 turns, f is 50 Hertz, B is flux density and A, the core cross sectional area is 12.5 cm^2. Inserting flux density values of 0.9 Tesla and 0.95 Tesla would lead to line to neutral voltages of 70.7 Volts and 74.6 Volts respectively.

4.4 DETERMINATION OF LABORATORY GAP THICKNESSES

In the modelling, it had been assumed that two E-cores make up uniform gaps. It had also been assumed that the two E-cores align onto each other perfectly. Practically, non-uniform gaps would always exist, three gaps would have slightly different lengths and alignment would be imperfect, which could result in leakage flux.

Figure 4. 4 Alignment and meeting of two cores

Compensation efforts were made to incorporate such effects into the gap thickness. In the modelling, excitation current is related to flux density and gap thickness for the single-phase units by equation (3.2) and the three-phase unit by equations (3.12) to (3.14).

A range of ac voltages was generated from 15.7 Volts (0.2 Teslas) to 74.5 Volts (0.95 Teslas) in steps of 7.9 Volts (0.1 Teslas) and current through each phases were recorded. Knowing measured currents, modelled currents were then determined by making gap thickness an independence variable using best fit method as applied by Cullimore [9] such that $\sum (I_{modelled} - I_{measured})^2$ is minimized at all points of comparison. Since resultant modelled currents are not pure sinusoidal, rms current values was treated as comprised of discrete values and hence they were found by:

$$I = \sqrt{\frac{1}{N} \sum_{i=0}^{t=t+167us} i^2(t)} \qquad (4.2)$$

where N is 120. Table 4. 1 shows resultant closest matching gap thickness.

Table 4. 1 Modelled currents versus measured currents over a range of 15.7 Volts to 74.6 reactors.

a. **Non-gapped single-phase reactor**
b. **250 micrometre gapped single-phase reactor**
c. **450 micrometre gapped single-phase reactor**
d. **250 micrometre gapped three-phase reactor**
e. **450 micrometre gapped three-phase reactor**

Voltage	ac Flux	Measured currents (A)				Modelled currents (A)			
(V)	(T)	Red	White	Blue	Neutral	Red	White	Blue	Neutral
15.7	0.2	0.02	0.02	0.02	0	0.0328	0.0351	0.029	0.0053
23.6	0.3	0.03	0.04	0.03	0	0.0486	0.052	0.0429	0.0081
31.4	0.4	0.04	0.05	0.04	0	0.0639	0.0685	0.0563	0.0108
39.3	0.5	0.06	0.06	0.06	0.01	0.079	0.0847	0.0695	0.0136
47.1	0.6	0.08	0.08	0.07	0.02	0.0937	0.1005	0.0823	0.0165
55.0	0.7	0.1	0.11	0.09	0.03	0.1083	0.1163	0.095	0.0192
62.8	0.8	0.12	0.13	0.11	0.05	0.123	0.1321	0.1077	0.0219
70.7	0.9	0.15	0.16	0.13	0.06	0.138	0.1482	0.1209	0.0244
74.6	0.95	0.17	0.18	0.14	0.08	0.1458	0.1566	0.1277	0.0255
Squared error sum of measured and modelled currents						0.0026	0.0026	0.0011	
Equivalent gap thickness (*micrometres)*						22.3	24.2	19.1	

Voltage	ac Flux	Measured currents (A)				Modelled currents (A)			
(V)	(T)	Red	White	Blue	Neutral	Red	White	Blue	Neutral
15.7	0.2	0.3	0.29	0.29	0.01	0.3197	0.3116	0.3125	0.0077
23.6	0.3	0.47	0.45	0.45	0.01	0.4788	0.4667	0.4681	0.0116
31.4	0.4	0.62	0.61	0.61	0.02	0.6376	0.6214	0.6233	0.0155
39.3	0.5	0.78	0.77	0.76	0.02	0.7961	0.7758	0.7782	0.0194
47.1	0.6	0.94	0.92	0.92	0.03	0.9542	0.9299	0.9327	0.0234
55.0	0.7	1.11	1.08	1.08	0.03	1.1123	1.0839	1.0872	0.0273
62.8	0.8	1.27	1.24	1.24	0.04	1.2703	1.2379	1.2417	0.0311
70.7	0.9	1.44	1.4	1.41	0.04	1.4288	1.3923	1.3966	0.0348
74.6	0.95	1.52	1.48	1.49	0.04	1.5083	1.4697	1.4743	0.0367
Squared error sum of measured and modelled currents						0.0016	0.0012	0.0022	
Equivalent gap thickness (*micrometres)*						262.6	255.8	256.6	

Table 4.1 (continued)

Voltage	ac Flux	Measured currents (A)				Modelled currents (A)			
(V)	(T)	Red	White	Blue	Neutral	Red	White	Blue	Neutral
15.7	0.2	0.54	0.53	0.53	0.02	0.5546	0.551	0.5487	0.0051
23.6	0.3	0.82	0.81	0.79	0.03	0.8312	0.8258	0.8224	0.0078
31.4	0.4	1.08	1.08	1.07	0.04	1.1074	1.1003	1.0957	0.0104
39.3	0.5	1.37	1.36	1.35	0.05	1.3834	1.3744	1.3687	0.0131
47.1	0.6	1.66	1.64	1.63	0.06	1.659	1.6482	1.6414	0.0158
55.0	0.7	1.92	1.93	1.92	0.08	1.9345	1.9219	1.914	0.0185
62.8	0.8	2.2	2.2	2.19	0.09	2.21	2.1957	2.1866	0.021
70.7	0.9	2.5	2.48	2.47	0.1	2.4859	2.4698	2.4596	0.0234
74.6	0.95	2.64	2.61	2.61	0.1	2.6241	2.6071	2.5963	0.0245
Squared error sum of measured and modelled currents						0.0022	0.0017	0.003	
Equivalent gap thickness (*micrometres*)						459.4	456.4	454.5	

Voltage	ac Flux	Measured currents (A)				Modelled currents (A)			
(V)	(T)	Red	White	Blue	Neutral	Red	White	Blue	Neutral
15.7	0.2	0.2	0.19	0.26	0.06	0.2225	0.2235	0.265	0.0421
23.6	0.3	0.31	0.31	0.38	0.07	0.3327	0.3348	0.3965	0.0629
31.4	0.4	0.43	0.43	0.53	0.11	0.4422	0.4457	0.5273	0.0835
39.3	0.5	0.53	0.54	0.65	0.13	0.5515	0.5566	0.658	0.1041
47.1	0.6	0.65	0.66	0.77	0.15	0.6608	0.6674	0.7885	0.1246
55.0	0.7	0.76	0.77	0.91	0.16	0.7702	0.7783	0.9192	0.1452
62.8	0.8	0.88	0.89	1.04	0.19	0.8798	0.8893	1.0501	0.1658
70.7	0.9	1	1.01	1.19	0.21	0.9903	1.0007	1.1819	0.1866
74.6	0.95	1.07	1.08	1.27	0.22	1.0462	1.0567	1.2484	0.1972
Squared error sum of measured and modelled currents						0.0026	0.0031	0.0015	
Equivalent gap thickness (*micrometres*)						271.8	277.2	325.3	

Voltage	ac Flux	Measured currents (A)				Modelled currents (A)			
(V)	(T)	Red	White	Blue	Neutral	Red	White	Blue	Neutral
15.7	0.2	0.38	0.38	0.42	0.03	0.3979	0.3972	0.4379	0.0403
23.6	0.3	0.58	0.58	0.63	0.05	0.5959	0.5953	0.6558	0.0602
31.4	0.4	0.77	0.78	0.85	0.1	0.7931	0.7931	0.873	0.0799
39.3	0.5	0.96	0.97	1.06	0.13	0.9902	0.9909	1.0901	0.0996
47.1	0.6	1.17	1.17	1.29	0.16	1.1872	1.1886	1.3071	0.1192
55.0	0.7	1.37	1.37	1.51	0.18	1.3843	1.3863	1.5242	0.1389
62.8	0.8	1.58	1.58	1.74	0.2	1.5817	1.5841	1.7415	0.1586
70.7	0.9	1.8	1.8	1.98	0.23	1.78	1.7824	1.9597	0.1786
74.6	0.95	1.9	1.9	2.09	0.23	1.8797	1.8818	2.0694	0.1887
Squared error sum of measured and modelled currents						0.0037	0.0027	0.0042	
Equivalent gap thickness (*micrometres*)						492.3	495.5	542.5	

4.5 CURRENT HARMONICS, REACTIVE POWER AND TEMPERATURE MEASUREMENTS

Ac voltages of 70.7 Volts and 74.6 Volts for the two separate sets on measurements were injected in the laboratory circuit. An adjusted equivalent gap thickness for a set-up concerned was fed into the model in the previous Chapter and as a result, dc current values were determined. The modelled dc currents were now fed into the neutral of the circuit by varying the variable resistor therefore making both modelled and measured currents the same. Respective current harmonics and reactive power were recorded by a power fluke and temperature was measured by a thermocouple sensor. 74.6 Volts' set of measurements can be found in the next subsections. 70.7 Volts' measurements can be found in Appendix C.

4.5.1 NON-GAPPED SINGLE-PHASE UNITS' MEASUREMENTS

A full range of dc currents could not be tested on non-gapped single-phase units due to the limited available minimum dc currents as mentioned earlier. Results are shown in Table 4. 2.

Table 4. 2 Measured current harmonic contents and reactive power for single-phase non-gapped units at 74.6 Volts.

a. **Red phase**
b. **White phase**
c. **Blue phase**

ac Flux	ac V	Current (A)			Current harmonics (% of fundamental current)									Reactive power
(T)	(V)	dc	total	fund.	2nd	3rd	4th	5th	6th	7th	8th	9th	10th	(VAR)
0.95	74.6	0	0.16	0.23	6.9	13.2	7	2.9	5.8	1.9	4.6	2.3	3.4	15
0.95	74.6	0.33	0.47	0.48	57	41.4	22.3	14.2	8.2	4.5	3.9	3.5	2.7	34
0.95	74.6	0.66	1	0.91	68.2	49.9	32.3	18.7	9.6	4.7	3.6	3.1	2.1	65

ac Flux	ac V	Current (A)			Current harmonics (% of fundamental current)									Reactive power
(T)	(V)	dc	total	1st	2nd	3rd	4th	5th	6^{th}	7th	8th	9th	10th	(VAR)
0.95	74.6	0	0.17	0.23	6.5	12.2	6.4	3.3	5.9	1.2	4.1	2	3.7	15
0.95	74.6	0.31	0.43	0.44	53.5	34.5	17.7	11.7	7	5.1	5.2	3.6	2.2	30
0.95	74.6	0.63	0.92	0.83	68.2	43.8	31.9	19.4	8.9	5.1	3.4	2	2.4	62

Table 4.2 (continued)

ac Flux	ac V	Current (A)			Current harmonics (% of fundamental current)									Reactive power
(T)	(V)	dc	total	1st	2nd	3rd	4th	5th	6^{th}	7th	8th	9th	10th	(VAR)
0.95	74.6	0	0.14	0.2	9.1	10	9.2	3.9	6.5	0.9	5.8	2.1	4.1	14
0.95	74.6	0.32	0.45	0.45	62.6	47.2	30	20.8	12	6.7	4.3	3.7	3.8	35
0.95	74.6	0.66	0.99	0.88	72.9	53.4	38.8	25.6	13	7.1	4.7	3.8	3.2	64

Dc currents varied from 0 to an average of 650 mA (per phase). The maximum value makes up 487 % compared to an average initial fundamental current of 130 mA. As shown in the tables, such an increase in dc currents resulted in total current, fundamental current, harmonics and reactive power changing as further graphically illustrated in Figure 4. 5 and Figure 4. 6 respectively.

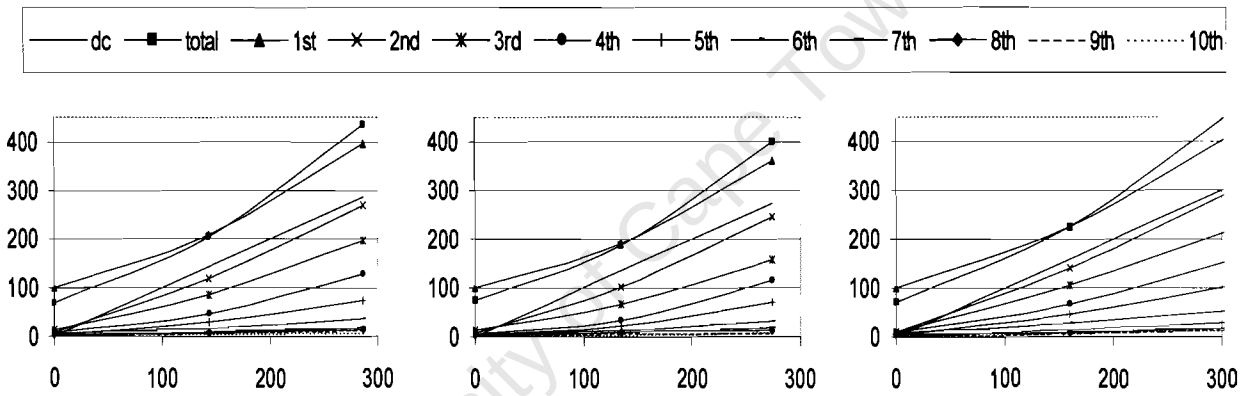

a) Red phase b) White phase c) Blue phase

Figure 4. 5 Measured current harmonics versus dc current both taken as a percentage of fundamental current (both at 0 dc current offset) for single-phase non-gapped units in the phases at 74.6 Volts.

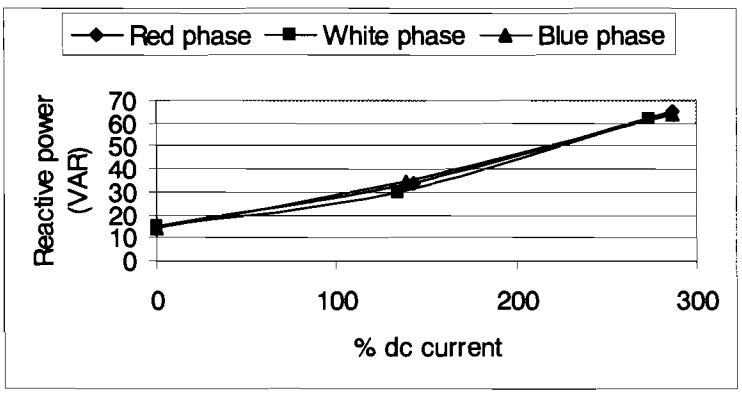

Figure 4. 6 Measured reactive power versus dc current as a percentage of fundamental current (at 0 dc current offset) for single-phase non-gapped units at 74.6 Volts.

In Figure 4. 5, there is a notable high harmonic percentage in the phases without the injection of dc currents. The main reason for this is because the power fluke's accuracy greatly deteriorates below values of 2 Amps and there was no better equipment available [16]. However as, dc current was injected, the overall trend for harmonic percentage decreased with increasing order for a particular injected dc current. None of the harmonics displayed were within the compatibility levels for harmonics in Table 2.1.

Figure 4. 6 shows how reactive power consumption increased above linearity as the injected dc current increased.

Table 4. 3 Measured current harmonic contents for single-phase non-gapped reactors in the neutral at 74.6 Volts.

Ac Flux	dc Flux	Current (A)			Current harmonics (% of fundamental current)								
(T)	(T)	dc	total	1st	2nd	3rd	4th	5th	6th	7th	8th	9th	10th
0.95	0	0	0.07	0.04	30	300	30	1	70	20	30	5	0
0.95	0.6	0.96	0.55	0.05	90	∞	80	80	360	20	30	50	10
0.95	0.65	1.69	1.39	0.08	90	∞	70	80	390	10	30	100	10

Results are graphically illustrated in Figure 4. 7.

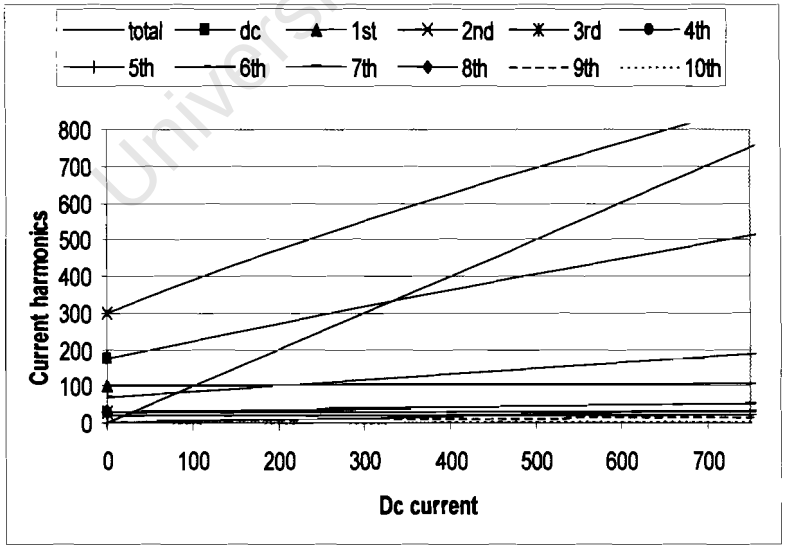

Figure 4. 7 Measured current harmonics versus dc current both taken as a percentage of fundamental current (both at 0 dc current offset) for single-phase non-gapped units in the neutral at 74.6 Volts.

As dc current increased, there was a notable increase total and fundamental currents and in the third, sixth and ninth harmonic contents in the neutral with the third being the highest, the sixth being the middle and the ninth being the lowest. The rest of the harmonics seemed to remain somewhat randomly distributed.

Table 4. 4 Measured temperature versus dc Flux for non-gapped units at an ambient temperature of 19.1 ^{0}C.

Dc Flux (T)	Temperature (°C)	Change in temperature (°C)
0	20.2	
0.6	21.4	1.2
0.65	22.4	1

Change in temperature between consecutive dc fluxes remained pretty much constant

4.5.2 GAPPED SINGLE-PHASE UNITS MEASUREMENTS

A full range of dc currents could be tested on both thin-gapped and thick-gapped single-phase units as modelled. The thin-gapped and thick-gapped reactors are made of gap thickness in Table 4. 1(b) and (c) respectively.

Table 4. 5 Measured current harmonic contents and reactive power for single-phase thin-gapped units at 74.6 Volts.

a. **Red phase**
b. **White phase**
c. **Blue phase**

Ac Flux	ac V	Current (A)			Current harmonics (% of fundamental current)									Reactive power
(T)	(V)	dc	total	1st	2nd	3rd	4th	5th	6th	7th	8th	9th	10th	(VAR)
0.95	74.6	0	1.51	1.51	0.1	2.1	0.2	0.8	0	0.4	0.1	0.4	0.1	110
0.95	74.6	0.17	1.5	1.51	0.5	2.1	0.1	0.9	0.2	0.4	0.1	0.5	0.2	111
0.95	74.6	0.32	1.5	1.51	0.9	1.8	0.1	1	0.2	0.4	0.2	0.6	0.2	111
0.95	74.6	0.51	1.52	1.53	1.7	1.6	0.3	1.1	0.3	0.4	0.2	0.7	0.1	112
0.95	74.6	0.64	1.53	1.54	2.6	1.1	0.5	1.3	0.5	0.2	0.2	0.7	0.1	113
0.95	74.6	0.86	1.59	1.59	4.7	1.4	1.7	2.1	1	0.3	0.4	0.6	0.3	117
0.95	74.6	1.27	1.78	1.82	14.9	8.5	8.1	6.3	4.2	2.1	1.2	0.7	0.7	133
0.95	74.6	1.55	2.06	2.13	25.8	17	14.4	10.6	10.6	4.2	2	1.1	1	156

Table 4.5 (continued)

Ac Flux	ac V	Current (A)			Current harmonics (% of fundamental current)									Reactive power
(T)	(V)	dc	total	1st	2nd	3rd	4th	5th	6th	7th	8th	9th	10th	(VAR)
0.95	74.6	0	1.48	1.45	0.2	2.8	0	0.7	0.1	0.8	0.2	0.6	0.2	108
0.95	74.6	0.15	1.48	1.44	0.6	2.5	0.2	0.7	0.3	0.7	0.2	0.6	0.7	108
0.95	74.6	0.31	1.48	1.46	0.8	2.8	0.4	0.7	0.3	0.6	0.2	0.5	0.4	109
0.95	74.6	0.45	1.49	1.48	1.2	3.1	0.4	0.9	0.6	0.5	0.2	0.5	0.3	109
0.95	74.6	0.6	1.49	1.48	1.5	2.6	0.2	0.8	0.5	0.6	0.2	0.5	0.1	109
0.95	74.6	0.83	1.51	1.49	3.1	1.7	0.7	1.4	1	0.2	0.2	0.6	0.3	111
0.95	74.6	1.03	1.56	1.59	5.9	1.8	3.2	3	2.5	0.9	0.5	1	0.7	119
0.95	74.6	1.5	1.91	1.98	21.5	15.4	13.7	10.7	8.6	4.9	2.6	1.7	1.4	148

Ac Flux	ac V	Current (A)			Current harmonics (% of fundamental current)									Reactive power
(T)	(V)	dc	total	1st	2nd	3rd	4th	5th	6th	7th	8th	9th	10th	(VAR)
0.95	74.6	0	1.48	1.43	0.1	1.8	0.2	0.8	0.1	0.9	0.1	0.5	0.1	107
0.95	74.6	0.17	1.47	1.42	0.8	1.7	0.2	0.8	0.2	1	0.2	0.5	0.1	108
0.95	74.6	0.31	1.47	1.46	1.3	1.8	0.3	1	0.3	0.8	0.2	0.5	0.1	107
0.95	74.6	0.45	1.48	1.46	2	1.9	0.3	1	0.4	0.8	0.3	0.5	0.2	109
0.95	74.6	0.68	1.5	1.46	3	1.9	0.4	1.2	0.7	0.7	0.3	0.6	0.3	111
0.95	74.6	0.81	1.51	1.52	4.4	0.6	0.9	1.6	1.1	0.6	0.3	0.5	0.3	111
0.95	74.6	1.22	1.76	1.75	17.7	9.9	8	6.9	5.1	2.3	0.8	0.7	0.8	130
0.95	74.6	1.34	1.92	1.95	23.6	15.2	11.6	9.1	6.5	3.1	1.2	0.8	0.8	147

Table 4. 6 Measured current harmonic contents and reactive power for single-phase thick-gapped units at 74.6 Volts.

a. **Red phase**
b. **White phase**
c. **Blue phase**

ac Flux	ac V	Current (A)			Current harmonics (% of fundamental current)									Reactive power
(T)	(V)	dc	total	1st	2nd	3rd	4th	5th	6th	7th	8th	9th	10th	(VAR)
0.95	74.6	0	2.64	2.66	0.1	1.9	0	0.5	0.1	0.3	0	0.2	0	195
0.95	74.6	0.27	2.64	2.71	0.2	1.9	0.1	0.5	0	0.3	0	0.3	0	197
0.95	74.6	0.56	2.64	2.72	0.6	1.8	0.2	0.5	0.2	0.3	0	0.2	0.1	199
0.95	74.6	0.73	2.66	2.71	1	2.2	0.3	0.5	0.2	0.3	0.1	0.3	0	199
0.95	74.6	1.18	2.68	2.72	1.8	1.7	0.6	0.6	0.4	0.3	0.1	0.2	0.1	201
0.95	74.6	1.46	2.72	2.68	2.8	0.8	1.2	1.2	0.7	0.2	0.2	0.2	0.1	202
0.95	74.6	1.87	2.89	2.88	8.7	3.4	4.7	3.5	2.4	1	0.7	0.4	0.3	214
0.95	74.6	2.23	3.07	3.08	13.8	7.4	5.9	5	2.9	1.6	1.1	0.7	0.8	230

Table 4.6 (continued)

ac Flux	ac V	Current (A)			Current harmonics (% of fundamental current)									Reactive power
(T)	(V)	dc	total	1st	2nd	3rd	4th	5th	6th	7th	8th	9th	10th	(VAR)
0.95	74.6	0	2.61	2.56	0.1	2.3	0	0.5	0.1	0.3	0	0.3	0	194
0.95	74.6	0.28	2.63	2.61	0.3	2.2	0.2	0.5	0.2	0.2	0	0.2	0	194
0.95	74.6	0.52	2.63	2.6	0.5	2.6	0.2	0.5	0.2	0.2	0	0.2	0.1	196
0.95	74.6	0.86	2.62	2.59	0.7	2.6	0.2	0.4	0.3	0.3	0	0.2	0	195
0.95	74.6	1.11	2.63	2.59	1	2.8	0.2	0.5	0.4	0.2	0	0.2	0	196
0.95	74.6	1.46	2.64	2.61	1.5	2.7	0.4	0.7	0.6	0.2	0.1	0.2	0	197
0.95	74.6	1.87	2.76	2.72	5.4	0.6	3.1	2.5	2.6	0.9	0.7	0.6	0.5	202
0.95	74.6	2.3	3.02	3.03	13.2	7.6	5.5	5.6	3.6	2	1.3	0.7	0.7	227

ac Flux	ac V	Current (A)			Current harmonics (% of fundamental current)									Reactive power
(T)	(V)	dc	total	1st	2nd	3rd	4th	5th	6th	7th	8th	9th	10th	(VAR)
0.95	74.6	0	2.6	2.55	0.1	1.8	0	0.5	0.1	0.3	0	0.3	0	193
0.95	74.6	0.28	2.61	2.57	0.5	1.7	0.2	0.6	0.2	0.4	0.1	0.2	0.1	195
0.95	74.6	0.54	2.61	2.58	0.7	2	0.2	0.6	0.2	0.5	0.1	0.2	0.1	195
0.95	74.6	0.8	2.61	2.56	1.1	2.2	0.3	0.8	0.3	0.4	0.1	0.2	0.1	196
0.95	74.6	1.04	2.62	2.57	1.7	2	0.3	0.8	0.4	0.4	0.1	0.3	0.1	197
0.95	74.6	1.37	2.68	2.63	3.4	0.9	1	1.3	0.8	0.3	0.2	0.3	0.1	199
0.95	74.6	1.79	2.81	2.77	7.9	2.4	3.4	3	2.2	0.8	0.5	0.4	0.2	209
0.95	74.6	2.07	3.02	3.03	13.2	6.9	5.7	4.9	2.8	1.5	1.2	0.7	0.7	228

Dc currents varied from 0 to an average of 1.46 A and 2.2 A (per phase) in thin-gapped and thick-gapped units respectively. The maximum values make up 99 and 85 percents respectively compared to respective average initial fundamental currents of 1.47 A and 2.6 A. As shown in the tables, such an increase in dc currents resulted in total currents, fundamental currents, harmonics and reactive powers changing as further graphically illustrated in Figure 4. 8 to Figure 4. 10.

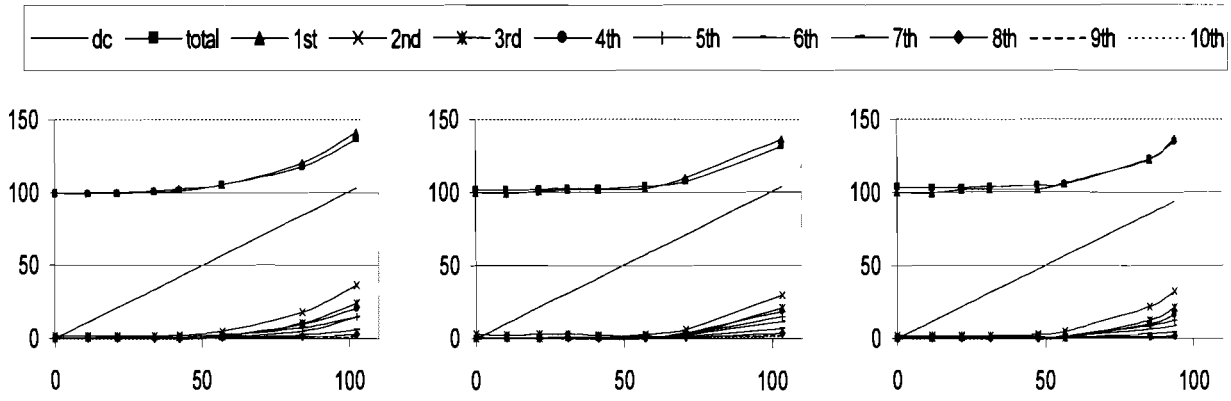

a) Red phase b) White phase c) Blue phase

Figure 4. 8 Measured current harmonics versus dc current both taken as a percentage of fundamental current (0 dc current offset) for single-phase thin-gapped units in the phases at 74.6 Volts.

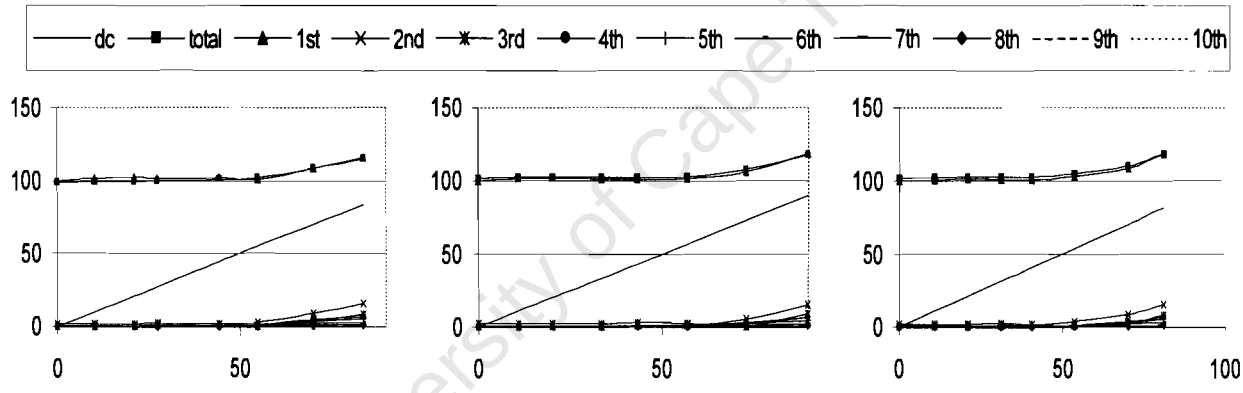

a) Red phase b) White phase c) Blue phase

Figure 4. 9 Measured current harmonics versus dc current both taken as a percentage of fundamental current 0 dc current offset) for single-phase thick-gapped units in the phases at 74.6 Volts.

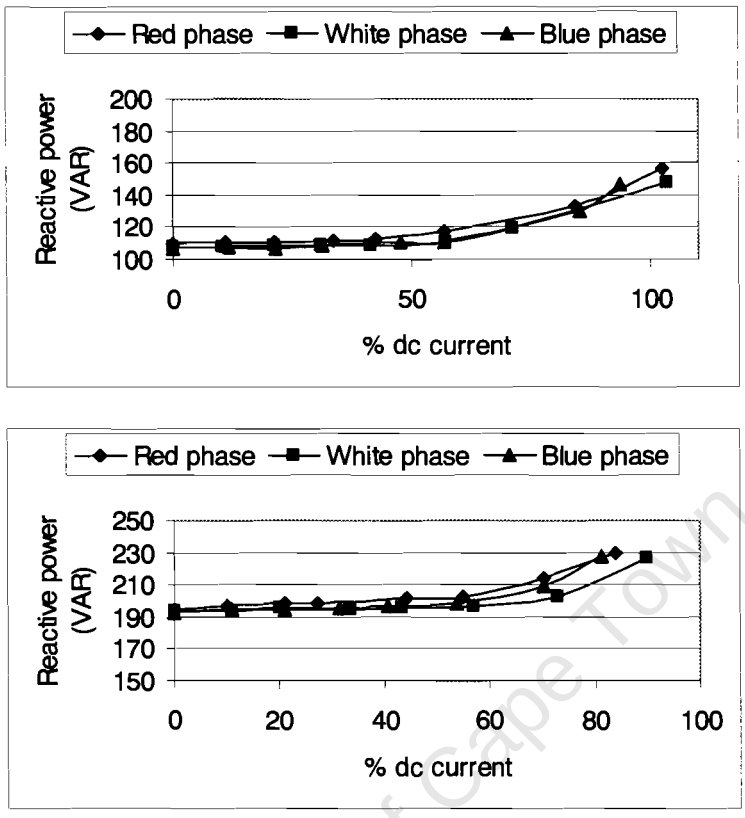

Figure 4. 10 Measured reactive power versus dc current as a percentage of fundamental current (at 0 dc current offset) for single-phase units at 74.6 Volts.

a. Thin-gapped
b. Thick-gapped

Harmonic currents are well within compatibility levels in Table 2.1 without the injection of dc flux. As dc flux increases, they stay within the range for more than half of the time. Harmonics began to increase exponentially over the last half at a decreasing rate as the harmonic number increased for a particular dc current. Both total and fundamental currents increased remarkably at least the last two values. Rates of increase for both harmonic contents and total and fundamental currents tended to be higher for thin-gapped units than for thick-gapped units.

Figure 4. 10 shows how reactive power consumption initially remained constant as the injected dc current increased only to increase above linearity more or less over the last third of the range.

Table 4. 7 Measured current harmonic contents for single-phase reactors in the neutral at 74.6 Volts.

a. Thin-gapped

b. Thick-gapped

ac Flux	dc Flux	Current (A)			Current harmonics (% of fundamental current)								
(T)	(T)	dc	total	1st	2nd	3rd	4^{th}	5th	6th	7th	8th	9th	10th
0.95	0	0	0.03	0.16	10	33	9	8	8	2	7	2	5
0.95	0.1	0.47	0.02	0.16	14	23	11	1	8	1	10	5	3
0.95	0.2	0.94	0.03	0.15	11	33	9	9	8	4	7	3	6
0.95	0.3	1.41	0.03	0.16	37	69	19	22	46	27	22	21	4
0.95	0.4	1.9	0.05	0.16	26	13	5	4	17	6	5	7	1
0.95	0.5	2.5	0.08	0.16	49	38	16	11	28	9	5	3	4
0.95	0.6	3.5	0.5	0.26	80	178	46	33	72	11	4	5	3
0.95	0.65	4.44	1.14	0.18	70	628	49	24	25	32	6	42	12

ac Flux	dc Flux	Current (A)			Current harmonics (% of fundamental current)								
(T)	(T)	dc	total	1st	2nd	3rd	4^{th}	5th	6th	7th	8th	9th	10th
0.95	0	0	0.1	0.14	13	106	19	6	6	10	8	5	6
0.95	0.1	0.82	0.07	0.14	9	87	17	7	8	11	10	8	6
0.95	0.2	1.65	0.1	0.13	13	113	13	12	2	13	6	10	8
0.95	0.3	2.47	0.11	0.14	7	109	9	7	7	15	9	8	5
0.95	0.4	3.32	0.09	0.19	14	628	2	9	13	4	5	2	4
0.95	0.5	4.27	0.1	0.16	37	45	6	21	45	10	2	5	7
0.95	0.6	5.63	0.3	0.18	57	170	31	17	114	5	8	15	5
0.95	0.65	6.75	0.51	0.17	34	800	29	18	277	20	17	40	3

Results are graphically illustrated in Figure 4. 11.

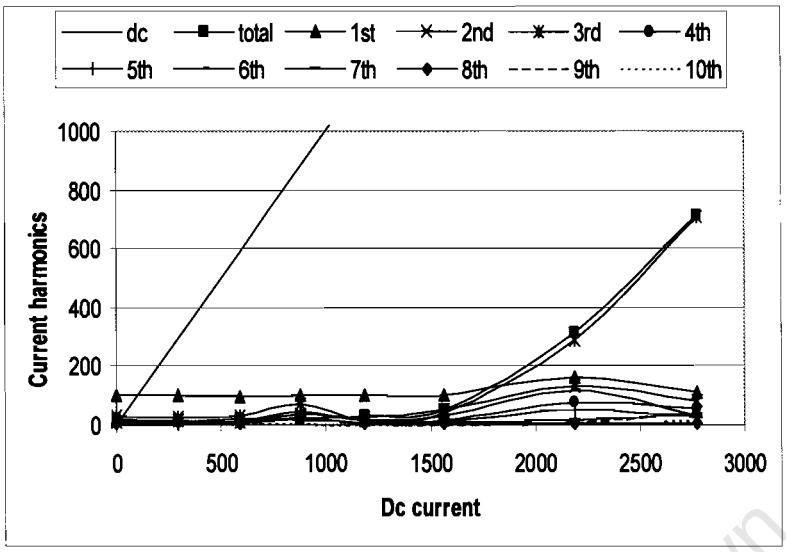

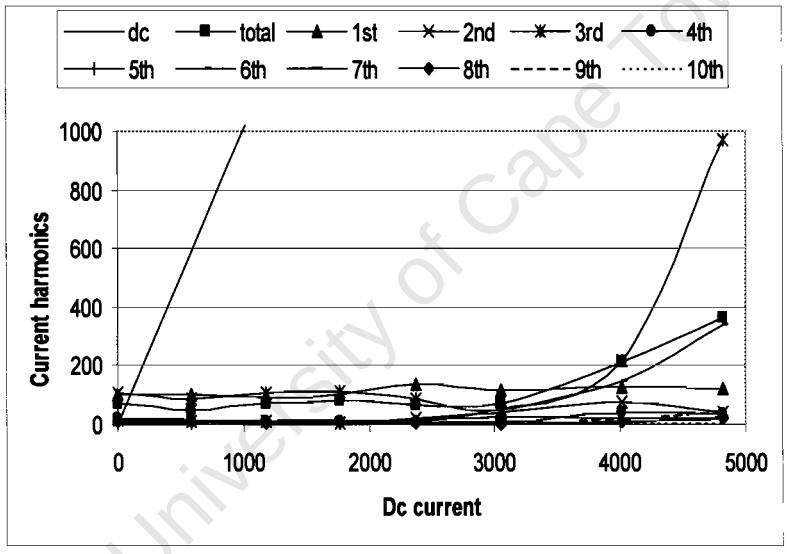

Figure 4. 11 Measured current harmonics versus dc current both taken as a percentage of fundamental current (0 dc current offset) for single-phase units in the neutral at 74.6 Volts.

a. Thin-gapped

b. Thick-gapped

As injected dc current increased, there was a notable increase in the third and sixth harmonics content in the neutral with the third being highest and sixth being lowest. The rest of the harmonics seemed to remain somewhat randomly distributed. Injected dc current was relatively higher than all the harmonics as depict Figure 4. 11.

Table 4. 8 Measured temperature versus dc Flux at an ambient temperature of 19.9 ^{0}C.

a. **Thin-gapped**
b. **Thick-gapped**

dc Flux (T)	Temperature (°C)	Change in temperature (°C)
0	23.6	
0.1	25	1.4
0.2	21.1	-3.9
0.3	24.2	3.1
0.4	25.7	1.5
0.5	27.8	2.1
0.6	23.8	-4
0.65	27.2	3.4

dc Flux (T)	Temperature (°C)	Change in temperature (°C)
0	26.9	
0.1	28.5	1.6
0.2	30.4	1.9
0.3	31.1	0.7
0.4	25.2	-5.9
0.5	27.5	2.3
0.6	27.1	-0.4
0.65	29.7	2.6

There were breaks during gapped reactor measurement periods as the shared generator supply was being for other purposes. Therefore breaks meant that reactors could cool down and hence negative temperature change. Change in temperature between consecutive dc fluxes remained more or less constant otherwise.

4.5.3 THREE-PHASE UNITS' MEASUREMENTS

Dc current values injected for these units were taken as if there was no dc flux cancelling effect. Modelled values without the cancelling effect can be found in Appendix C. Again a range of dc currents was tested on both thin-gapped and thick-gapped units. Adjusted gap thickness can be found in Table 4. 1 (d) and (e) respectively.

Table 4. 9 Measured current harmonic contents and reactive power for three-phase thin-gapped reactors at 74.6 Volts.

a. **Red phase**
b. **White phase**
c. **Blue phase**

ac Flux	ac V	Current (A)			Current harmonics (% of fundamental current)									Reactive Power
(T)	(V)	dc	total	1st	2nd	3rd	4^{th}	5th	6th	7th	8th	9th	10th	(VAR)
0.95	74.6	0	1.09	1.08	0.3	1.7	0.3	1.7	0.2	0.4	0.2	0.5	0.3	95
0.95	74.6	0.12	1.08	1.08	0.4	1.5	0.3	1.6	0.4	0.6	0.2	0.6	0.2	94
0.95	74.6	0.25	1.09	1.08	0.3	1.6	0.2	1.5	0.3	0.6	0.2	0.4	0.3	93
0.95	74.6	0.37	1.09	1.09	0.4	1.6	0.2	1.4	0.2	0.7	0.2	0.3	0.3	94
0.95	74.6	0.51	1	1.09	0.4	1.5	0.3	1.6	0.3	0.7	0.3	0.4	0.2	94
0.95	74.6	0.69	1.1	1.09	0.4	1.6	0.2	1.4	0.3	0.8	0.2	0.5	0.2	94
0.95	74.6	1.13	1.1	1	0.4	1.7	0.2	1.5	0.4	0.6	0.2	0.4	0.2	94
0.95	74.6	1.6	1.12	1.11	0.5	1.5	0.2	1.5	0.4	0.7	0.2	0.5	0.3	94

ac Flux	ac V	Current (A)			Current harmonics (% of fundamental current)									Reactive Power
(T)	(V)	dc	total	fund.	2nd	3rd	4th	5th	6th	7th	8th	9th	10th	(VAR)
0.95	74.6	0	1.07	1.06	0.1	0.8	0.2	1	0.3	0.8	0.1	0.6	0.1	93
0.95	74.6	0.11	1.07	1.06	0.2	1	0.1	1	0.2	0.9	0.3	0.5	0.1	93
0.95	74.6	0.23	1.07	1.06	0.1	1.1	0.2	1.1	0.2	0.8	0.2	0.6	0.2	91
0.95	74.6	0.35	1.07	1.06	0.3	1.2	0.1	1	0.2	0.8	0.2	0.7	0.1	92
0.95	74.6	0.49	1.07	1.07	0.2	1.1	0.1	1	0.3	0.8	0.1	0.5	0.1	92
0.95	74.6	0.63	1.07	1.06	0.1	1	0.1	1.2	0.2	0.8	0.3	0.6	0.2	91
0.95	74.6	1.11	1.06	1.06	0.2	1.2	0.1	1.1	0.2	0.9	0.2	0.6	0.1	91
0.95	74.6	1.57	1.06	1.06	0.3	1	0.1	1.2	0.2	0.8	0.3	0.7	0.2	89

ac Flux	ac V	Current (A)			Current harmonics (% of fundamental current)									Reactive Power
(T)	(V)	dc	total	fund.	2nd	3rd	4th	5th	6th	7th	8th	9th	10th	(VAR)
0.95	74.6	0	1.29	1.27	0.1	0.8	0.2	1	0.3	0.8	0.1	0.6	0.1	112
0.95	74.6	0.11	1.28	1.28	0.2	1	0.1	1	0.2	0.9	0.3	0.5	0.1	111
0.95	74.6	0.22	1.28	1.28	0.3	1	0.2	1.1	0.2	0.8	0.2	0.6	0.1	109
0.95	74.6	0.34	1.29	1.27	0.3	1.2	0.1	1	0.2	0.8	0.2	0.7	0.1	111
0.95	74.6	0.48	1.29	1.28	0.2	1.1	0.1	1	0.2	0.9	0.3	0.6	0.2	113
0.95	74.6	0.63	1.3	1.29	0.1	1	0.1	1.2	0.2	0.8	0.3	0.6	0.2	111
0.95	74.6	1.1	1.31	1.3	0.3	1.1	0.2	1.2	0.3	0.8	0.2	0.7	0.1	112
0.95	74.6	1.55	1.32	1.31	0.3	1	0.1	1.2	0.2	0.8	0.2	0.7	0.2	111

Table 4. 10 Measured current harmonic contents and reactive power for three-phase thick-gapped reactors at 74.6 Volts.

a. **Red phase**
b. **White phase**
c. **Blue phase**

ac Flux	ac V	Current (A)			Current harmonics (% of fundamental current)									Reactive Power
(T)	(V)	dc	total	1st	2nd	3rd	4^{th}	5th	6th	7th	8th	9th	10th	(VAR)
0.95	74.6	0	1.93	1.93	0.2	1.2	0.1	0.8	0	0.4	0.1	0.4	0.1	155
0.95	74.6	0.22	1.94	1.95	0.1	1.3	0.2	0.8	0	0.4	0.2	0.5	0	155
0.95	74.6	0.43	1.95	1.94	0.2	1.2	0.1	0.9	0.1	0.3	0.1	0.5	0.1	154
0.95	74.6	0.62	1.96	1.96	0.1	1.2	0.2	0.8	0	0.2	0.1	0.5	0.1	154
0.95	74.6	0.87	1.95	1.95	0.1	1.1	0.2	0.9	0.1	0.3	0.2	0.6	0.2	154
0.95	74.6	1.14	1.97	1.96	0.1	1	0.1	0.9	0.1	0.2	0.1	0.6	0.1	155
0.95	74.6	1.66	1.97	1.96	0.1	1.1	0.1	0.9	0	0.4	0.1	0.5	0.1	154
0.95	74.6	2.18	1.98	1.98	0.2	0.9	0.1	1	0	0.3	0.1	0.6	0.2	157

ac Flux	ac V	Current (A)			Current harmonics (% of fundamental current)									Reactive Power
(T)	(V)	dc	total	fund.	2nd	3rd	4th	5th	6th	7th	8th	9th	10th	(VAR)
0.95	74.6	0	1.9	1.85	0.1	1.3	0.1	0.7	0	0.4	0	0.4	0.1	153
0.95	74.6	0.19	1.89	1.84	0.1	1.4	0.1	0.7	0.1	0.4	0.1	0.4	0.1	151
0.95	74.6	0.41	1.89	1.84	0.1	1.5	0.1	0.6	0.1	0.5	0.1	0.5	0	149
0.95	74.6	0.61	1.88	1.83	0.2	1.5	0.1	0.7	0	0.4	0.1	0.4	0.1	148
0.95	74.6	0.85	1.89	1.84	0.2	1.4	0.1	0.7	0	0.4	0.1	0.4	0.1	149
0.95	74.6	1.08	1.9	1.85	0.1	1.5	0.1	0.7	0	0.4	0.2	0.4	0.1	149
0.95	74.6	1.6	1.89	1.85	0.2	1.4	0.1	0.7	0.1	0.4	0.1	0.4	0.1	148
0.95	74.6	2.07	1.89	1.84	0.1	1.5	0.1	0.6	0.1	0.5	0.2	0.4	0.1	150

ac Flux	ac V	Current (A)			Current harmonics (% of fundamental current)									Reactive Power
(T)	(V)	dc	total	fund.	2nd	3rd	4th	5th	6th	7th	8th	9th	10th	(VAR)
0.95	74.6	0	2.11	2.11	0	0.3	0	0.8	0.1	0.3	0	0.5	0.1	169
0.95	74.6	0.16	2.12	2.12	0.1	0.6	0.1	0.8	0.1	0.2	0.1	0.5	0.1	169
0.95	74.6	0.38	2.11	2.12	0.1	0.4	0.1	0.8	0	0.4	0.1	0.4	0.1	167
0.95	74.6	0.58	2.11	2.12	0.1	0.5	0	0.8	0.1	0.2	0	0.5	0.1	166
0.95	74.6	0.84	2.12	2.12	0.2	0.5	0.1	0.8	0.1	0.3	0.1	0.5	0.1	167
0.95	74.6	1.11	2.12	2.11	0.1	0.5	0.1	0.8	0.1	0.2	0.1	0.4	0.1	167
0.95	74.6	1.63	2.12	2.11	0.1	0.4	0	0.8	0.1	0.2	0.1	0.4	0	166
0.95	74.6	2.2	2.13	2.12	0.2	0.3	0.1	0.8	0.1	0.4	0	0.4	0.1	169

Results for harmonics average for the eight readings are graphically plotted in Figure 4. 12.

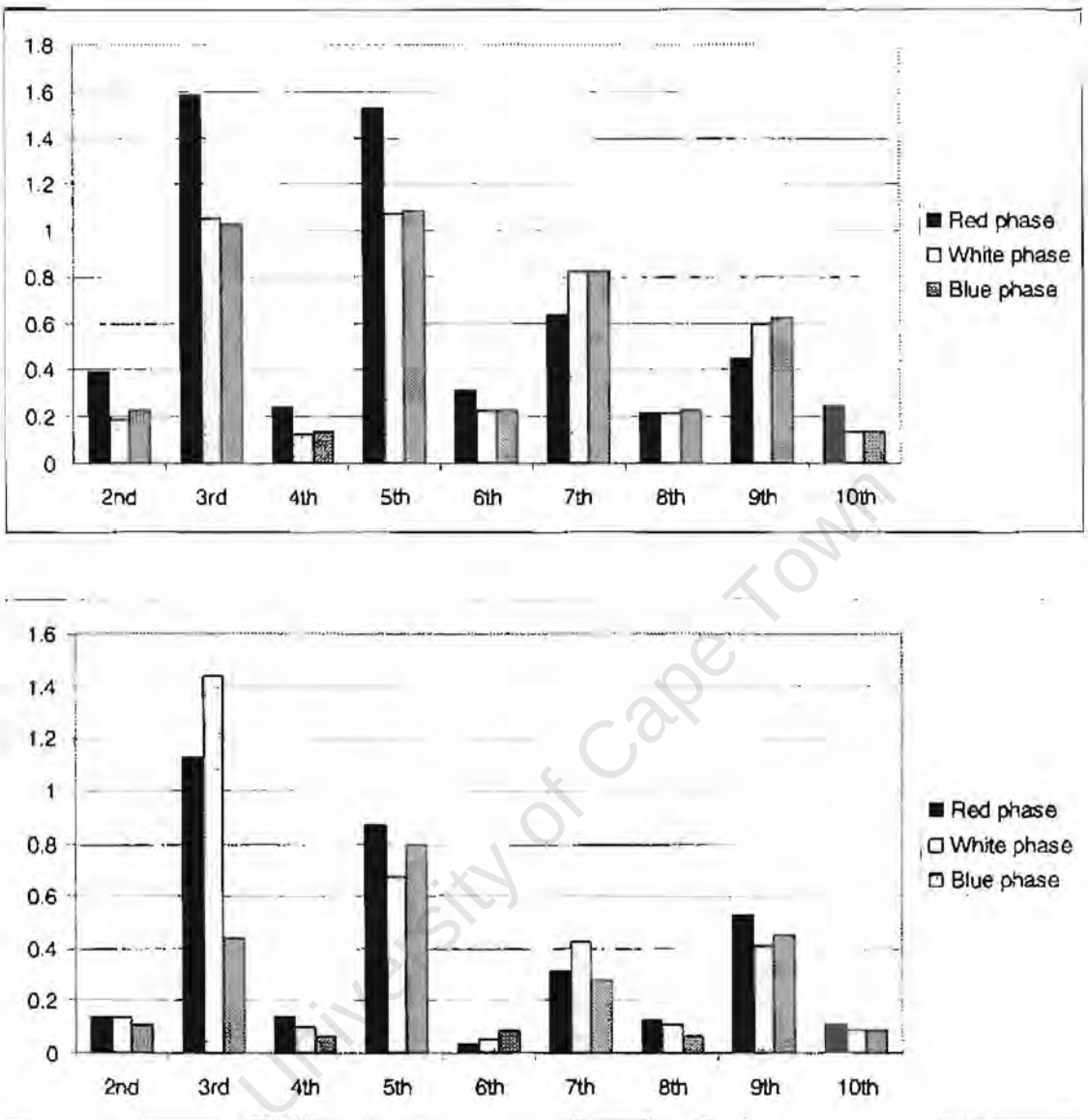

Figure 4. 12 Average measured harmonics as percentage of fundamental current for three-phase reactors at 74.6 Volts.

a. Thin-gapped

b. Thick-gapped

There are slight high harmonic percentages in the phases especially odd harmonics, without the injection of dc currents. These harmonic percentages could be attributed to the power fluke's inaccuracy [16]. Odd harmonics' overall trend for percentage dominated even harmonics' trend. The odd harmonics' trend decreased with increasing order at a given current magnitude while all even harmonics remained somewhat equal. As injected dc currents increased, harmonics remained unaffected. There seemed to be

slight increases in both total and fundamental currents. These increases did not seem to affect reactive power, except with the thick-gapped reactor, which could be due to instrument error.

Table 4. 11 Measured current harmonic contents for three-phase reactors in the neutral at 74.6 Volts.

a. Thin-gapped

b. Thick-gapped

ac Flux	dc Flux	Current (A)			Current harmonics (% of fundamental current)								
(T)	(T)	dc	total	1st	2nd	3rd	4th	5th	6th	7th	8th	9th	10th
0.95	0	0	0.19	0.25	6	9	6	2	5	2	5	2	4
0.95	0.1	0.35	0.01										
0.95	0.2	0.7	0.02										
0.95	0.3	1.07	0.01	0.04	52	61	40	30	11	10	3	4	3
0.95	0.4	1.46	0										
0.95	0.5	2.04	0.02	0.10	48	19	5	16	14	3	4	9	6
0.95	0.6	3.32	0.01										
0.95	0.65	4.74	0.03	0.12	32	5	16	15	2	9	9	4	7

Ac Flux	dc Flux	Current (A)			Current harmonics (% of fundamental current)								
(T)	(T)	dc	total	1st	2nd	3rd	4th	5th	6th	7th	8th	9th	10th
0.95	0	0	0.21	0.27	5	11	4	4	4	19	4	1	3
0.95	0.1	0.61											
0.95	0.2	1.23	1.23										
0.95	0.3	1.85	0.03	0.10	43	27	2	17	16	6	1	6	9
0.95	0.4	2.51	2.6										
0.95	0.5	3.35	0.02	0.10	46	27	3	16	15	5	4	6	9
0.95	0.6	4.89	4.9										
0.95	0.65	6.45	0.02	0.13	27	1	15	12	4	10	5	4	7

Readings for measurements in Table 4. 11 were fluctuating most of the times and blanks in such tables represent those readings that could not be taken. As injected dc current increased, harmonics seemed to remain somewhat randomly distributed.

4.6 INTERPRETATION OF RESULTS

Under balanced conditions, a presence of harmonics of both odd and even harmonics with the overall trend for magnitude to decrease with decreasing order at a given ac excitation and dc excitation indicates saturation. The harmonics were present in fractions of fundamental currents did not result in physical damage but indicated concealed effects.

4.7 SUMMARY

The laboratory testing was based on the expectations derived from the mathematical modelling with special focus paid to the saturation of the reactors' magnetic cores; the condition appeared to be related to the generation of harmonics.

Two types of reactors were tested: three matched single-phase unit reactors and a three-phase unit reactor. For both types, testing was done for gapped and non-gapped reactors. Testing equipment included a three-phase source and variac, dc current source, ammeters, power flukes and thermocouple sensor.

Ac voltage of equivalent ac flux density excited gapped and non-gapped reactors. Varying dc current was injected into the circuit while recording harmonics and observing any strange behaviour in the reactors.

Without dc current injection, current measurements indicated very low harmonic contents. As injected dc current increased, single-phase units began to consist of both even and odd harmonics, which may have exceeded recommended compatibility levels for harmonics. Subsequently reactive power started to increase exponentially while increase in temperature remained constant. The harmonics decreased as the harmonic number for a particular dc current increased. Non-gapped single-phase units harmonic content was higher than gapped units and so was the rate of increase in reactive power.

Three-phase units did not get to saturate at all and in fact, no change in harmonic content was observed despite a slight increase in fundamental current in one or two phases.

CHAPTER 5

CORRELATION OF MODELLING AND LABORATORY RESULTS

Simulations were carried out on reactors in Chapter 4. The same reactors were tested in the laboratory in Chapter 5 under similar modelling conditions. In these chapters, reactors were excited under two constant ac conditions of 0.9 Teslas (70.7 Volts) and 0.95 Teslas (74.6 Volts) close to the saturation point while varying dc flux/currents. This chapter shall present similarities under the latter condition between the results obtained from two methods for any possible correlations.

5.1 SINGLE-PHASE UNITS

Even though ac flux density/voltage remained constant, fundamental current in the phases changed as injected dc current increased for single-phase units. Injection of dc current also introduced both even and odd harmonics both in the phases and in the neutral. It resulted in an increase of reactive power consumption as well.

5.1.1 PHASE FUNDAMENTAL CURRENTS

Without the injection of dc current, the single-phase non-gapped units operated at an average predominant fundamental current of about 150 mA per phase. As injected dc current increased from 0 to an average of 650 mA (448% of the initial excitation current) per phase, fundamental current subsequently increased as displayed in Figure 5. 1.

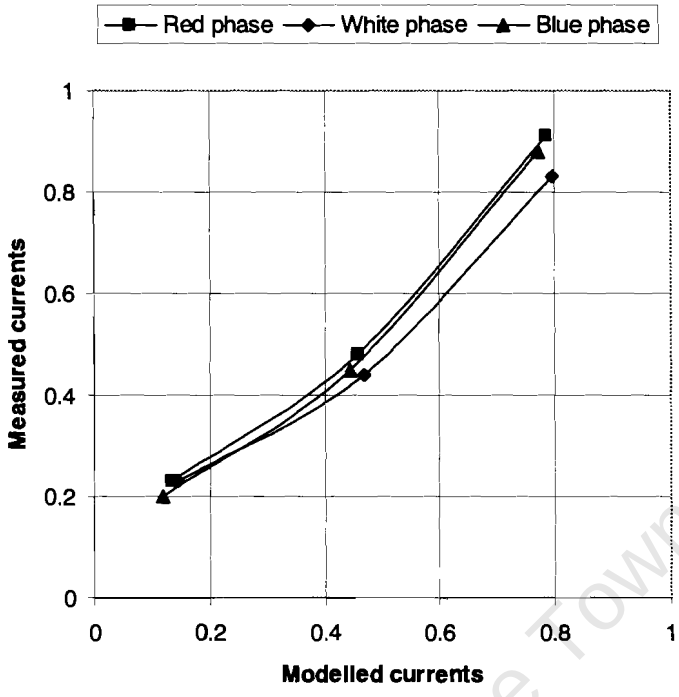

Figure 5. 1 Measured fundamental currents versus modelled fundamental currents at 74.6 Volts over a range of varying dc currents for single-phase thin-gapped reactors in the phases.

The single-phase thin-gapped units operated at an average predominant fundamental current of about 1.48 A per phase without the injection of dc current. As injected dc current increased from 0 to an average of 1.46 A (99% of the initial excitation current) per phase, fundamental current subsequently increased as displayed in Figure 5. 2.

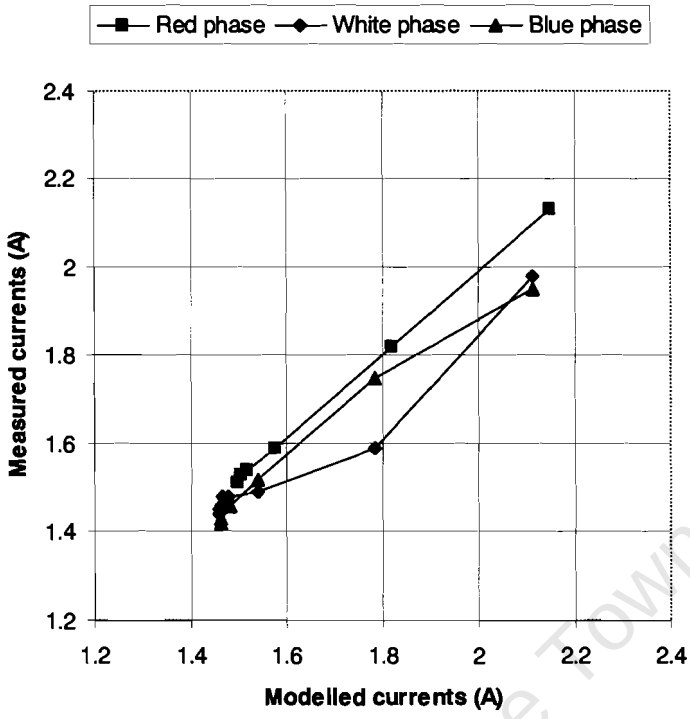

Figure 5. 2 Measured fundamental currents versus modelled fundamental currents at 74.6 Volts over a range of varying dc currents for single-phase non-gapped reactors in the phases.

The single-phase thin-gapped units operated at an average predominant fundamental current of about 2.61 A per phase without the injection of dc current. As injected dc current increased from 0 to an average of 2.2 A (84% of the initial excitation current) per phase, modelled and measured fundamental currents subsequently increased as displayed in Figure 5. 3.

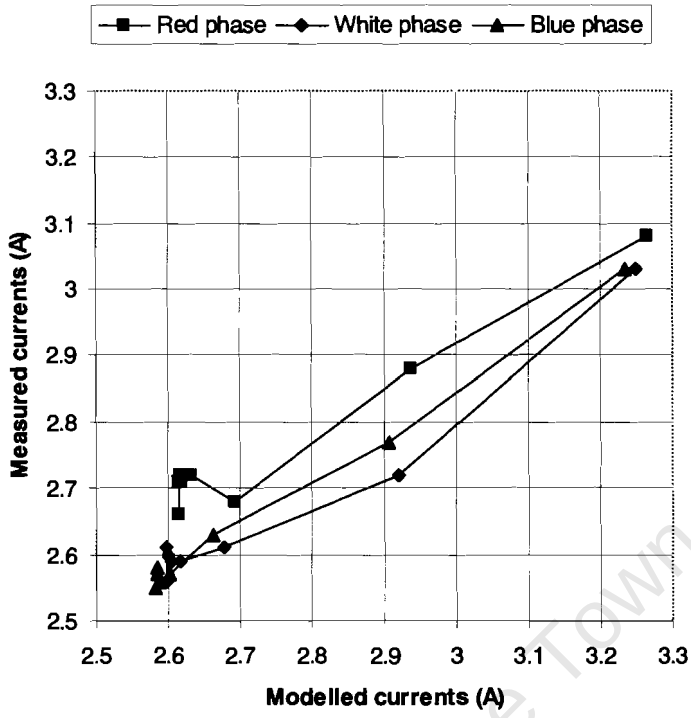

Figure 5. 3 Measured fundamental currents versus modelled fundamental currents at 74.6 Volts over a range of varying dc currents for single-phase thick-gapped reactors in the phases.

Figure 5. 1 to Figure 5. 3 depicts an almost diagonally linear relationship between measured and modelled currents at 74.6 Volts, which indicates how closely correlated the two methods are. The graphs could have been perfectly and diagonally linear had it not been because of errors introduced by measuring equipment and neglect of hysteresis loop.

Graphical illustrations between measured and modelled fundamental currents at 70.7 Volts in the phases can be found in Appendix D.

5.1.2 PHASE CURRENT HARMONICS

Without the injection of dc currents, modelled harmonics were rarely present while small quantities of harmonics were measured. As injected dc current increased, both even and odd harmonics were being introduced in the circuit as depicted in Figure 5. 4.

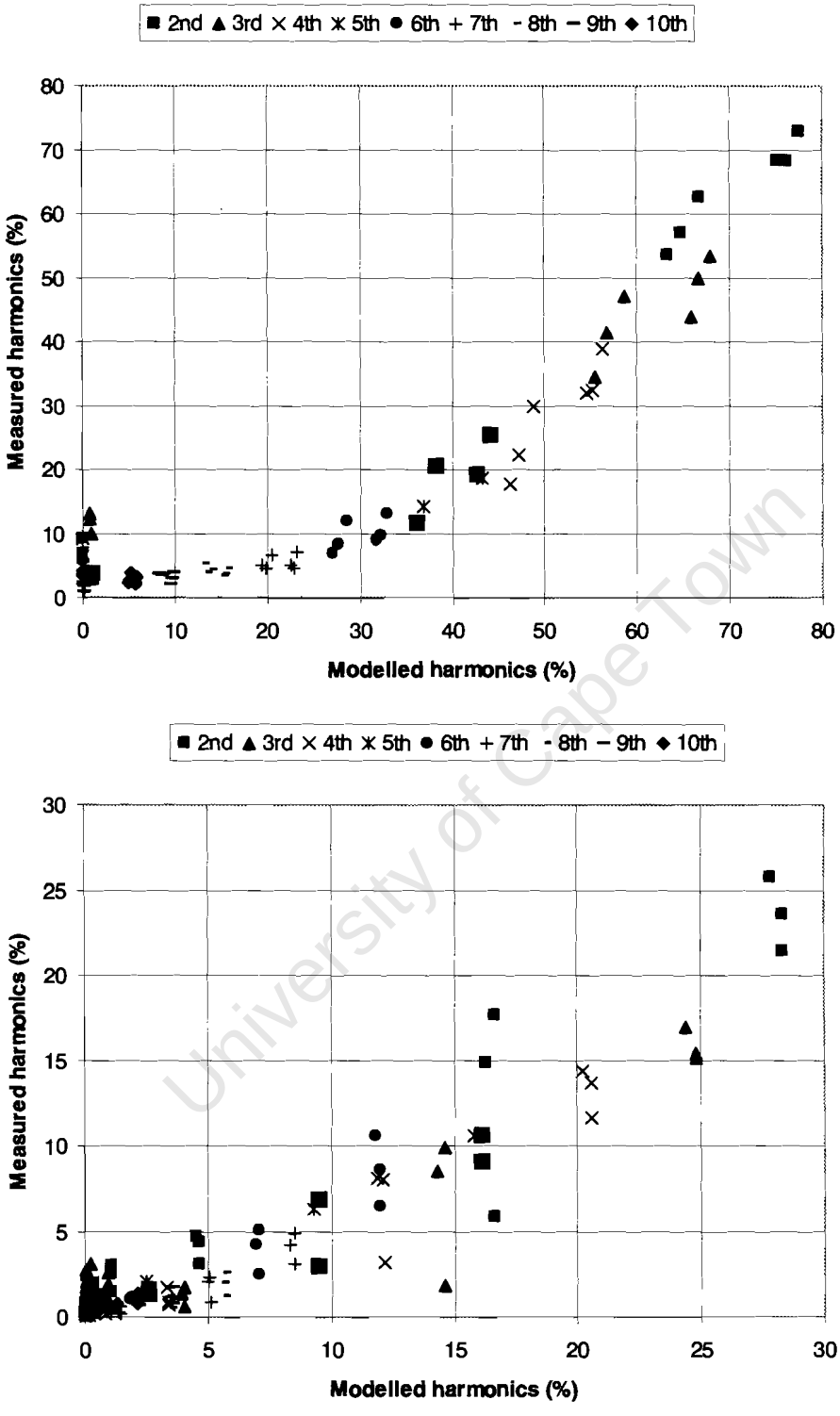

Figure 5. 4 Measured current harmonics versus modelled current harmonics at 74.6 Volts over a range of varying dc currents for single-phase reactors in the phases.

a. **Non-gapped**
b. **Thin-gapped**
c. **Thick-gapped**

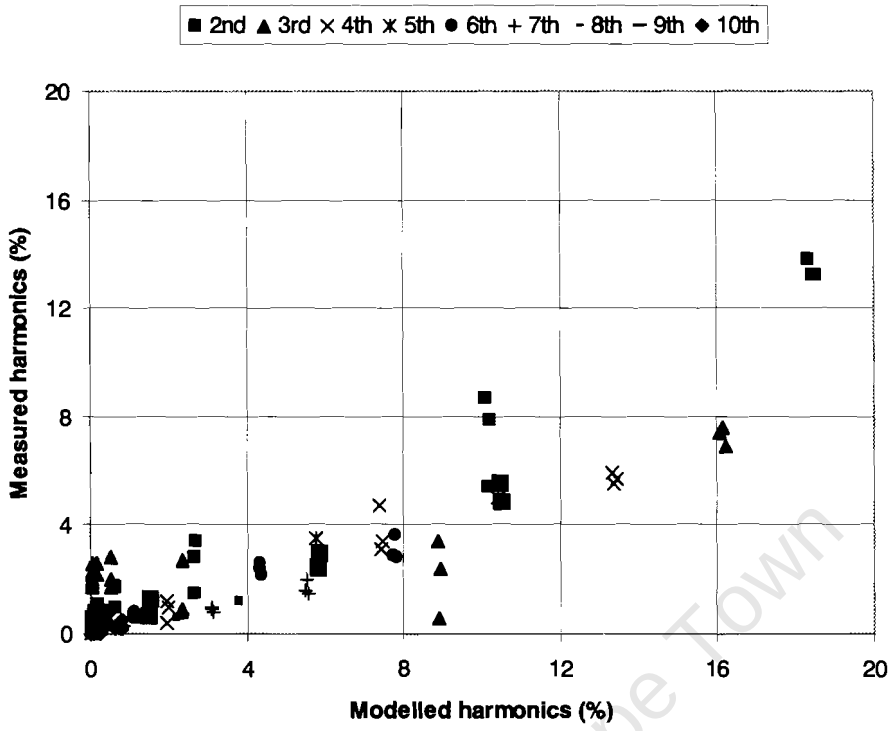

Figure 5.4 (continued)

Figure 5. 4 (a) depicts a somewhat parabolic relationship between respective measured and modelled harmonics. In Figure 5. 4 (a) and (b), it improves to a more linear relationship. The graphs could have been once again perfectly and diagonally linear had it not been because of errors introduced by measuring equipment and neglect of hysteresis loop.

Graphical illustrations between measured and modelled current harmonics at 70.7 Volts in the phases can be found in Appendix D.

5.1.3 NEUTRAL FUNDAMENTAL CURRENTS

As injected dc current increases, modelled fundamental current remained constant while measured current changed as illustrated in Figure 5. 5.

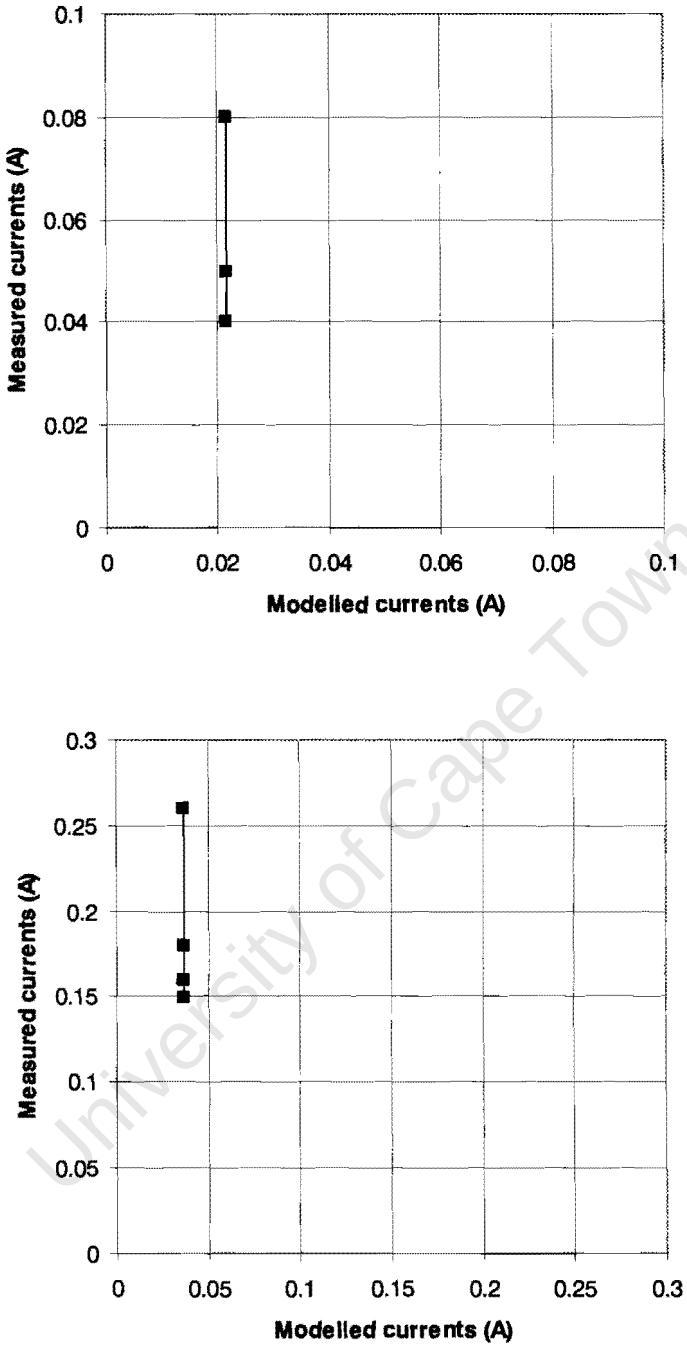

Figure 5. 5 Measured fundamental current versus modelled fundamental current at 74.6 Volts over a range of varying dc currents for single-phase reactors in the neutral.

a. **Non-gapped**
b. **Thin-gapped**
c. **Thick-gapped**

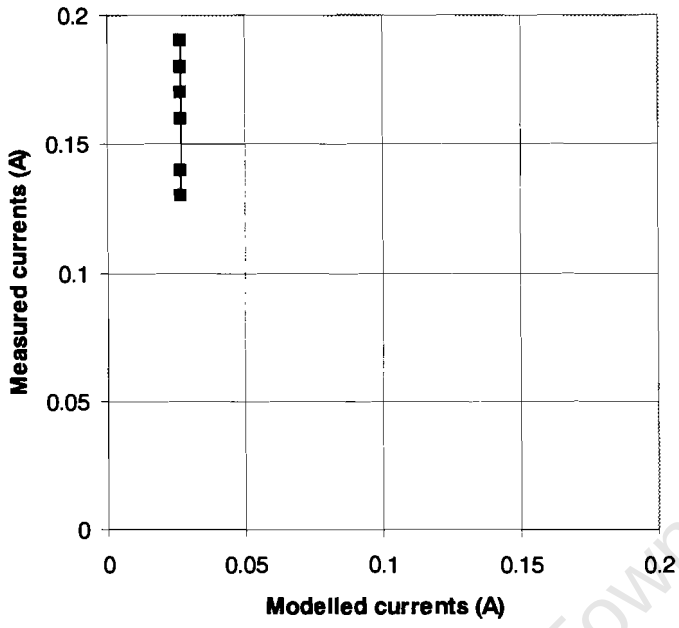

Figure 5.5 (continued)

Measured and modelled currents could have followed a similar pattern in Figure 5. 5 but they did not due to errors introduced mainly by measuring equipment at low current values and by neglecting hysteresis losses.

Graphical illustrations between measured and modelled fundamental currents at 70.7 Volts in the neutral can be found in Appendix D.

5.1.4 NEUTRAL HARMONIC CURRENTS

Without the injection of dc currents, a predominant amount of third harmonics was present. Relatively small amount of other harmonics were present too. As injected dc current increased, third, sixth and ninth harmonics greatly increased as depicted in Figure 5. 6.

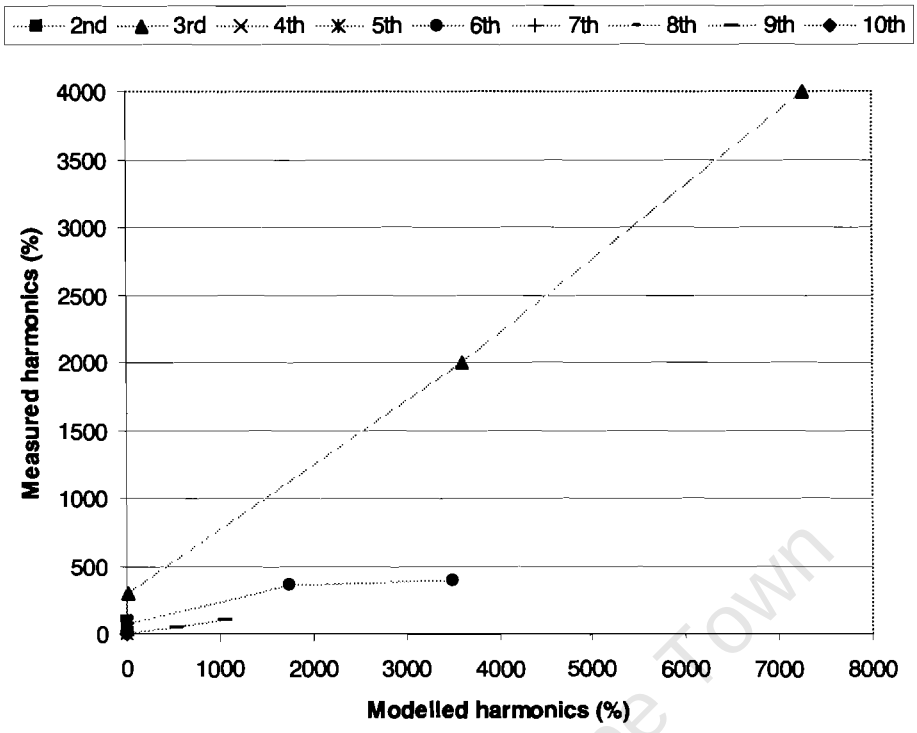

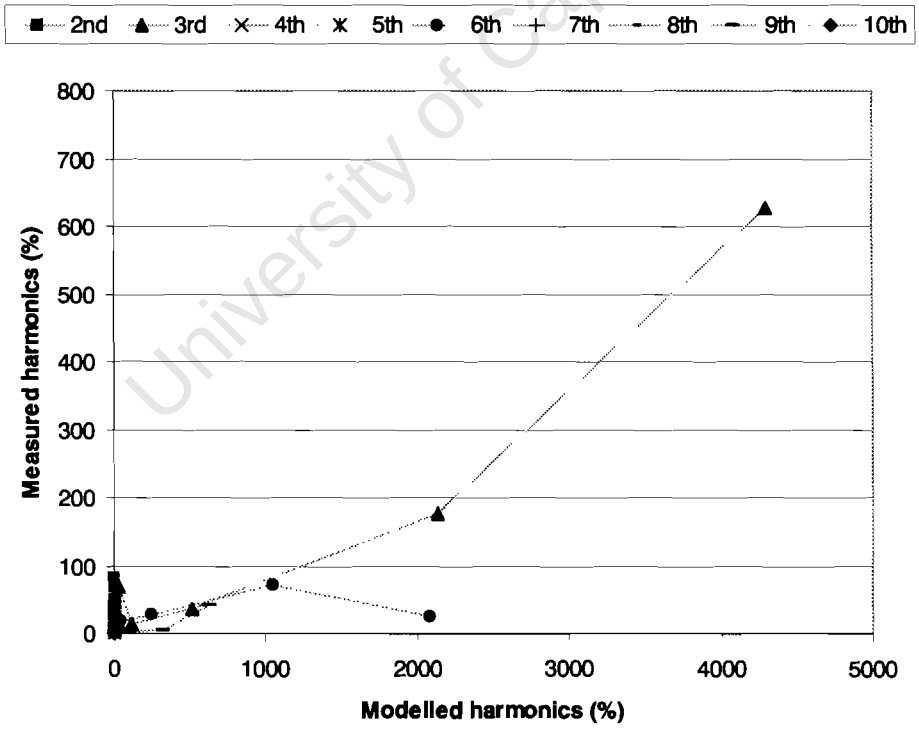

Figure 5. 6 Measured current harmonics versus modelled current harmonics at 74.6 Volts over a range of varying dc currents for single-phase reactors in the neutral.

a. **Non-gapped**
b. **Thin-gapped**
c. **Thick-gapped**

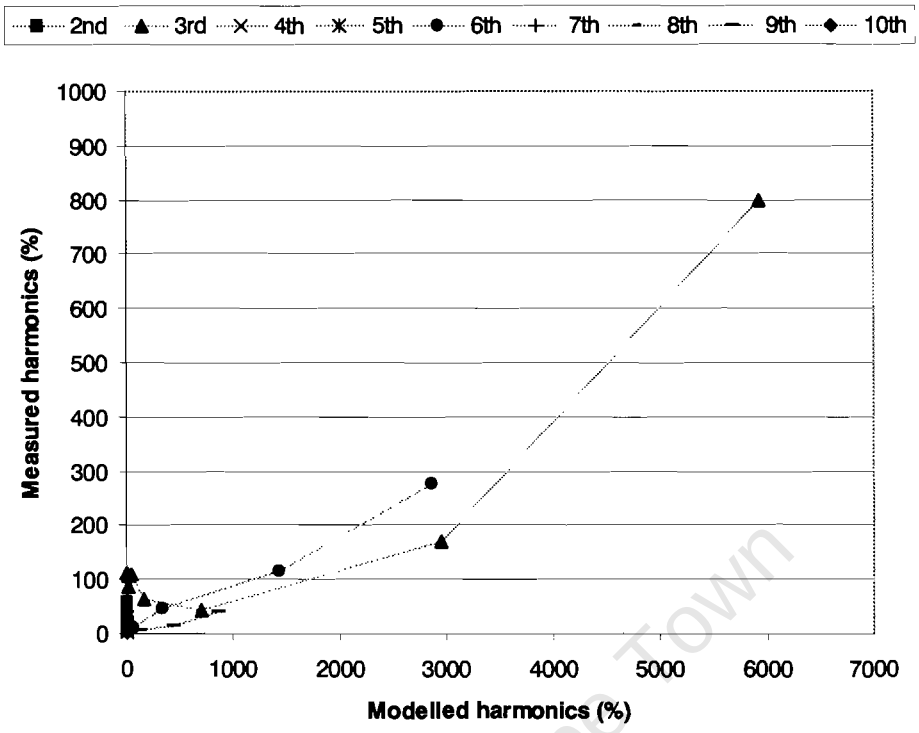

Figure 5.6 (continued)

Measured and modelled current harmonics in the neutral could have followed a similar pattern in Figure 5. 6 but they did not due to errors introduced mainly by measuring equipment at low current values and by neglecting hysteresis losses.

Graphical illustrations between measured and modelled current harmonics at 70.7 Volts in the neutral can be found in Appendix D.

5.1.5 REACTIVE POWER

As injected dc current increased, reactive power increased almost proportionally to the fundamental current in the phases as illustrated in Figure 5. 7.

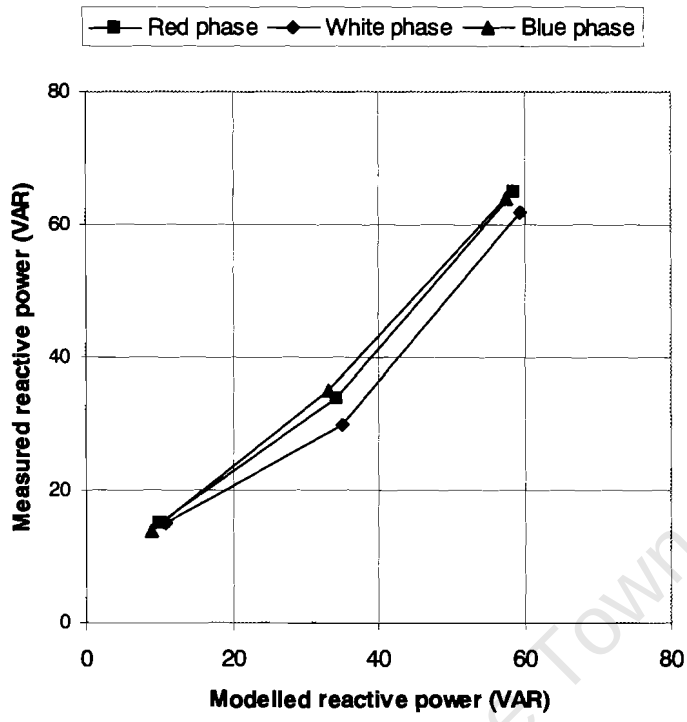

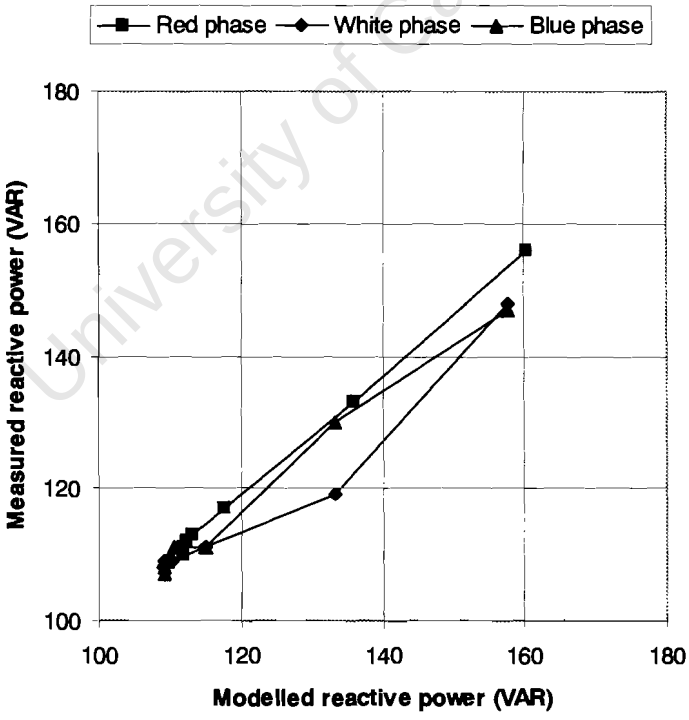

Figure 5. 7 Measured reactive power versus modelled reactive power at 74.6 Volts over a range of varying dc currents for single-phase reactors.

a. **Non-gapped**
b. **Thin-gapped**
c. **Thick-gapped**

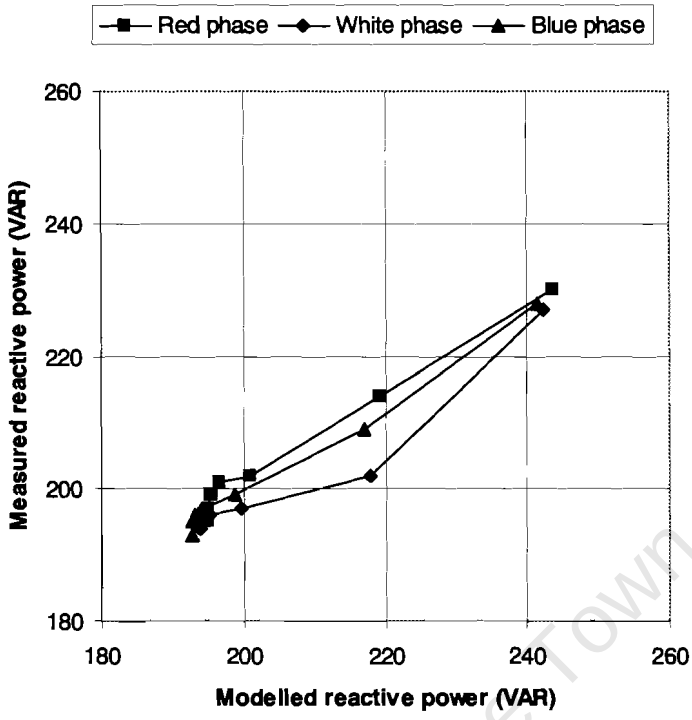

Figure 5.7 (continued)

Figure 5. 7 depict an almost diagonally linear relationship between measured and modelled reactive power at 74.6 Volts, which indicates how closely correlated the two methods are. The graphs could have been perfectly and diagonally linear had it not been because of errors introduced by measuring equipment and neglect of hysteresis losses.

Graphical illustrations between measured and modelled power harmonics at 70.7 Volts can be found in Appendix D.

5.2 THREE-PHASE UNITS

Unlike single-phase units, three-phase units' fundamental current in the phases rarely changed as injected dc current increased at constant ac voltages. Although a small portion of harmonics was produced in the circuit, it rarely changed as injected dc current increased and so was consumed reactive power. Table 5. 1 and Table 5. 2 summarize measured and modelled results obtained.

Table 5. 1 Summary of current harmonic contents and reactive power for three-phase thin-gapped units at 74.6 Volts.

a. **Modelled**
b. **Measured**

	Current (A)			Current harmonics (% of fundamental current)									Reactive power
Phase	dc	total	1st	2nd	3rd	4th	5th	6th	7th	8th	9th	10th	(VAR)
Red	-0	1.03	1.03	0	0.04	0	0.18	0	0.02	0	0.03	0	77
White	0	1.04	1.04	0	0.02	0	0.08	0	0.01	0	0.01	0	77
Blue	0	1.24	1.24	0	0.03	0	0.15	0	0.02	0	0.02	0	92

	Current (A)			Current harmonics (% of fundamental current)									Reactive power
Phase	dc	total	1st	2nd	3rd	4th	5th	6th	7th	8th	9th	10th	(VAR)
Red	0	1.09	1.08	0.39	1.59	0.24	1.53	0.31	0.64	0.21	0.45	0.25	95
White	0	1.07	1.06	0.19	1.05	0.13	1.08	0.23	0.83	0.21	0.6	0.14	93
Blue	0	1.29	1.27	0.23	1.03	0.14	1.09	0.23	0.83	0.23	0.63	0.14	112

Table 5. 2 Summary of current harmonic contents and reactive power for three-phase thick-gapped units at 74.6 Volts.

a. **Modelled**
b. **Measured**

	Current (A)			Current harmonics (% of fundamental current)									Reactive power
Phase	dc	total	1st	2nd	3rd	4th	5th	6th	7th	8th	9th	10th	(VAR)
Red	-0	1.87	1.87	0	0.02	0	0.1	0	0.01	0	0.01	0	139
White	0	1.87	1.87	0	0.01	0	0.05	0	0.01	0	0.01	0	139
Blue	0	2.05	2.05	0	0.02	0	0.09	0	0.01	0	0.01	0	153

	Current (A)			Current harmonics (% of fundamental current)									Reactive power
Phase	dc	total	1st	2nd	3rd	4th	5th	6th	7th	8th	9th	10th	(VAR)
Red	0	1.93	1.93	0.14	1.13	0.14	0.88	0.04	0.31	0.13	0.53	0.11	155
White	0	1.9	1.85	0.14	1.44	0.1	0.68	0.05	0.43	0.11	0.41	0.09	153
Blue	0	2.11	2.11	0.11	0.44	0.06	0.8	0.09	0.28	0.06	0.45	0.09	169

Fundamental currents in Table 5. 1 are quite close to each other indicating how the two correlates with one another and so are fundamental currents Table 5. 2.

Between measured and modelled reactive power, modelled reactive power slightly lags behind measured power.

It is different with current harmonics however as measured and modelled harmonics are not of the same magnitude perhaps due to power harmonic analyser inaccuracy at low harmonics' contents at low current levels. What is notable though is a similar trend for magnitude that measured and modelled harmonics tended to follow as illustrated in

Figure 5. 8 and Figure 5. 9 (note scale difference between modelled and measured harmonic contents).

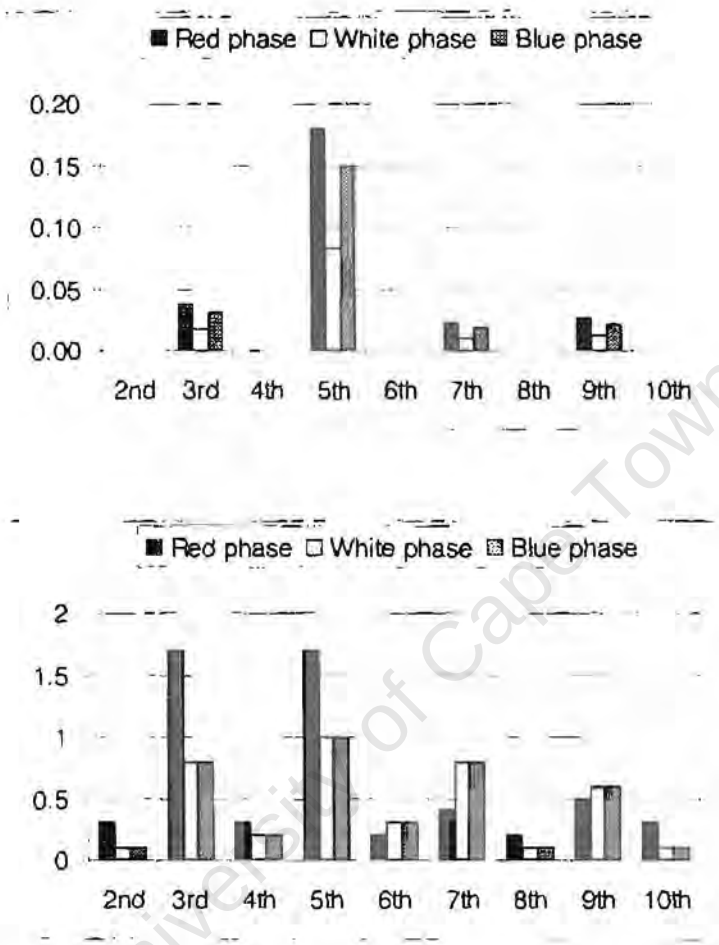

Figure 5. 8 Current harmonic contents for three-phase thin-gapped units at 74.6 Volts.

a. **Modelled**
b. **Measured**

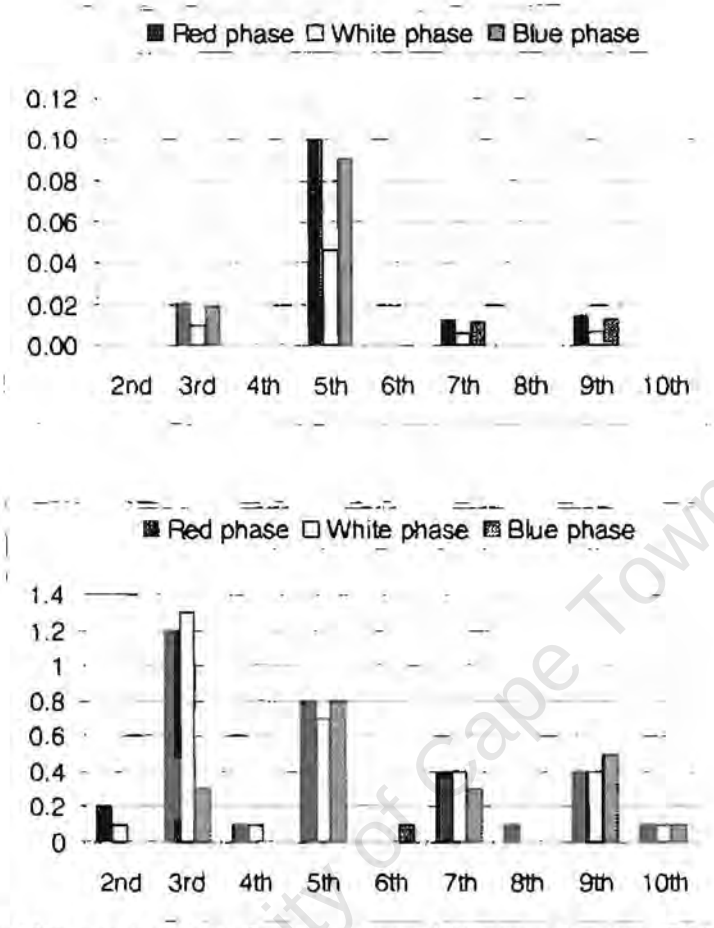

Figure 5. 9 Current harmonic contents for three-phase thick-gapped units at 74.6 Volts.

a. **Modelled**
b. **Measured**

Between measured and modelled harmonics, fifth harmonics is larger than all other harmonics on several occasions but it cannot be explained why the model 5^{th} harmonic significantly larger that of measurements. It is usually followed by third and then either ninth or seventh harmonics. Present in minorities are second, fourth, eight and tenth harmonics.

5.3 SUMMARY

Comparisons between measured and modelled quantities were carried out for single-phase and three-phase reactor units. These quantities, which included phase fundamental

currents, phase current harmonics, neutral fundamental harmonics, neutral harmonic currents and reactive power were obtained under similar conditions in Chapter 4 and Chapter 5.

Comparisons were done by using XY plots for single-phase units. Modelled quantities were presented on the x-axis while measured quantities were presented on the y-axis. A linear relationship between modelled and measured quantities such that corresponding quantities are equal at all points indicates a perfect correlation. Results between the two methods showed a satisfactory correlation for phase fundamental currents, phase current harmonics, neutral harmonic currents and reactive power. Modelled neutral fundamental current remained constant while measured neutral fundamental current slightly increased.

In three-phase units, both measured fundamental currents and reactive were quite close to their modelled counterparts despite modelled reactive power slightly lagging behind measured power. Pie charts were used to compare harmonic currents for these units. Although measured and modelled harmonics were not quite of the same magnitude they followed a similar trend for magnitude.

Errors that lead to imperfect correlations were identified and were measuring equipment errors, which greatly deteriorates at low current levels and low harmonic currents' content, and neglect of hysteresis loop.

CHAPTER 6

CORRELATION WITH FIELD MEASUREMENTS

Sunburst monitoring equipment was installed in December 2000 at Grassridge and Hydra to measure essential data such as geomagnetic data, GICs currents in the neutral, fundamental currents, harmonic components (from second to the sixth harmonic) that gas monitoring units could not measure. Only two substations were chosen due to limited number of equipment and the fact that they were expected to be more susceptible than others in the country [30]. Sunburst is a program initiated by the Electric Power Research Institute (EPRI) in 1992 to monitor power system network globally [8].

The sunburst-monitoring equipment collected data during the three major storms occurred on 31 March 2001, 06 November 2001 and 24 November 2001. None of the transformers onto which the equipment was fitted developed faults. Data collected, which included essential geomagnetic data, GICs currents in the neutral, fundamental currents, harmonic components (from second to the sixth harmonic) together with mathematical modelling results and laboratory results would finalize an insight to what extent GICs could cause damages [30].

This chapter shall present and analyse the collected data for any indicators of saturation.

6.1 MAGNETIC FIELD MEASUREMENTS

The geomagnetic field is commonly described by a geometric co-ordinate system comprised of three independent vector components shown in Table 6. 1 [48].

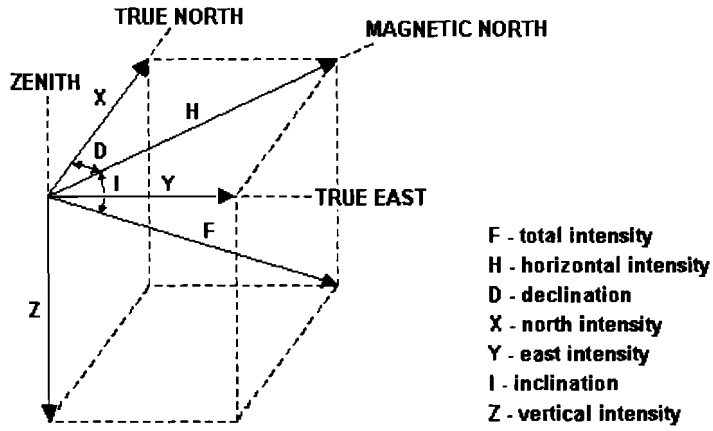

Figure 6. 1 The co-ordinate system commonly used to describe ground-based observations in geomagnetism [48].

During a geomagnetic storm encounter, all components of the geomagnetic field get disturbed. There are measures that indicate the degree of disturbance, which in turn determine the amount of GICs expected. The K index that will be dealt with in this thesis is one of such measures [30].

The K-index is a quasi-logarithmic scale that represents a maximum variation in the north field intensity (X) within a three-hour interval with integer values from 0 (minimum storm activity) to 9 (super storm activity). The K-index values and corresponding variation ranges are shown in Table 6. 1 [30].

Table 6. 1 Limits of amplitude ranges (nT) for defining the K-index at the Hermanus Observatory [48].

K index	0	1	2	3	4	5	6	7	8	9
Range (nT)	3	6	12	24	42	72	120	198	300	

Magnetic storm conditions are considered to prevail when the degree of magnetic activity is taken to be a K-index of 5 or greater. It is considered a major storm when K is 6 and a severe storm when K exceeds 6 [30]. Table 6. 2 shows such K values for a few days in 2001 including those classified to have had major storms. This data was collected from the Hermanus Magnetic Observatory (HMO) and assumed to be the same in the whole country even though there are generally slight variations from place to place.

Table 6. 2 Dates and corresponding K-index values for some major activities in 2001 [10].

Date	31 March	25 September	21 October	06 November	24 November
K-Index	7775 6667	1221 1167	2211 2667	7654 4565	3597 7645

Figure 6. 2 to Figure 6. 5 graphically show north field intensity (X) and the rate of change in the field intensity for a 24-hour period for the days indicated in Table 6. 2.

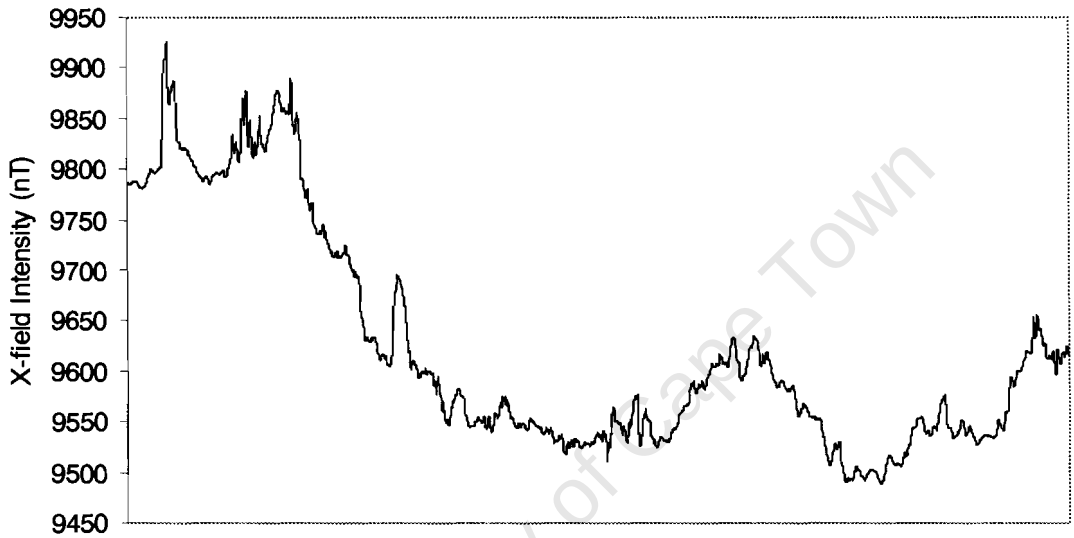

Figure 6. 2 X-component of the magnetic field measured on 31 March 2001.

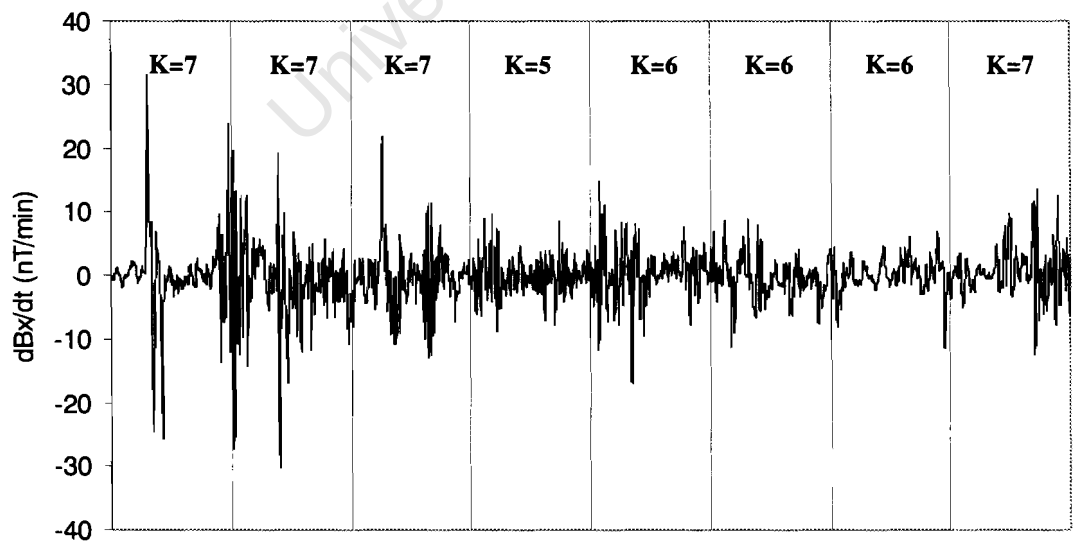

Figure 6. 3 K-index and a rate of change in the X-component on 31 March 2001 [10].

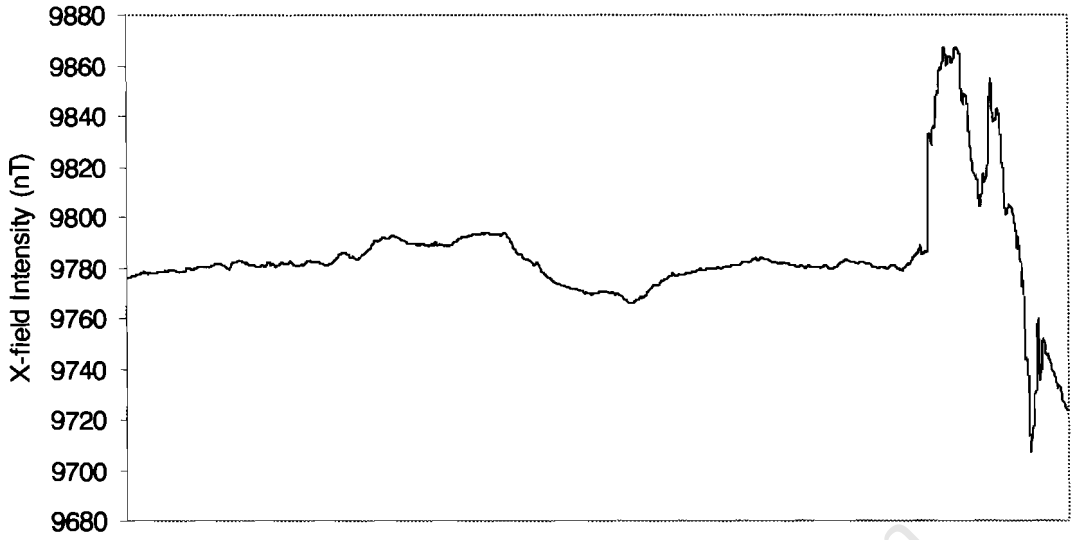

Figure 6. 4 X-component of the magnetic field measured on 25 September 2001 [10].

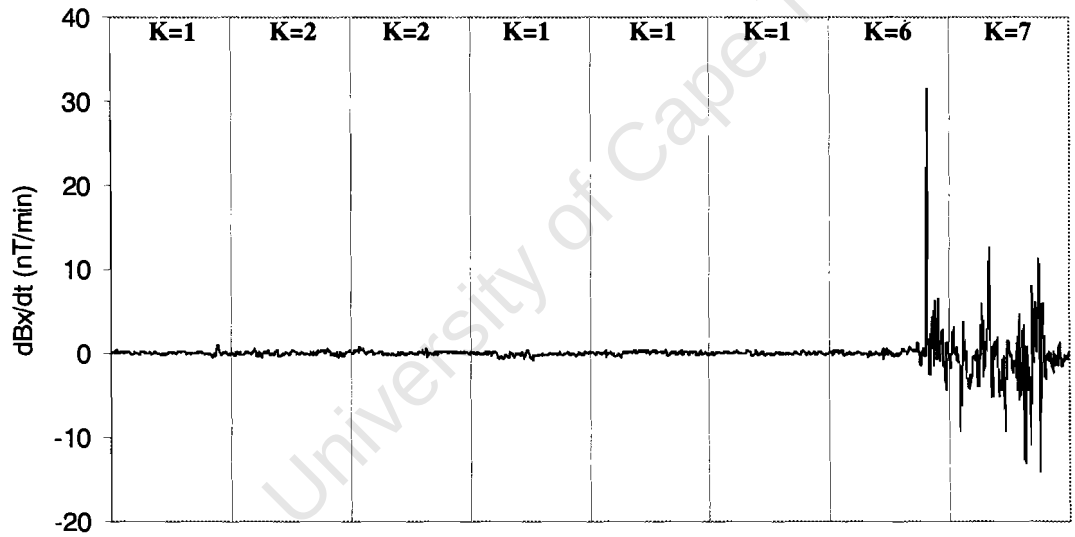

Figure 6. 5 K-index and a rate of change in the X-component on 25 September 2001 [10].

The first three quarters of Figure 6. 4 is an example of how much variations in the X-field intensity for calm day as far as geomagnetic storms are concerned.

6.2 SUBSTATION MEASUREMENTS AND THEIR ANALYSIS

The position of Hydra and Grassridge substations in the power grid network make them very susceptible to GICs and thus they were chosen to install the Sunburst monitoring equipment [30].

Since they were installed, the Sunburst monitoring equipment had been measuring GICs currents in the neutral, fundamental currents in the neutral and on the phases and harmonic components (from second to the sixth harmonic) both in the neutral and on the phases.

6.2.1 HYDRA SUBSTATION

A single 400 / 132 / 15 kV, 240 MVA (1043A rating current), three-phase, five-limb, core type autotransformer manufactured in 1968 was monitored at Hydra Substation. Since the installation of the Sunburst monitoring equipment, the transformer was rarely utilized beyond 10% of its rating [30].

Figure 6. 6 to Figure 6. 8 show current measured (per minute for 24 hours) on the phase A of the transformer as provided by Eskom. From left to right, the graphs are divided up into five vertical blocks for data collected on 31 March 2001, 25 September 2001, 21 October 2001, 06 November 2001 and on 24 November 2001 respectively.

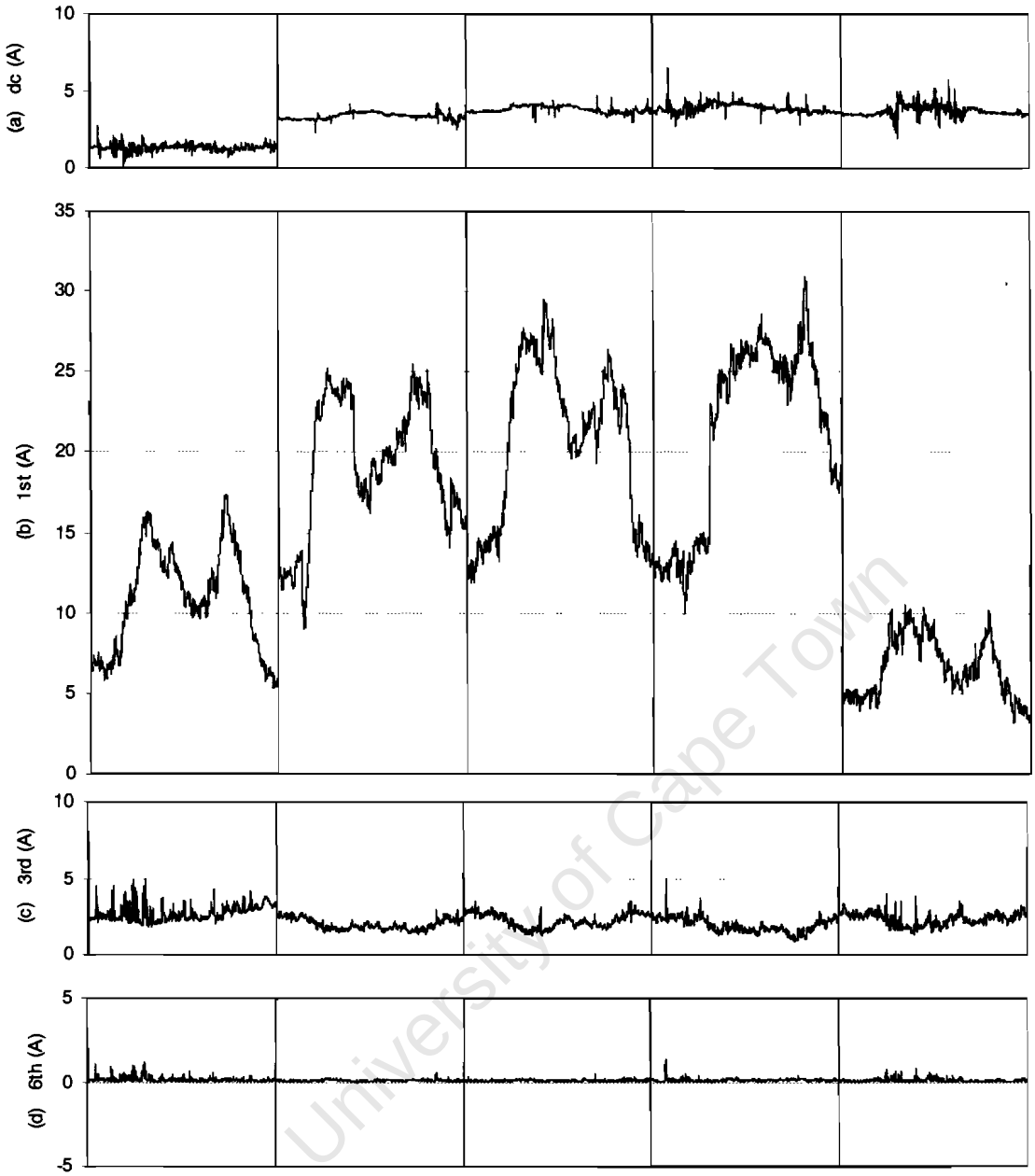

Figure 6. 6 Currents measured in the neutral of the Hydra substation transformer.

There are dc currents present in the neutral of the transformer with or without much storm activities occurring in Figure 6. 6(a). In most cases, the frequency of these currents' fluctuations increases as the K-index increases, responding to the presence of storm activities. Similarly, there are third and sixth harmonics present in the neutral of the transformer with or without much storm activities occurring in Figure 6. 6(c) and (d). The harmonics fluctuate alongside dc currents' fluctuations. Third harmonics fluctuations exceed those of dc currents in terms of magnitude white sixth harmonics are lesser than dc currents'.

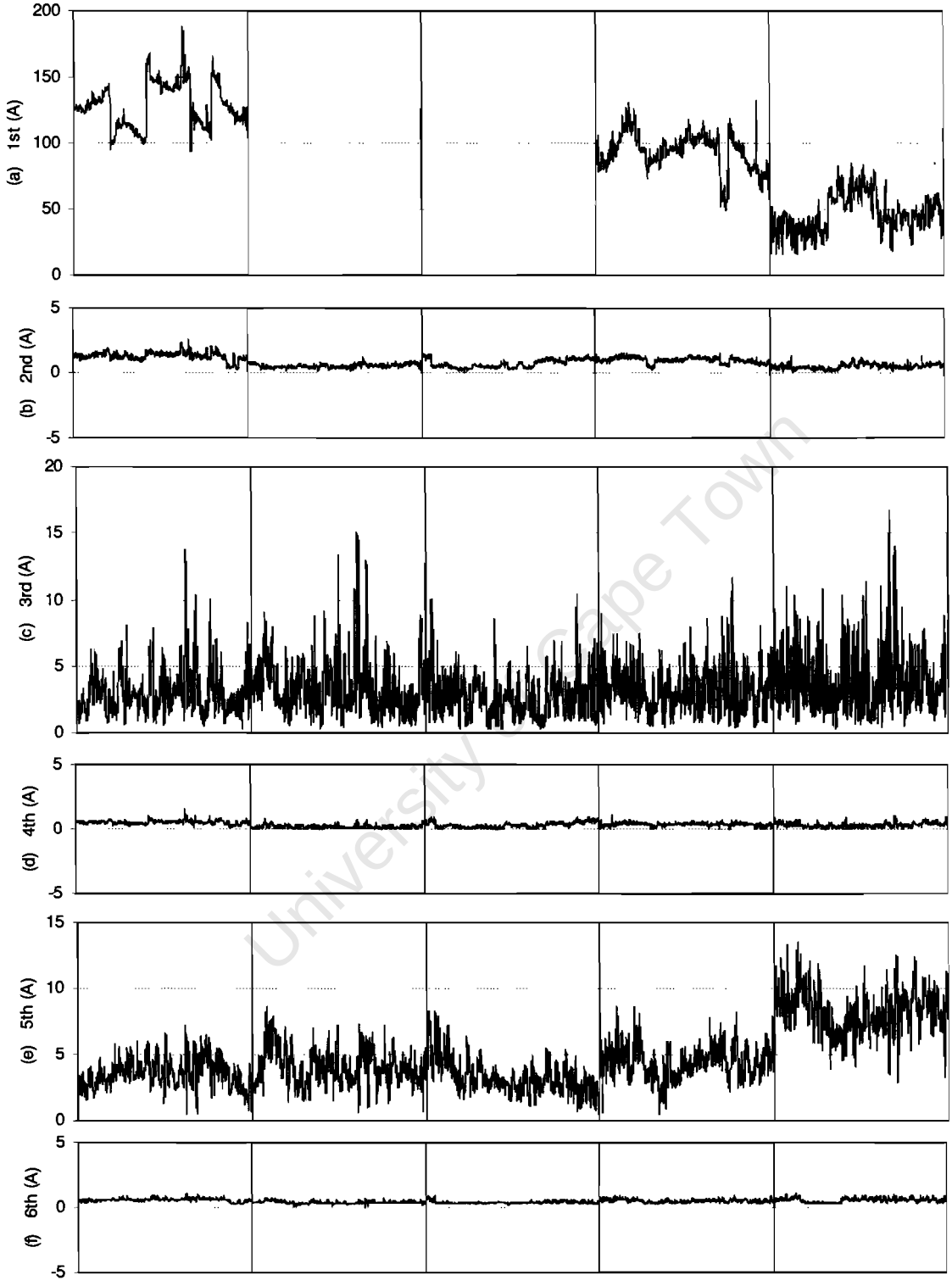

Figure 6. 7 Currents measured on the low voltage side of the Hydra substation transformer.

The neutral dc currents would ideally split up in equal proportions among the three phases. Second, third, fourth, fifth and sixth harmonics are present in the phase and each constantly fluctuating at the same pace throughout, not necessarily fluctuating with dc currents' fluctuations. The presence of dc currents in the measured phase contributed by the neutral is hence not having any effects on the current harmonics' content.

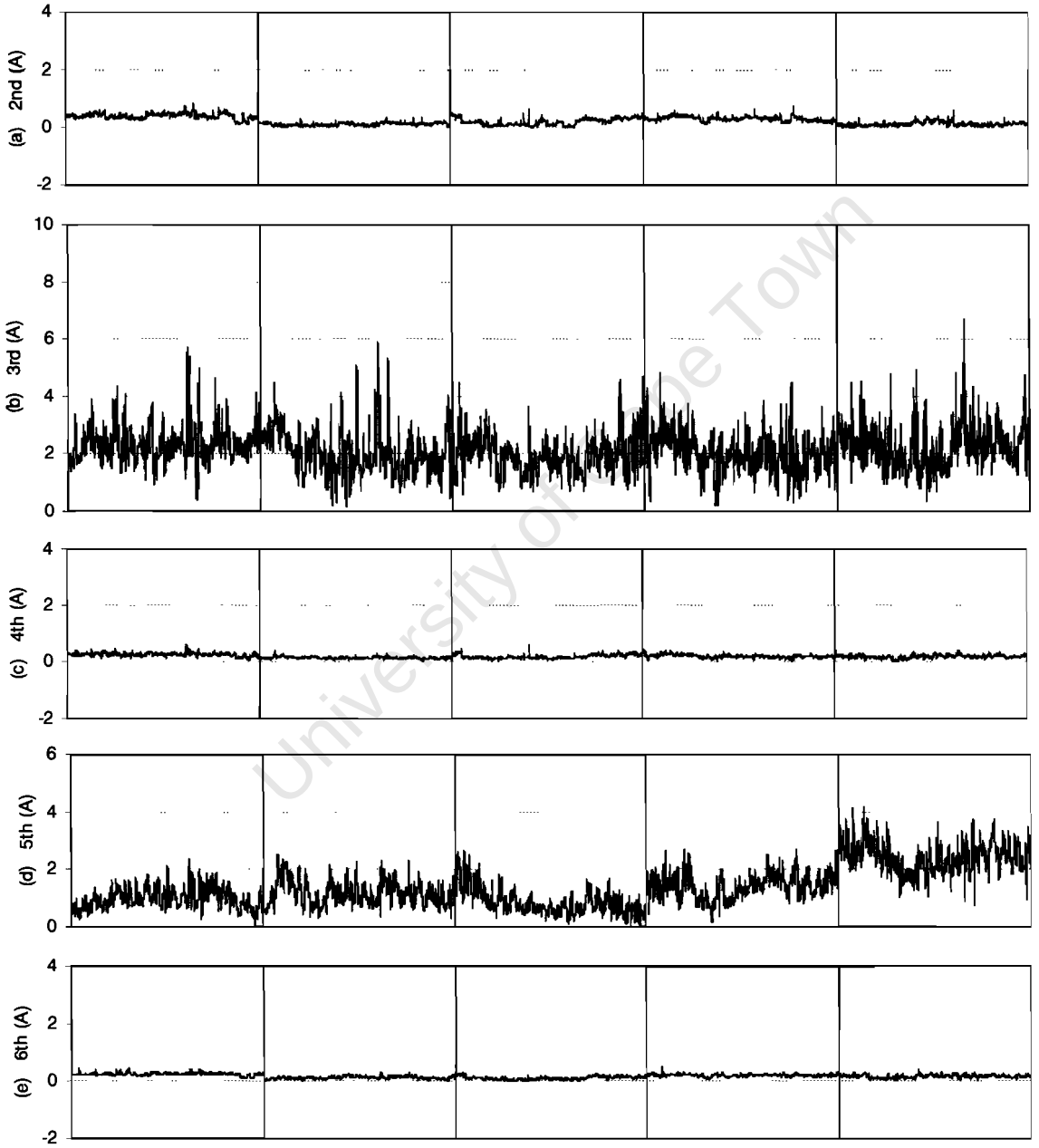

Figure 6. 8 Currents measured on the high voltage side of the Hydra substation transformer.

High voltage measurements kept the similar trend to that of low voltage measurements in every way. Harmonics were still present and each fluctuated at the same pace and remained unaffected by fluctuations in dc currents. The presence of dc currents in the measured phase contributed by the neutral is hence not having any effects on the current harmonics' content.

6.2.2 GRASSRIDGE SUBSTATION

A single 400 / 132 / 22 kV, 500 MVA, three-phase, three-limb, core type autotransformer manufactured in 1991 was monitored at Grassridge Substation. Since the installation of the Sunburst monitoring equipment, the transformer was utilized at about 50% of its rating [30].

Figure 6. 6 to Figure 6. 8 show current measured (per minute for 24 hours) on the phase A of the transformer as provided by Eskom. From left to right, the graphs are divided up into five vertical blocks for data collected on 31 March 2001, 25 September 2001, 21 October 2001, 06 November 2001 and on 24 November 2001 respectively.

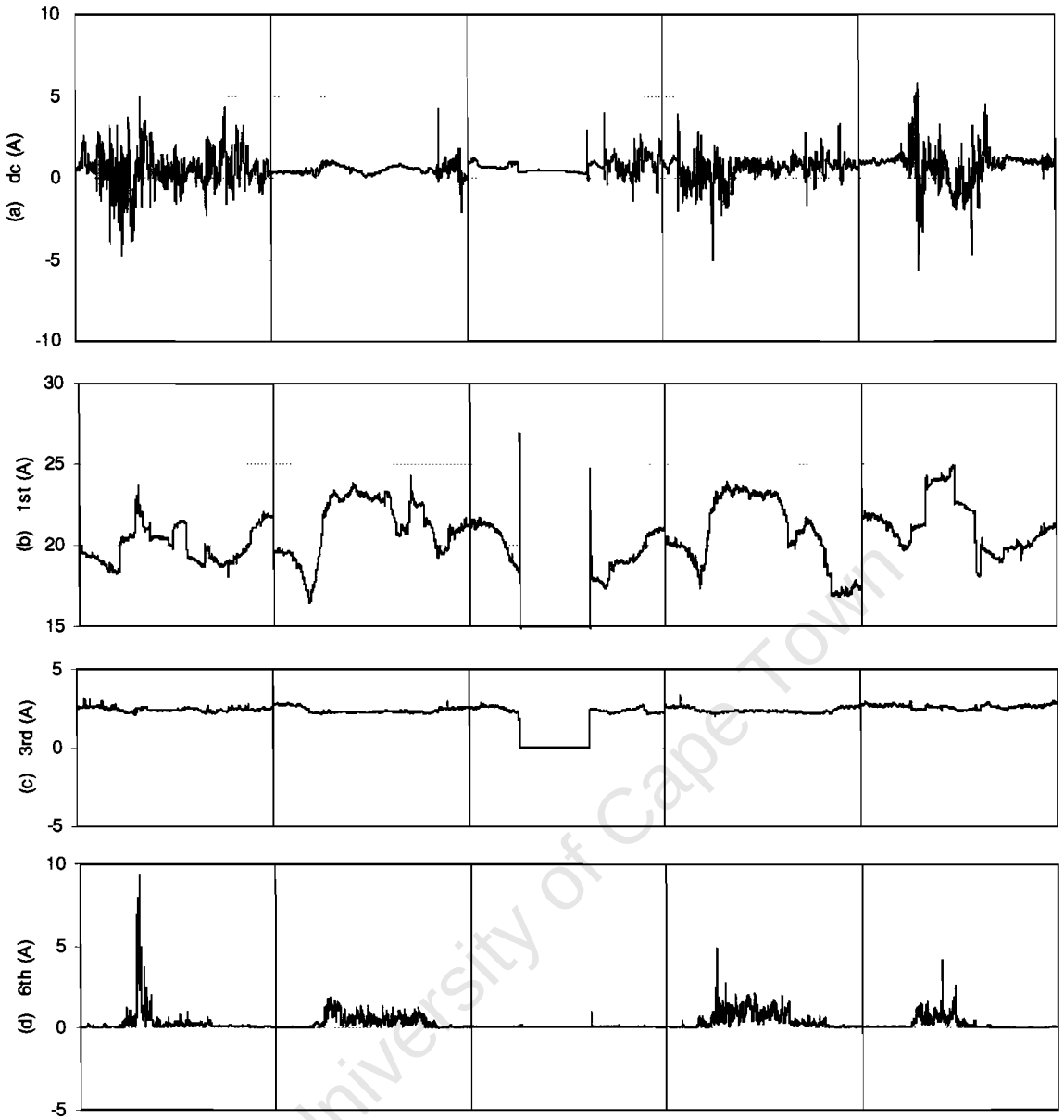

Figure 6. 9 Currents measured in the neutral of the Grassridge substation transformer.

There are dc currents present in the neutral of the transformer in Figure 6. 9(a) with or without much storm activities occurring. The currents fluctuate greatly as the K-index increases, responding to the presence of storm activities. Similarly, there are third harmonics present in the neutral of the transformer in Figure 6. 9(c) without much storm activities occurring, which rarely fluctuate with increasing storm activities. Sixth harmonics is the opposite of third harmonics; they are present in small quantities at lower K-index and fluctuate greatly alongside dc currents as higher K-index with magnitudes exceeding those of dc currents in terms of magnitudes at times.

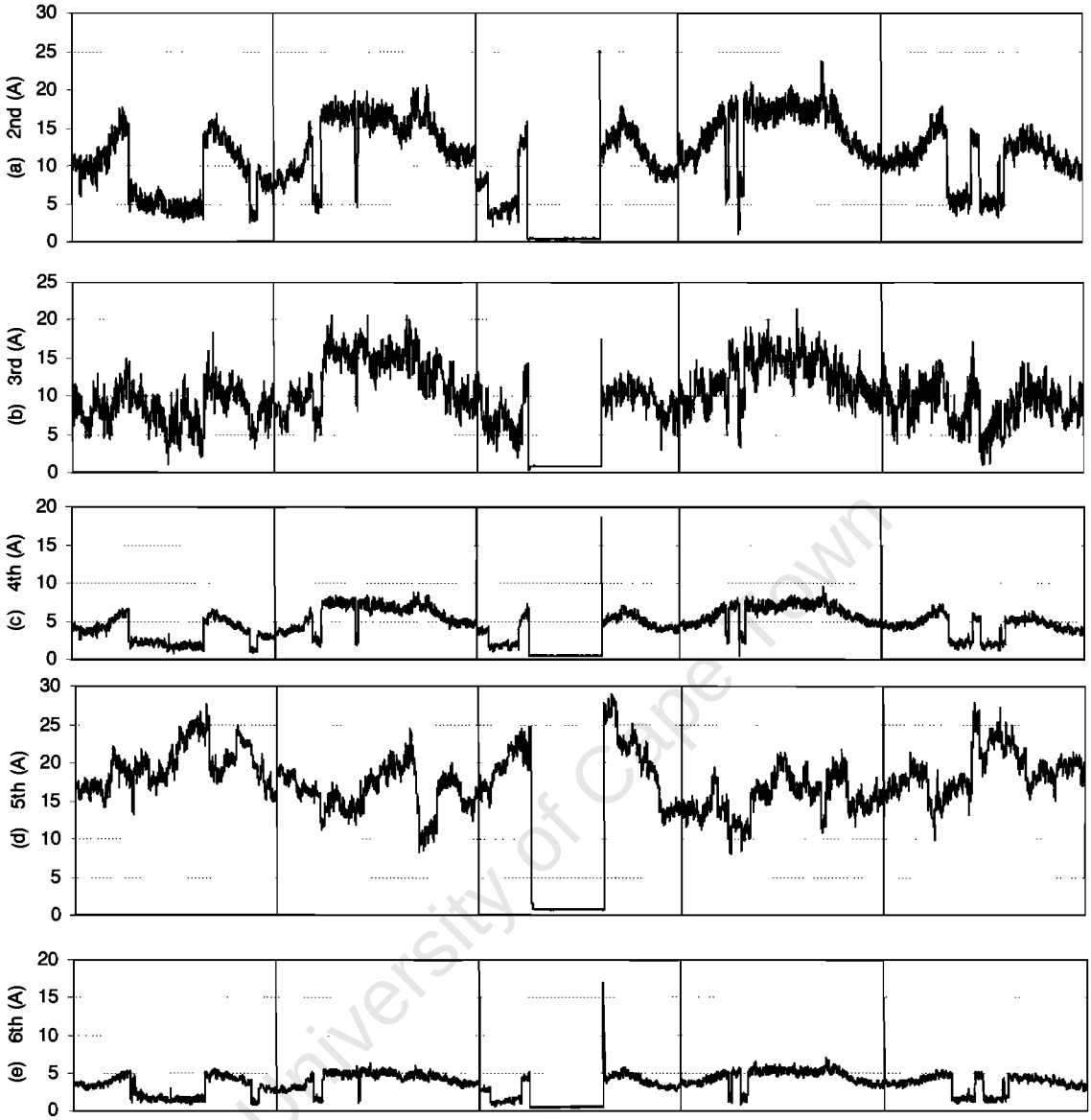

Figure 6. 10 Currents measured on the low voltage side of the Grassridge substation transformer.

The neutral dc currents would ideally split up in equal proportions among the three phases. Second, third, fourth, fifth and sixth harmonics are present in the phase and each constantly fluctuating at the same pace throughout, not necessarily fluctuating with dc currents' fluctuations. The presence of dc currents in the measured phase contributed by the neutral is hence not having any effects on the current harmonics' content.

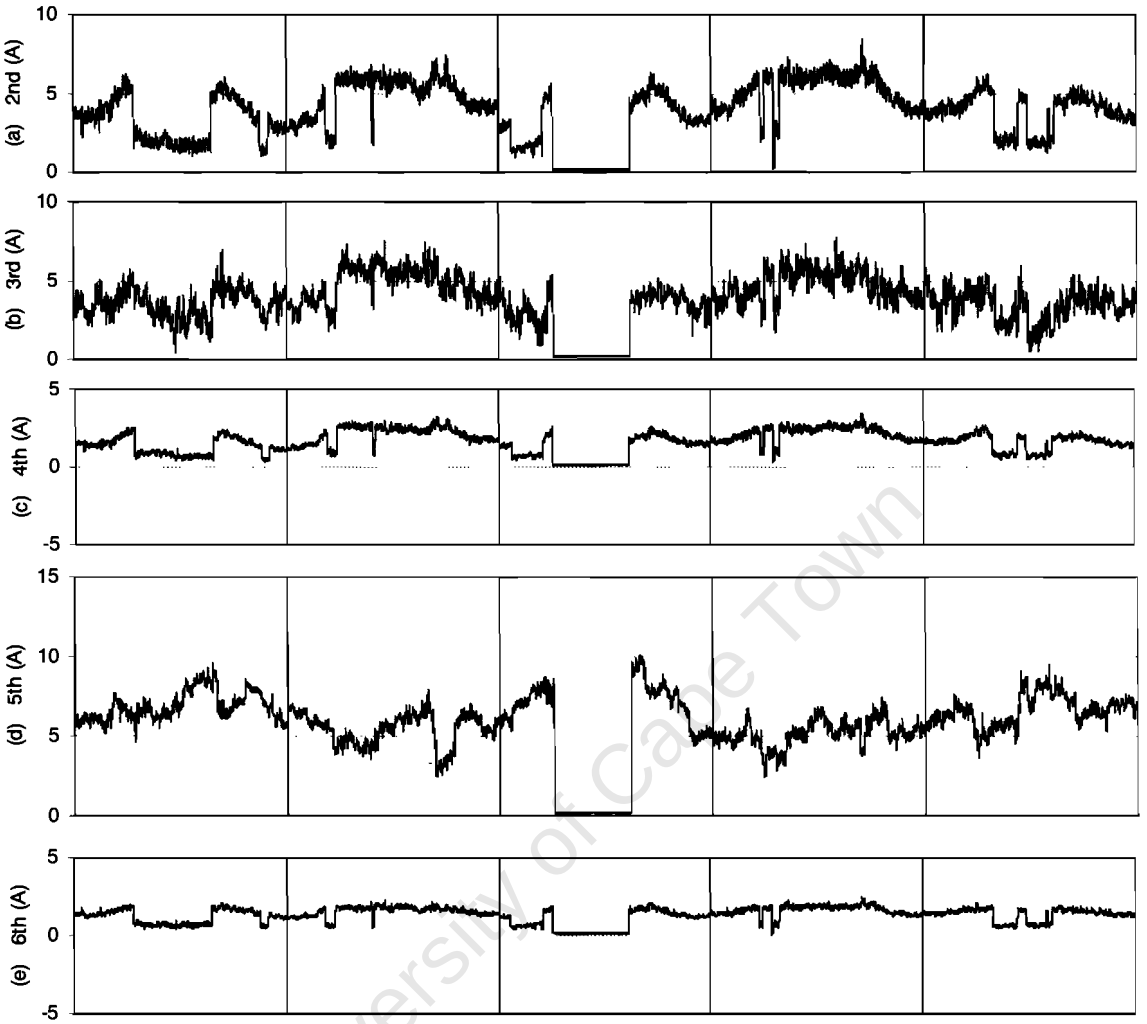

Figure 6. 11 Currents measured on the high voltage of the Grassridge substation transformer.

High voltage measurements kept the similar trend to that of low voltage measurements in every way. Harmonics were still present and each fluctuated at the same pace and remained unaffected by fluctuations in dc currents. The presence of dc currents in the measured phase contributed by the neutral is hence not having any effects on the current harmonics' content.

6.3 COMPARISONS OF FIELD RESULTS TO MODELLING AND LABORATORY RESULTS

Comparisons would only be done for Grassridge transformer whose magnetization properties could be obtained and whose configuration (three limb) had been modelled. They are closely correlated to those of the reactors used in this project as Figure 6. 12 illustrates.

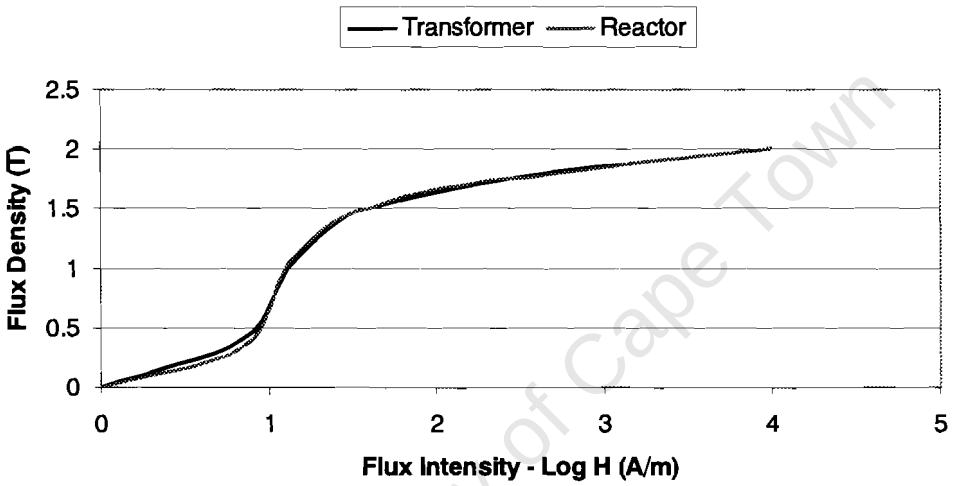

Figure 6. 12 Magnetisation curve for Grassridge transformer and project's reactor [41].

Figure 6. 13 and Figure 6. 14 display current harmonics as percentage of fundamental currents in the Grassridge transformer phase and neutral respectively. High voltage and low voltage sides consisted of the same harmonics' percentage.

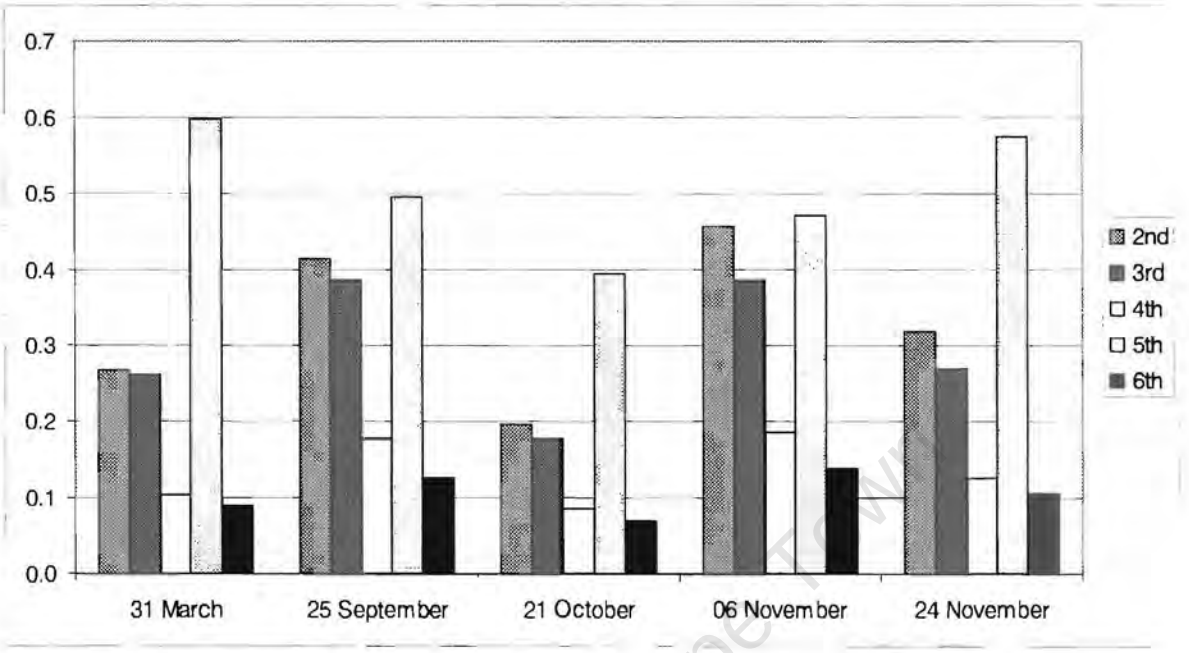

Figure 6. 13 Current harmonics in the Grassridge transformer phase as percentage of fundamental currents.

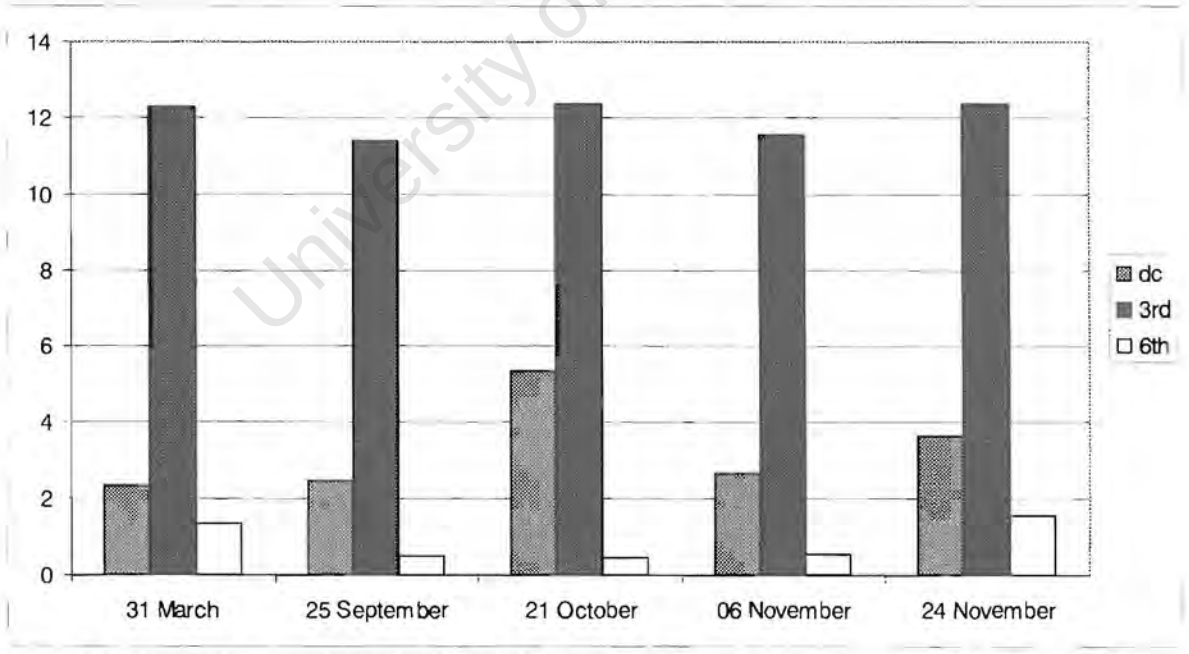

Figure 6. 14 Current harmonics in the Grassridge transformer neutral as percentage of fundamental currents.

6.3.1 FIELD RESULTS VERSUS MODELLED RESULTS

Due to a lack of detailed design information, comparing field results with modelled results becomes very difficult. What is apparent in the Grassridge transformer phase though is that the levels of harmonics in Figure 6. 13 measured in the Grassridge transformer seemed to be achievable by injecting a level of dc flux between 0 and 0.1 Tesla when assuming that there is no dc flux cancelling effect among the phases (Appendix E) as the measurement trend falls between 0 and 0.1 dc flux injection shown in Figure 6. 15 and Figure 6. 16. This level of dc flux injection is light and would only lead transformers into light saturation still within compatibility levels.

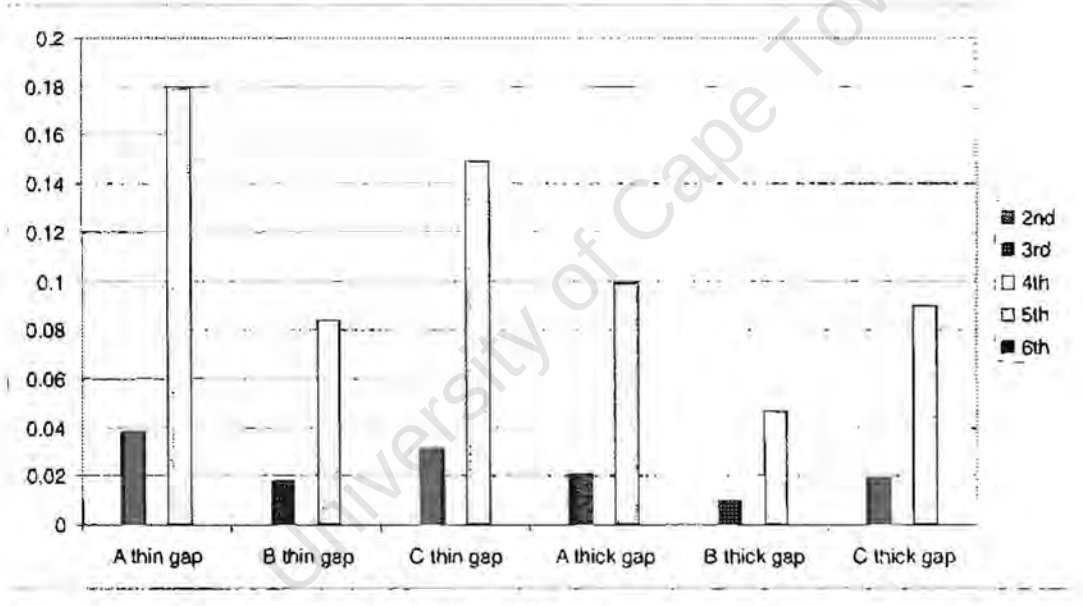

Figure 6. 15 Modelled current harmonics in the three-phase reactor units as percentage of fundamental currents without dc flux injection.

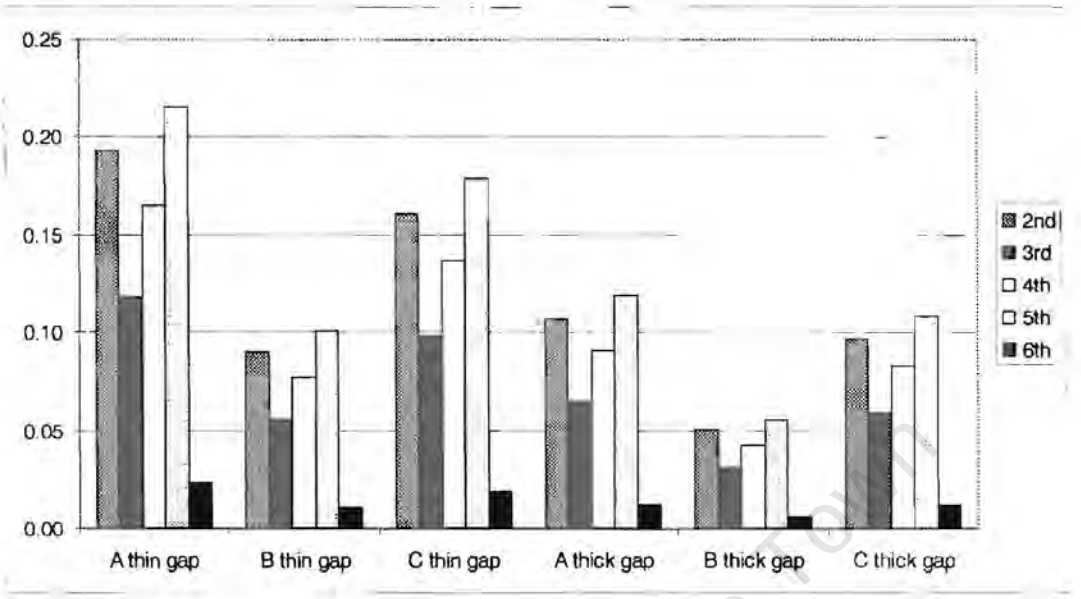

Figure 6. 16 Modelled current harmonics in the three-phase reactor units as percentage of fundamental currents with 0.1 dc flux injection.

In these illustrations, both modelled harmonics and Grassridge transformer's harmonics both follow a similar trend of magnitudes (just as thin and thick gapped reactors do although they have different magnitudes and design information – air gap); fifth harmonics is commonly higher followed by second, then third, fourth and fifth lastly.

Modelled neutral measurements follow the same trend as field neutral measurement through in that third harmonics are usually higher, then dc and last sixth harmonics.

6.3.2 FIELD RESULTS VERSUS MEASURED RESULTS

Compared to laboratory phase current harmonics for three-phase reactor units, Grassridge tend to follow a similar trend. In the Grassridge phase, fifth harmonics is commonly higher followed by second, then third, fourth and fifth lastly as depicted in Figure 6. 13. The laboratory results followed this trend half of the time perhaps because of the E-cores imperfect alignment and thus the trend was only followed in phase B and phase C of the thin-gapped units and in phase C of the thick-gapped units in Figure 6. 17.

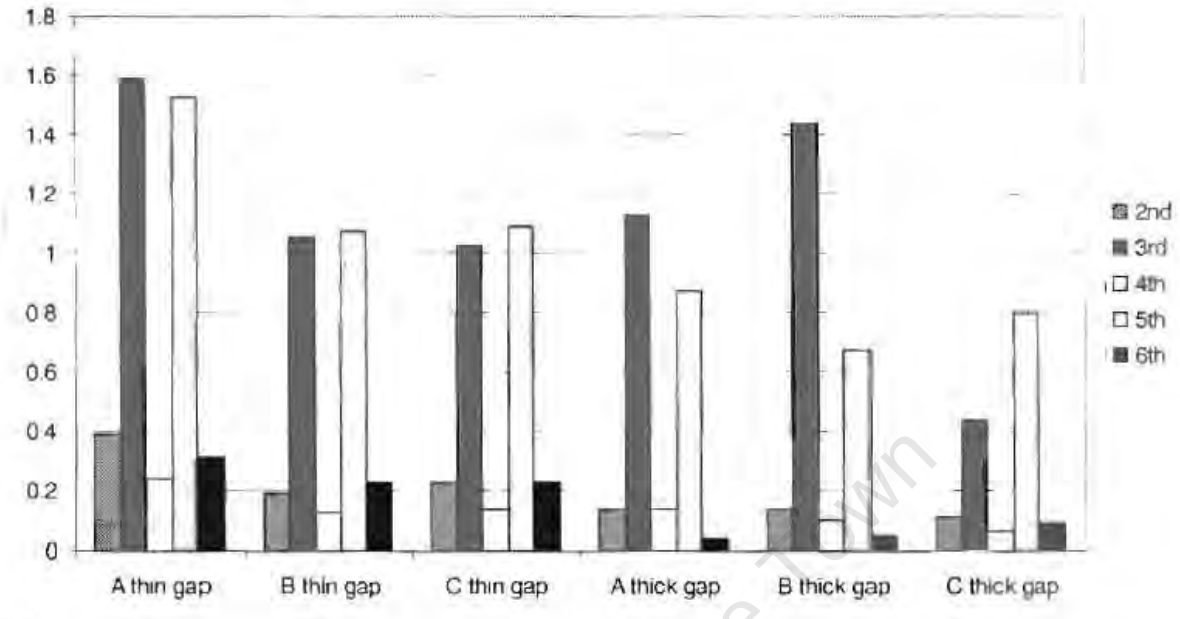

Figure 6. 17 Laboratory measured current harmonics in the three-phase reactor units as percentage of fundamental currents.

6.4 INTEPRETATION OF RESULTS

GICs only affected third and sixth harmonics in the neutrals of both Hydra and Grassridge transformers. Phase harmonics remained unchanged by GICs. Therefore either measured GICs were too small to cause any impact in the phases of the transformers or dc currents contribution from different phases cancelled out. The dc currents however only cancel each out in the case of three-phase three-limb transformers and not in the three-phase five-limb transformers. It therefore seems that measured and modelled results of reactors alone are not sufficient to explain the reason why GICs were only affecting the neutral currents and not the phase currents.

6.5 SUMMARY

Field measurements such as dc currents in the neutral, fundamental currents, harmonic components (from second to the sixth harmonic) were collected by sunburst monitoring

equipment fitted on Hydra and Grassridge transformers prior to the major storms reported on 31 March 2001, 06 November 2001 and 24 November 2001 and minor storms on 25 September 2001 and 21 October 2001.

Hydra measurements indicated a presence of dc currents in the neutral of the transformer with or without much storm activities increasing as the storm activities increase. Similarly, third and sixth harmonics were present in the neutral of the transformer with or without much storm activities fluctuating alongside dc currents' fluctuations. High voltage measurements were very similar to low voltage measurements in terms of percentages. Harmonics were still present but remained unaffected by the presence of dc currents in the neutrals.

Grassridge measurements also indicated a presence of dc currents in the neutral of the transformer with or without much storm activities increasing as the storm activities increase. Third and sixth harmonics were measured in the neutral of the transformers fluctuating alongside dc currents' fluctuations. High voltage measurements' relationship to low voltage measurements was similar to Hydra measurements. Both remained unaffected by the presence of dc currents in the neutral.

Grassridge transformer measurements were correlated to modelled and measured quantities since its transformer's magnetization properties are known and its configuration (three limb) was modelled in Chapter 4. Despite the lack of detailed design information that could lead to effective comparison, it was observed that Grassridge measurements looked similar to modelled measurements with a slight injection of dc flux density between 0 and 0.1 Teslas. It's only this time that fifth harmonics is predominantly higher followed by second, then third, fourth and fifth lastly. Measured harmonics also followed this trend and hence in agreement with Grassridge measurements.

CHAPTER 7

CONCLUSIONS AND RECOMMENDATIONS

In an event of a geomagnetic storm, it could take relatively low GICs, compared to fundamental currents, to drive single-phase reactors into saturation. Unless there is an unbalance in the magnetic circuit, three-phase units do not get driven into saturation by GICs as GICs from all three phases cancel each other.

Saturation in transformers and reactors are accompanied with concealed and physical effects. Concealed effects are production of odd and even harmonics and increase in reactive power flow. Physical effects that usually result in equipment failure and physical damage are: intense stray flux, heating and gas evolution and even core deformation.

Concealed effects usually occur first in the early stages of saturation when GICs are a fraction of fundamental currents while physical effects occur under extreme saturation beyond the knee of the magnetization curve. In the early stages of saturation, operation of power system equipment may seem normal. The concealed effects such as introduction of both odd and even harmonics beyond recommended compatibility levels in the long run could be very detrimental to end-users' appliances and equipment such as motors.

Physical effects could occur as a result of repeated light GICs exposure over several solar cycles and when failure eventually occurs, the cause of failure might be in combination with and usually attributed to other factors. These extended duration raises the likelihood of loss-of-life to transformer and reactor insulations.

Based on the findings in this research, the following recommendations were made to reduce the sensitivity of transformers and reactors to GICs' damages.

Koen [30] recommended that reactors should be removed from the network prior to reported major geomagnetic events if possible but in this research, it is being recommended that only single-phase reactors should be disconnected.

For new transformers/reactors, use three-phase three-limb units as they are less susceptible to GICs than any other unit type and hence decreasing chances of saturation

REFERENCES

1. Acres Consulting Services Limited, "Study of the disruption of electric power systems by magnetic storms", Earth Physics Branch Open File 77-19, Department of Energy, Mines and Resources, Ottawa, 1975.
2. Albertson, V.D., J.M. Thorson, Jr., "Power system disturbances during a K-8 geomagnetic storm: August 4, 1972", IEEE Transaction on Power Apparatus and Systems, Vol. PAS-93, pp. 1025-1030, 1974.
3. Albertson, V.D., Thorson, J.M., and Miske, S.A., "The Effects of Geomagnetic Storms on Electrical Power Systems", IEEE PAS-93, No. 4, pp 1031-1044, July/August 1974.
4. Alloy Magnetic Cores (Pty) Ltd, "AMC Catalogue", May 2001.
5. Ashok, S., "Effects of power system harmonics on power system equipment and loads", Department of Electrical Engineering, R.E.C., Calicut.
6. Bolduc, L., and Aubin, J., "Effects of direct currents in power transformer, Part II. Simplified calculations for large transformers", Electr. Power Syst. Res (1977/1978), pp. 299-304.
7. Boteler, D.H., Pirjola, R.J., Nevanlinna, H., "The effects of geomagnetic disturbances on electrical systems at the earth's surface", Advances in Space Research 22 (1), 1998, pp. 17-27.
8. Cloete, R., Report No. 100098576, 28 September 2001; Report No. 100098932, 8 November 2001; Report No. 100098992, 14 November 2001, Analytical Services Cape, Eskom.
9. Cullimore, B.A., "Optimisation and automated data correlation in the NASA standard thermal/fluid system analyser", 33rd Intersociety Engineering Conference on Energy Conversion, Colorado Springs, August 1998.
10. Data obtained form the Hermanus Magnetic Observatory.
11. Davidson, W.F., "The Magnetic Storm of March 24, 1940 – Effects in the power system, Presentation to the Edison Electric Institute", May 07, 1940.

12. Della Tore, E., "Magnetic Hysteresis", IEEE Press, New York, NY, 1999.
13. Electric Research and management, Inc., SUNBURST GIC Network – Phase II Progress Report, February 1997.
14. Elovaara, J., P. Lindblad, A. Viljanen, T. Mäkinen, R. Pirjola, S. Larsson, and B. Kielen, "Geomagnetically induced currents in the Nordic power system and their effects on equipment, control, protection and operation", pres. CIGRE Colloquium, 30 Aug – 5 Sept., 1992.
15. Fink, D.G., "Standard Handbook for Electrical Engineers", 10th Edition, 1968.
16. Fluke Corporation "39/41 B Power harmonics tester users manual", 1996.
17. Harris, C.M., "Handbook of noise control", McGraw-Hill Book Co., 1957, pp. 1-14.
18. http://science.msfc.nasa.gov/ssl/pad/solar/images/grandad.jpg, April 2002.
19. http://science.nasa.gov/ssl/PAD/SOLAR, April 2002.
20. http://www.geolab.nrcan.gc.ca/geomag/e_history-1.html, May 2002.
21. http://www.mpelectric.com/storms/lrgtrans.htm, May 2002.
22. http://www.nepsi.com/nepsihome.reactn.htm, May 2002.
23. http://www.powerstudies.com/content/resources/MikesHarmArticle.pdf, An introduction to power system harmonics, July 2003.
24. http://www.spacetoday.org/SolSys/Sun/Sunspots.html, May 2002.
25. http://www.wws.princeton.edu/cgi-bin/byteserv.prl/~ota/disk2/1990/9034/903404.PDF, April 2002.
26. IEEE Transmission and Distribution Committee, "Geomagnetic Disturbance Effects on Power Systems", IEEE Transactions on Power Delivery, Vol. 8, No.3, pp 1206-1216, July 1993.
27. Kappenman, J.G., "Geomagnetic storms and impacts on power systems: Lessons learned from Solar Cycle 22 and outlook for Solar Cycle 23", IEEE Power Engineering Review, May 1996.
28. Kappenman, J.G., and Albertson, V.D., "Bracing for the Geomagnetic Storms", IEEE Spectrum Magazine, pp. 27-33, March 1990.
29. Koen, J., "Geomagnetically Induced currents and their presence in the Eskom transmission network", MSc (Eng.) Thesis, University of Cape Town, February 2000.

30. Koen, J., "Geomagnetically Induced currents in the Southern African Electricity Transmission Network", PhD Thesis, University of Cape Town, April 2002.
31. Koen, J., and Gaunt, C.T., "Disturbances in the Southern African Power Network due to Geomagnetically Induced Currents", CIGRE, August 2001.
32. Langevin, M.P. "Magnetisme et theorie des electrons", Ann. Chim. et Phys., Vol. 70, 1905.
33. Lu, S., and Liu, Y., "FEM Analysis of DC Saturation to Assess Transformer Susceptibility to Geomagnetically Induced Currents", IEEE Transactions on Power Delivery, Vol. 8, No.3, July 1993.
34. Lu, S., and Liu, Y., "Fundamental analysis of transformer GIC magnetisation using finite element approach", Proceedings of the 53rd Annual Meeting of the American Power Conference. Vol. 53, Pt.2, Chicago, IL, USA, 1991, pp. 1173-1178.
35. Lu, S., Liu, Y., and De La Ree, J., "Harmonics generated from a dc biased transformer", IEEE Transactions on Power Delivery, Vol. 8, No.2, April 1993, pp. 725-731.
36. Mafani, A.L., "Effect of direct current on power system reactors", BSc (Eng), University of Cape Town, October 2001.
37. Mayergoyz, I.D., "Mathematical Models of Hysteresis", Springer-Verlag, New York, NY, 1991.
38. Molinski, T.S., "Why utilities respect geomagnetically induced currents", Journal of atmospheric and solar-terrestrial physics, 2000, pp. 1-14.
39. Morrison, N., "Introduction to Fourier Analysis", John Wiley & Sons, 1994.
40. NRS 048-2 Standards, "Electricity supply – Quality of supply", 1996.
41. Online communication with Mr. A. Wellard, ABB, South Africa, May 2002.
42. Online communication with Mr. Antti Pulkkinen, Finnish Meteorological Institute, Finland, June 2002.
43. Preisach, F., "Über die magnetishe Nachwirkung", Z. Phys., Vol. 94, pp.277, 1935.
44. Private communication with Mr. Jacko Koen, Eskom, South Africa, June 2002.
45. Ringlee, R.G., and Stewart, J.R., "Geomagnetic effects on Power Systems", IEEE Power Engineering Review, Vol. 9, No.7, July 1989, pp. 6-9.

46. Roters, H.C., "Electromagnetic devices", NY, John Wiley and Sons, 1941, pp. 95&117.
47. Sen, PC, "Principles of electric machines and power electronics", Second Edition, John Wiley & Sons, 1997.
48. Sutcliffe, P.R. and P.B. Kotzé, "Proceedings of the workshop on the Hermanus Magnetic Observatory's Geophysical Services," no publisher, February 1992.
49. Takács, J., "A phenomenological mathematical model of hysteresis", COMPEL, Vol. 20, No.4, pp. 1002-1014, 2001.
50. Takasu, N., Oshi, T., Miyawaki, F., Saito, S., and Fujiwara, Y., "An experimental analysis of dc excitation of transformers by geomagnetically induced currents", IEEE Transactions on Power Delivery, Vol. 9, No. 2, April 1994, pp. 1173 – 1182.
51. Tattersfield, G.M., "Electromagnetic Field Theory", Student Manual, 1998 Edition.
52. Terörde, G., Schneider, J., and Hameyer, K., "Investigations of the audible noise of inductors with respect to different ferromagnetic materials", COMPEL, Vol. 18, No.4, 1999, pp. 647-655.
53. Tousignant, D., Bolduc, L., and Dutil, A., "A method for the indication of power transformer saturation", Electric Power Systems Research, Vol. 37, Issue 2, pp 115-120, May 1996.
54. Trutt, F.C., Erdelyi, E.A., and Hopkins, R.E., "Representation of the magnetization characteristic of DC machines for computer use", IEEE Transaction Power Apparatus and Systems, vol. PAS-87, No. 3, 1986, pp. 665-669.
55. Walling, R.A., and Khan, A.H., "Characteristics of transformer exciting-current during geomagnetic disturbances", IEEE Transaction on Power Delivery, Vol. 6, No. 4, October 1991, pp. 1707-1712.
56. Weiss, P.E., "L' Hypothese du Champ Moleculare et la Propriete Ferromagnetique", J. de Phys., VI, p.661, 1907.
57. Weiss, P.E., "La variation du ferromagnetisme avec la temperature", Comptes Rendus, Vol. 143, p.1136, 1906.

Appendix A: Cycle Numbers and their respective periods as given by scientists since 1755[1].

Number	Began	Duration
1	March 1755	11 years, 3 months
2	June 1766	9 years
3	June 1775	9 years, 3 months
4	September 1784	13 years, 8 months
5	May 1798	12 years, 7 months
6	December 1810	12 years, 5 months
7	May 1823	10 years, 6 months
8	November 1833	9 years, 8 months
9	July 1843	9 years, 8 months
10	December 1855	12 years, 5 months
11	March 1867	11 years, 9 months
12	December 1878	11 years, 3 months

Number	Began	Duration
13	March 1890	11 years, 11 months
14	February 1902	11 years, 6 months
15	August 1913	10 years
16	August 1923	10 years, 1 month
17	September 1933	10 years, 5 months
18	February 1944	10 years, 2 months
19	April 1954	10 years, 6 months
20	October 1964	11 years, 8 months
21	June 1976	10 years, 3 months
22	September 1986	9 years, 8 months
23	May 1996	
24	*circa*2007	

1. http://www.spacetoday.org/SolSys/Sun/Sunspots.html, April 2002

Appendix B: Modelled currents, current harmonics and reactive power at ac flux of 0.9 Teslas.

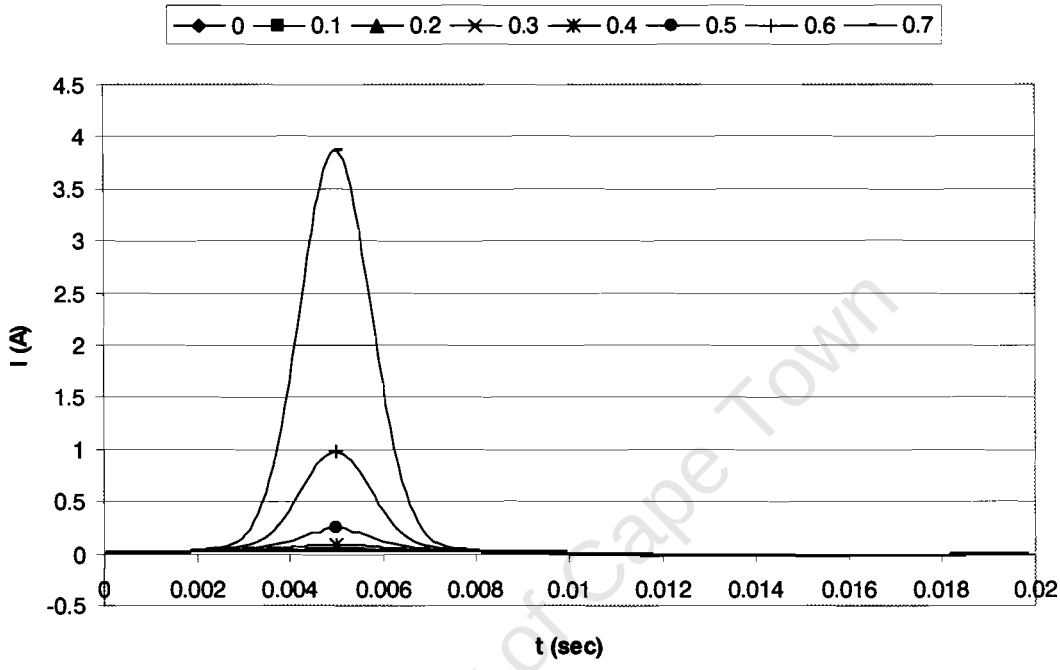

Figure 1 Current waveforms resulting from ac flux of 0.9 Teslas plus a range of dc flux offset of 0.1 to 0.7Teslas for the non-gapped single-phase reactor.

a. **One phase**
b. **Neutral**

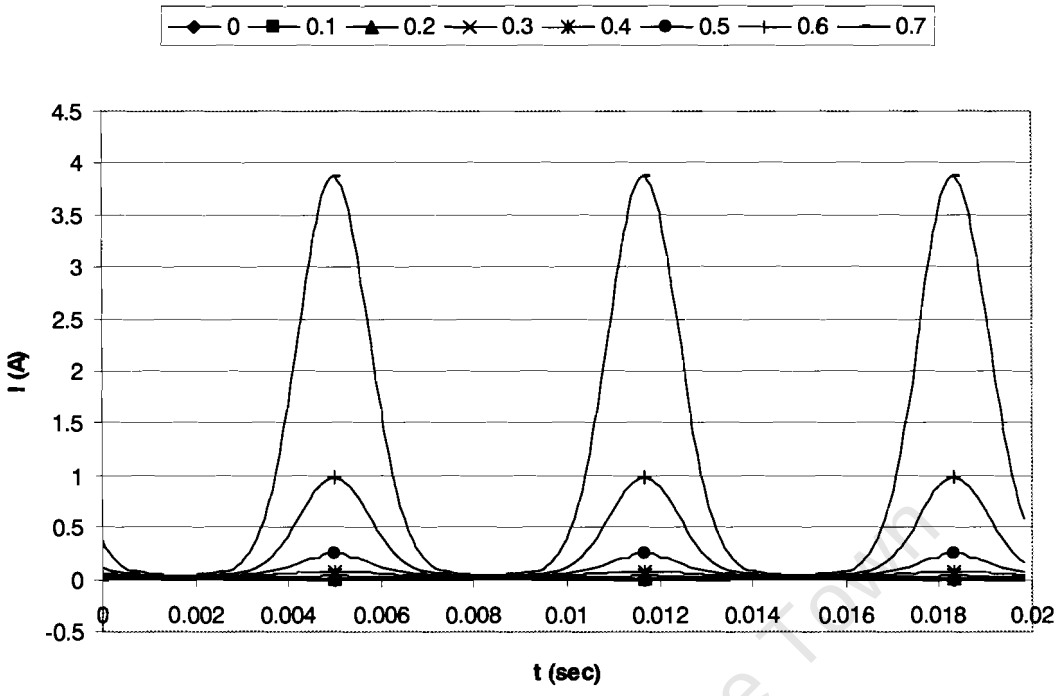

Figure 1 (continued)

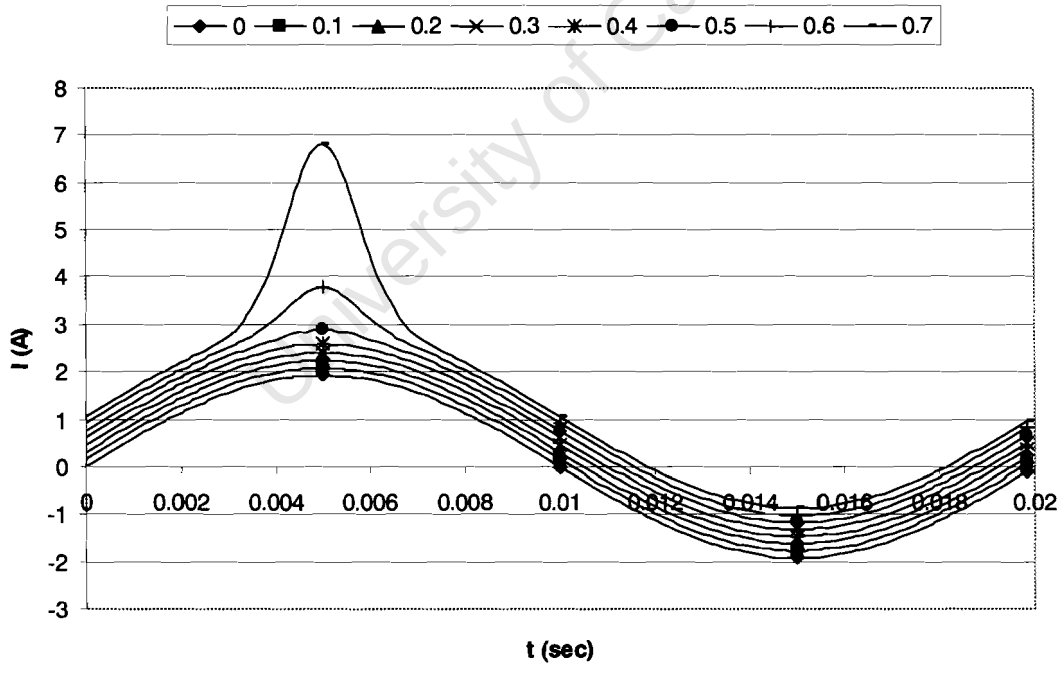

Figure 2 Current waveforms resulting from ac flux of 0.9 Teslas plus a range of dc flu x offset of 0.1 to 0.7 Teslas for the 250 micrometre gapped single-phase reactor in one-phase.

a. One phase

b. Neutral

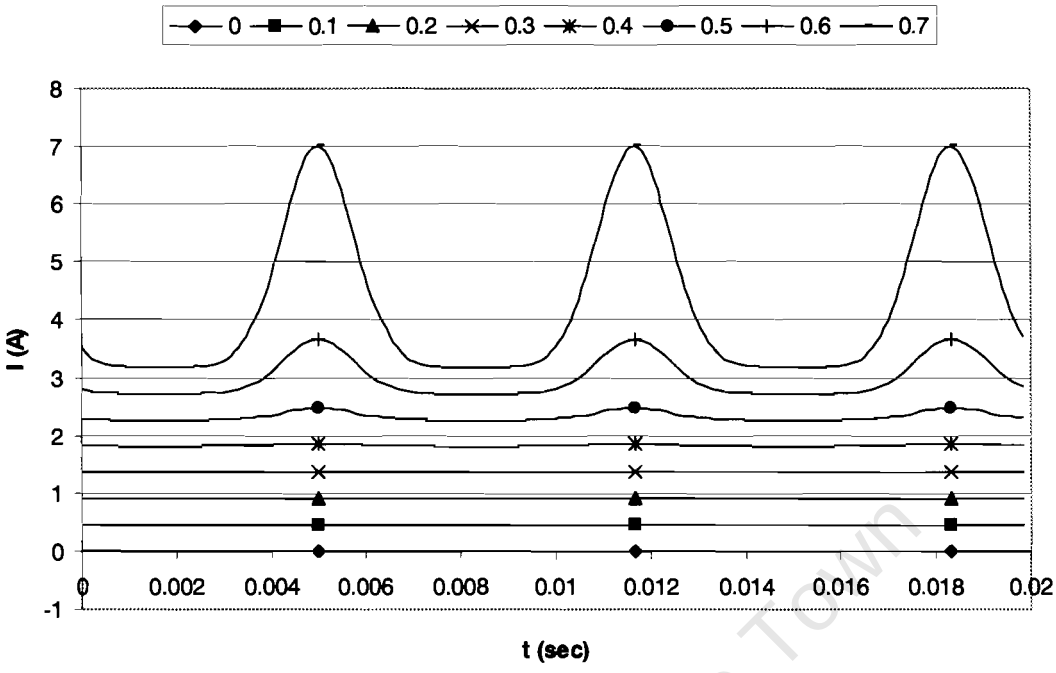

Figure 2 (continued)

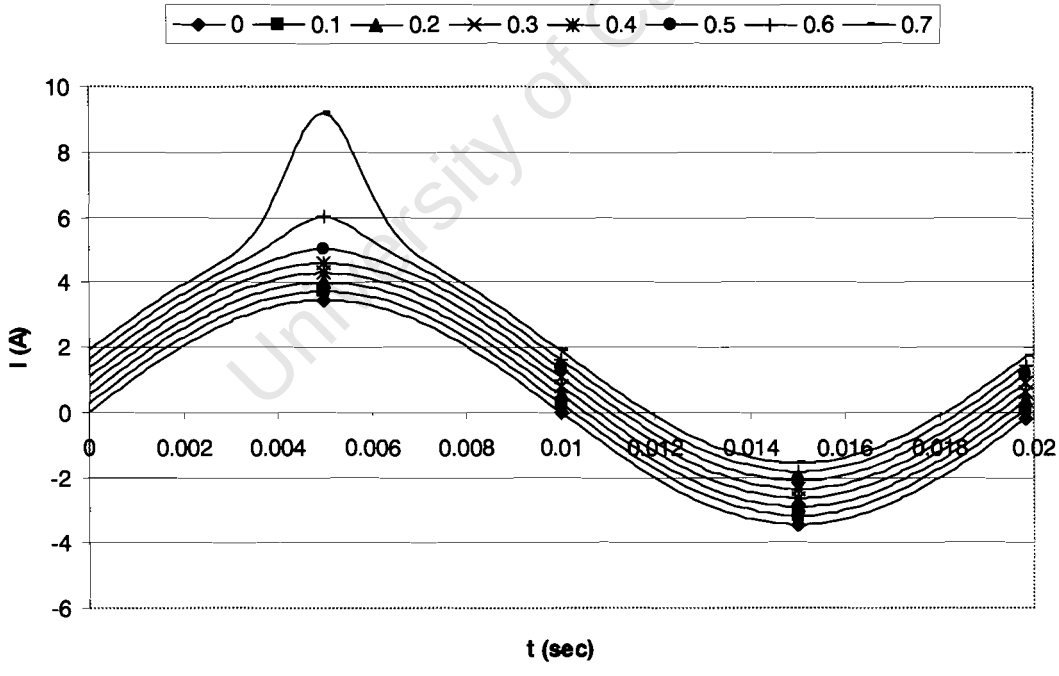

Figure 3 Current waveforms resulting from ac flux of 0.9 Teslas plus a range of dc flux offset of 0.1 to 0.7 Teslas for the 450 micrometre gapped single-phase reactor in one-phase.

a. **One phase**
b. **Neutral**

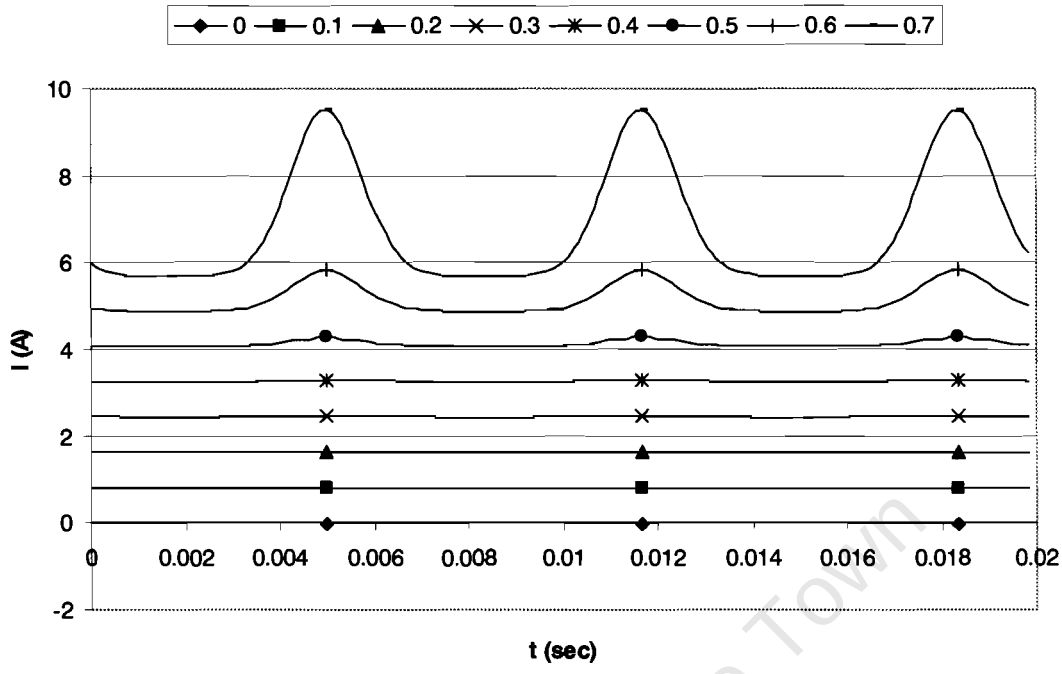

Figure 3 (continued)

Table 1 Harmonic current contents of current waveform and reactive power at ac flux of 0.9 Teslas for single-phase non-gapped reactors in one phase.

ac Flux	dc Flux	Current (A)			Current harmonics (% of fundamental current)									Reactive power
(T)	(T)	dc	total	1st	2nd	3rd	4th	5th	6th	7th	8th	9th	10th	(VAR)
0.9	0	-0	0.02	0.02	0.0	7.8	0.0	5.4	0.0	0.8	0.0	0.4	0.0	1.29
0.9	0.1	0	0.02	0.02	0.3	6.6	3.8	5.3	0.3	0.6	0.4	0.4	0.1	1.30
0.9	0.2	0	0.02	0.02	3.2	1.6	8.5	6.0	0.3	0.5	1.1	0.4	0.1	1.38
0.9	0.3	0.01	0.02	0.02	10.0	6.9	13.7	7.2	1.5	1.6	1.2	0.2	0.2	1.53
0.9	0.4	0.01	0.03	0.03	24.2	20.9	21.5	11.4	5.5	4.3	2.6	1.2	0.9	1.91
0.9	0.5	0.03	0.07	0.05	52.0	45.9	38.9	26.7	19.0	14.4	10.2	7.1	5.1	3.33
0.9	0.6	0.1	0.26	0.14	78.4	68.9	56.9	43.4	32.4	23.4	15.8	10.0	6.0	9.94
0.9	0.7	0.38	1.01	0.52	88.1	76.7	62.9	48.6	35.8	24.9	16.3	10.1	5.8	36.67

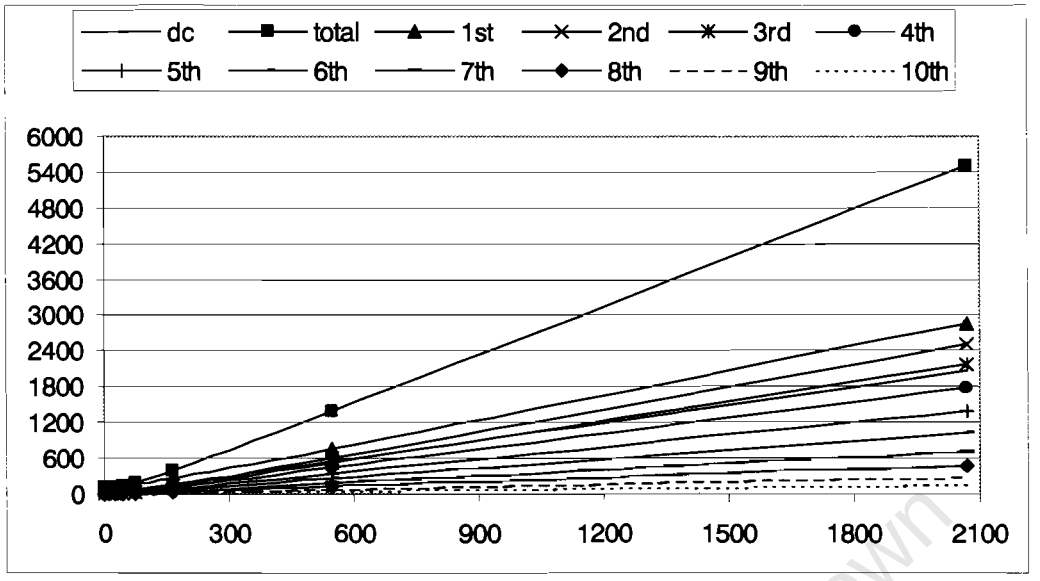

Figure 4 Current harmonics versus dc current both taken as a percentage of fundamental current (both at 0 dc current offset) at ac flux of 0.9 Teslas for single-phase non-gapped units in one phase.

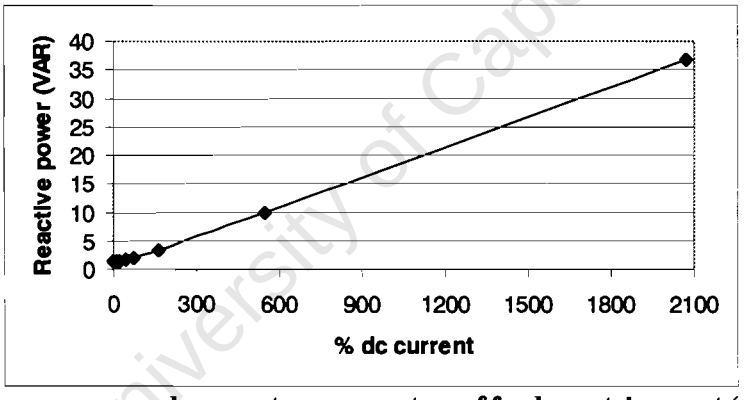

Figure 5 Reactive power versus dc current as a percentage of fundamental current (at 0 dc current offset) at ac flux of 0.9 Teslas for single-phase non-gapped units.

Table 2 Harmonic current contents of current waveform and reactive power for single-phase non-gapped reactors in the neutral.

ac Flux	dc Flux	Current (A)			Current harmonics (% of fundamental current)								
(T)	(T)	dc	total	1st	2nd	3rd	4th	5th	6th	7th	8th	9th	10th
0.9	0	0	0	0.00	663	∞	1305	454	492	115	87.1	∞	224
0.9	0.1	0.01	0.01	0.00	130	∞	151	52.3	∞	30	22.6	∞	23
0.9	0.2	0.01	0.01	0.00	62	∞	25	20.0	∞	20	15.0	∞	9
0.9	0.3	0.02	0.02	0.00	33	∞	45	8.0	∞	27	7.6	∞	7
0.9	0.4	0.04	0.04	0.00	5	∞	116	7.6	∞	53	12.6	∞	21
0.9	0.5	0.09	0.12	0.00	55	∞	197	42.4	∞	135	37.4	∞	79
0.9	0.6	0.3	0.44	0.00	109	∞	308	82.4	∞	245	36.3	∞	121
0.9	0.7	1.13	1.74	0.00	131	∞	331	89.2	∞	262	27.6	∞	120

Table 3 Harmonic current contents of current waveform and reactive power for single-phase 250 micrometre gapped reactors in one phase.

ac Flux	dc Flux	Current (A)			Current harmonics (% of fundamental current)									Reactive power
(T)	(T)	dc	total	1st	2nd	3rd	4th	5th	6th	7th	8th	9th	10th	(VAR)
0.9	0	-0	1.36	1.36	0.0	0.1	0.0	0.1	0.0	0.0	0.0	0.0	0.0	96.21
0.9	0.1	0.15	1.37	1.36	0.0	0.1	0.1	0.1	0.0	0.0	0.0	0.0	0.0	96.23
0.9	0.2	0.3	1.4	1.36	0.0	0.0	0.1	0.1	0.0	0.0	0.0	0.0	0.0	96.30
0.9	0.3	0.46	1.44	1.36	0.2	0.1	0.2	0.1	0.0	0.0	0.0	0.0	0.0	96.45
0.9	0.4	0.61	1.5	1.37	0.5	0.4	0.4	0.2	0.1	0.1	0.1	0.0	0.0	96.83
0.9	0.5	0.78	1.59	1.39	1.8	1.6	1.3	0.9	0.6	0.5	0.3	0.2	0.2	98.26
0.9	0.6	1	1.8	1.48	7.4	6.5	5.4	4.1	3.1	2.2	1.5	1.0	0.6	104.86
0.9	0.7	1.42	2.47	1.86	24.6	21.4	17.5	13.5	10.0	6.9	4.6	2.8	1.6	131.60

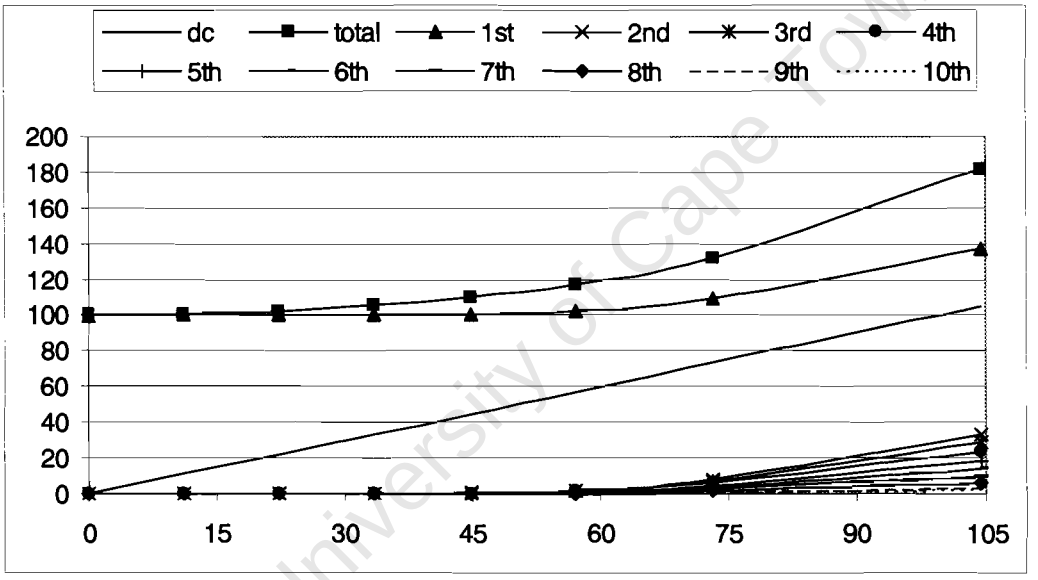

Figure 6 Current harmonics versus dc current both taken as a percentage of fundamental current (both at 0 dc current offset) at ac flux of 0.9 Teslas for single-phase 250 micrometre gapped units in one phase.

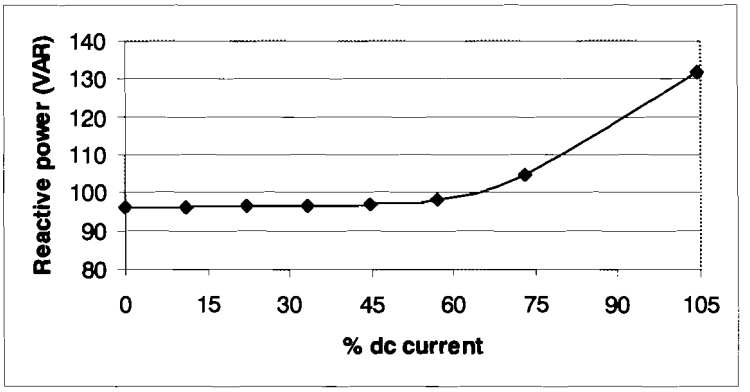

Figure 7 Reactive power versus dc current as a percentage of fundamental current (at 0 dc current offset) at ac flux of 0.9 Teslas for single-phase 250 micrometre gapped units.

Table 4 Harmonic current contents of current waveform and reactive power for single-phase 250 micrometre gapped reactors in the neutral.

ac Flux	dc Flux	Current (A)			Current harmonics (% of fundamental current)								
(T)	(T)	dc	total	1st	2nd	3rd	4th	5th	6th	7th	8th	9th	10th
0.9	0	0	0	0.00	268	∞	537	167	∞	87.0	22.9	∞	173
0.9	0.1	0.45	0.45	0.00	63.0	∞	13.8	14.6	∞	20.5	10.0	∞	0.7
0.9	0.2	0.91	0.91	0.00	58.1	∞	13.1	12.4	∞	20.9	10.0	∞	0.9
0.9	0.3	1.37	1.37	0.00	63.6	∞	11.2	12.8	∞	20.9	10.0	∞	0.2
0.9	0.4	1.83	1.83	0.00	61.0	∞	10.0	13.5	∞	21.0	11.1	∞	1.0
0.9	0.5	2.33	2.33	0.00	65.2	∞	9.0	14.8	∞	24.0	12.6	∞	3.0
0.9	0.6	2.99	3	0.00	52.0	∞	20.7	16.2	∞	28.5	12.9	∞	9.2
0.9	0.7	4.27	4.47	0.00	23.9	∞	66.3	29.0	∞	64.9	14.7	∞	26.3

Table 5 Harmonic current contents of current waveform and reactive power for single-phase 450 micrometre gapped reactors in one phase.

ac Flux	dc Flux	Current (A)			Current harmonics (% of fundamental current)									Reactive power
(T)	(T)	dc	total	1st	2nd	3rd	4th	5th	6th	7th	8th	9th	10th	(VAR)
0.9	0	0	2.44	2.44	0.0	0.1	0.0	0.0	0.0	0.0	0.0	0.0	0.0	172.15
0.9	0.1	0.27	2.45	2.44	0.0	0.1	0.0	0.0	0.0	0.0	0.0	0.0	0.0	172.16
0.9	0.2	0.54	2.5	2.44	0.0	0.0	0.1	0.0	0.0	0.0	0.0	0.0	0.0	172.23
0.9	0.3	0.81	2.57	2.44	0.1	0.1	0.1	0.1	0.0	0.0	0.0	0.0	0.0	172.39
0.9	0.4	1.09	2.68	2.44	0.3	0.2	0.2	0.1	0.1	0.0	0.0	0.0	0.0	172.77
0.9	0.5	1.37	2.82	2.46	1.0	0.9	0.7	0.5	0.4	0.3	0.2	0.1	0.1	174.19
0.9	0.6	1.71	3.08	2.56	4.3	3.8	3.1	2.4	1.8	1.3	0.9	0.6	0.3	180.80
0.9	0.7	2.26	3.78	2.94	15.6	13.6	11.1	8.6	6.3	4.4	2.9	1.8	1.0	207.53

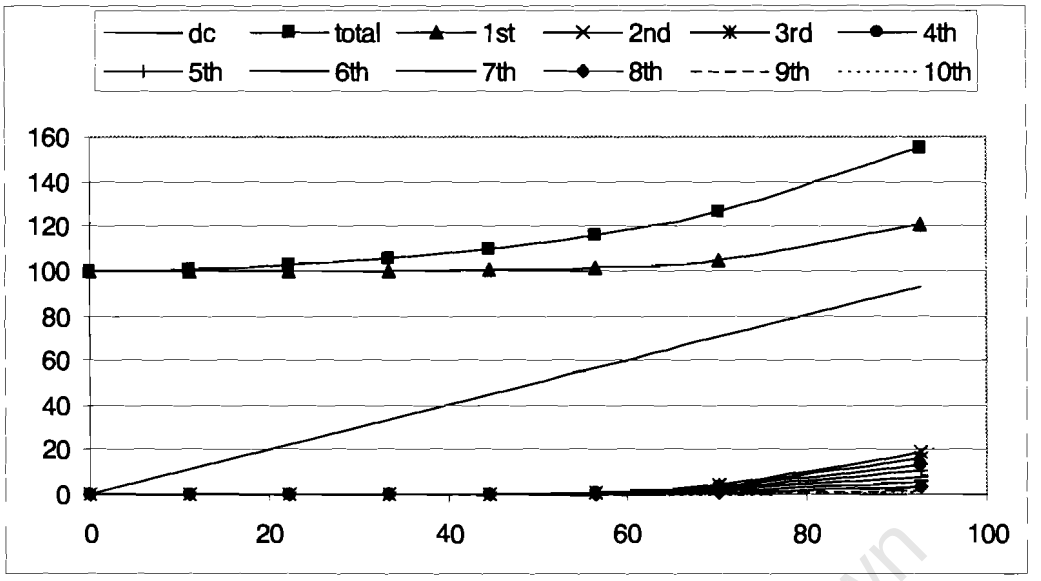

Figure 8 Current harmonics versus dc current both taken as a percentage of fundamental current (both at 0 dc current offset) at ac flux of 0.9 Teslas for single-phase 450 micrometre gapped units in one phase.

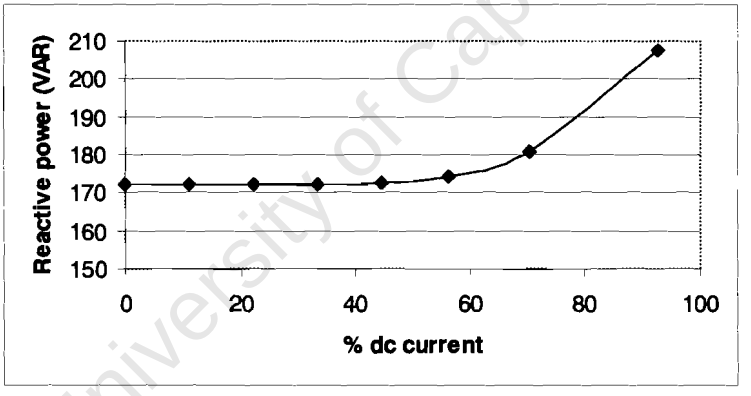

Figure 9 Reactive power versus dc current as a percentage of fundamental current (at 0 dc current offset) at ac flux of 0.9 Teslas for single-phase 450 micrometre gapped units.

Table 6 Harmonic current contents of current waveform and reactive power for single -phase 450 micrometre gapped reactors in the neutral.

ac Flux	dc Flux	Current (A)			Current harmonics (% of fundamental current)								
(T)	(T)	dc	total	1st	2nd	3rd	4th	5th	6th	7th	8th	9th	10th
0.9	0	0	0	0.00	415	∞	562	386	∞	266	510	∞	113
0.9	0.1	0.81	0.81	0.00	60.8	∞	13.3	11.5	∞	20.1	10.2	∞	1.0
0.9	0.2	1.63	1.63	0.00	59.0	∞	10.4	12.0	∞	19.9	10.2	∞	1.3
0.9	0.3	2.44	2.44	0.00	57.7	∞	12.3	11.3	∞	21.1	10.0	∞	0.3
0.9	0.4	3.26	3.26	0.00	60.7	∞	12.3	14.0	∞	22.4	10.4	∞	0.4
0.9	0.5	4.12	4.12	0.00	60.1	∞	10.6	12.9	∞	22.3	9.9	∞	1.6
0.9	0.6	5.13	5.14	0.00	56.7	∞	11.8	14.7	∞	25.1	11.8	∞	5.4
0.9	0.7	6.77	6.9	0.00	36.5	∞	36.8	20.6	∞	40.5	11.7	∞	15.7

Appendix C: Measured currents, current harmonics and reactive power at ac flux of 0.9 Teslas.

Table 1 Measured current harmonic contents and reactive power for single-phase non-gapped units at 70.7 Volts.

a. **Red phase**
b. **White phase**
c. **Blue phase**

ac Flux	ac V	Current (A)			Current harmonics (% of fundamental current)									Reactive power
(T)	(V)	dc	total	1st	2nd	3rd	4th	5th	6th	7th	8th	9th	10th	(VAR)
0.9	70.7	0	0.15	0.21	9.9	9.3	8.6	2.9	6	1.1	3.8	3.9	3.3	13
0.9	70.7	0.18	0.24	0.29	40.7	17.1	3.8	5	3.6	5.6	3.8	1.2	2.6	19
0.9	70.7	0.47	0.67	0.63	65.4	43.4	28.8	17.9	8	4.1	2.7	3	2.5	43

ac Flux	ac V	Current (A)			Current harmonics (% of fundamental current)									Reactive power
(T)	(V)	dc	total	1st	2nd	3rd	4th	5th	6th	7th	8th	9th	10th	(VAR)
0.9	70.7	0	0.16	0.22	8.8	12.9	7.7	3.3	5.6	2.4	4.3	2.3	4	14
0.9	70.7	0.16	0.24	0.28	37	11.2	2.4	3.4	3.1	5.1	2.7	1.2	3.4	18
0.9	70.7	0.44	0.61	0.59	62.2	37.6	26.9	16.2	8.2	5.3	3.9	3.1	2.4	40

ac Flux	ac V	Current (A)			Current harmonics (% of fundamental current)									Reactive power
(T)	(V)	dc	total	1st	2nd	3rd	4th	5th	6th	7th	8th	9th	10th	(VAR)
0.9	70.7	0	0.13	0.2	10.0	12.6	8.9	5.5	6.7	0.9	5.4	2.3	3.5	12
0.9	70.7	0.18	0.23	0.28	44.7	22.8	10.6	10.3	7.1	5.1	4.5	3.0	2.3	18
0.9	70.7	0.45	0.64	0.6	69.6	47.9	36.6	24.4	13.1	7.6	4.1	3.4	3.6	42

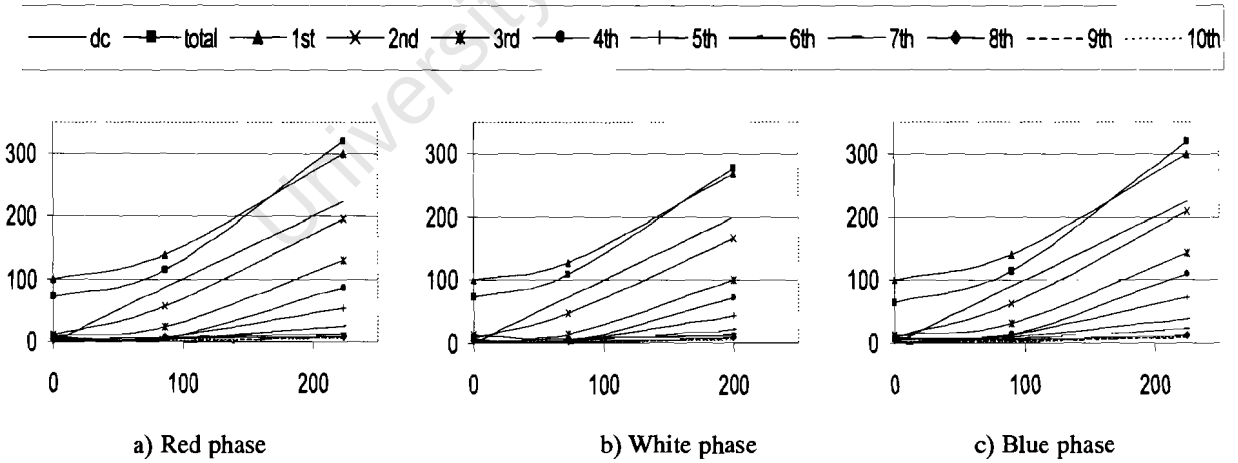

a) Red phase b) White phase c) Blue phase

Figure 1 Measured current harmonics versus dc current both taken as a percentage of fundamental current (both at 0 dc current offset) for single-phase non-gapped units in the phases at 70.7 Volts.

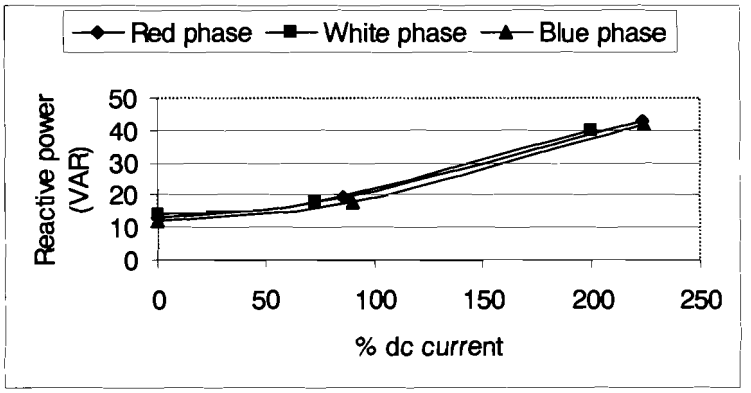

Figure 2 Measured reactive power versus dc current as a percentage of fundamental current (at 0 dc current offset) for single-phase non-gapped units at 70.7 Volts.

Table 2 Measured current harmonic contents for single-phase non-gapped reactors in the neutral at 70.7 Volts.

ac Flux	dc Flux	Current (A)			Current harmonics (% of fundamental current)								
(T)	(T)	dc	total	1st	2nd	3rd	4th	5th	6th	7th	8th	9th	10th
0.9	0	0	0.06	0.03	30	340	20	10	110	20	40	10	50
0.9	0.6	0.52	0.16	0.02	80	1000	80	80	260	10	30	40	30
0.9	0.7	1.38	0.86	0.07	80	1800	80	80	380	20	30	70	10

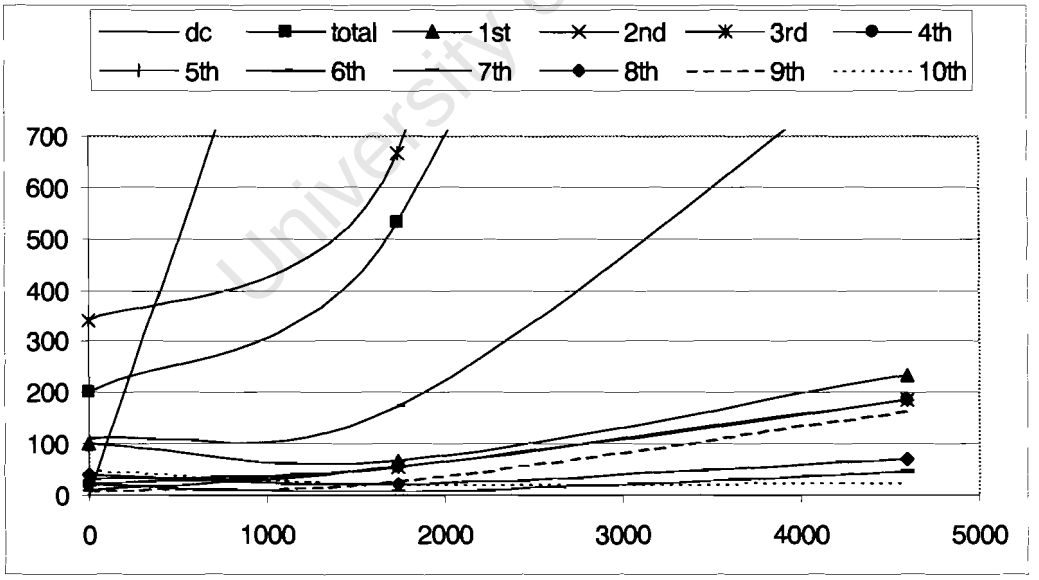

Figure 3 Measured current harmonics versus dc current both taken as a percentage of fundamental current (both at 0 dc current offset) for single-phase non-gapped units in the neutral at 70.7 Volts.

Table 3 Measured current harmonic contents and reactive power for single-phase thin-gapped units at 70.7 Volts.

a. **Red phase**
b. **White phase**
c. **Blue phase**

ac Flux	ac V	Current (A)			Current harmonics (% of fundamental current)									Reactive power
(T)	(V)	dc	total	1st	2nd	3rd	4th	5th	6th	7th	8th	9th	10th	(VAR)
0.9	70.7	0	1.42	1.41	0.2	2.3	0.1	0.9	0.1	0.8	0.2	0.7	0.2	98
0.9	70.7	0.18	1.42	1.41	0.5	1.9	0.1	1	0.2	0.7	0.2	0.7	0.1	97
0.9	70.7	0.31	1.42	1.43	0.8	2.1	0.1	1	0.2	0.8	0.2	0.6	0.1	99
0.9	70.7	0.48	1.43	1.43	1.4	2	0.1	0.9	0.2	0.8	0.2	0.6	0.2	99
0.9	70.7	0.68	1.45	1.45	2.2	1.7	0.3	1	0.3	0.6	0.2	0.7	0.2	101
0.9	70.7	0.82	1.48	1.48	3.5	0.9	1	1.5	0.8	0.7	0.2	0.7	0.3	104
0.9	70.7	1.06	1.54	1.54	8	2.3	3.5	3	2	0.7	0.6	0.6	0.4	108
0.9	70.7	1.45	1.82	1.82	21.4	13.1	11.5	8.7	5.8	3.2	1.5	0.8	0.9	130

ac Flux	ac V	Current (A)			Current harmonics (% of fundamental current)									Reactive power
(T)	(V)	dc	total	1st	2nd	3rd	4th	5th	6th	7th	8th	9th	10th	(VAR)
0.9	70.7	0	1.4	1.39	0.2	2.7	0.1	0.9	0.2	0.9	0.2	0.6	0.2	96
0.9	70.7	0.15	1.4	1.38	0.5	2.6	0.2	0.7	0.3	0.8	0.2	0.6	0.2	96
0.9	70.7	0.33	1.38	1.39	0.8	3	0.2	0.9	0.4	0.7	0.1	0.6	0.2	97
0.9	70.7	0.47	1.4	1.39	1.1	3.1	0.3	0.9	0.6	0.8	0.1	0.5	0.3	97
0.9	70.7	0.61	1.4	1.39	1.5	2.7	0.1	0.7	0.5	0.8	0.1	0.6	0.3	99
0.9	70.7	0.77	1.42	1.42	1.9	2.6	0.4	1	0.7	0.7	0.1	0.5	0.2	101
0.9	70.7	1.03	1.45	1.46	3.5	1.1	1.3	1.7	1.6	0.2	0.1	0.7	0.3	103
0.9	70.7	1.49	1.76	1.82	19.5	14.2	12.1	9.6	7.9	4.2	2.4	1.5	1.2	127

ac Flux	ac V	Current (A)			Current harmonics (% of fundamental current)									Reactive power
(T)	(V)	dc	total	1st	2nd	3rd	4th	5th	6th	7th	8th	9th	10th	(VAR)
0.9	70.7	0	1.4	1.35	0.7	1.8	0.1	1	0.2	0.8	0.2	0.6	0.1	93
0.9	70.7	0.17	1.39	1.35	0.8	1.8	0.2	1	0.2	0.9	0.3	0.5	0.3	92
0.9	70.7	0.28	1.37	1.36	1.2	1.9	0.2	1	0.3	0.8	0.3	0.7	0.2	94
0.9	70.7	0.45	1.39	1.37	2	2	0.4	1.3	0.6	0.9	0.4	0.6	0.3	94
0.9	70.7	0.6	1.4	1.39	2.7	1.8	0.3	1.3	0.5	0.8	0.3	0.6	0.2	96
0.9	70.7	0.76	1.43	1.42	4	1.1	0.6	1.5	0.9	0.6	0.2	0.6	0.3	101
0.9	70.7	0.9	1.46	1.47	6.5	0.8	1.6	2.3	1.8	0.5	0.6	0.6	0.4	104
0.9	70.7	1.29	1.8	1.82	22.5	14	10.8	8.4	5.2	2.3	0.9	0.7	0.6	131

Table 4 Measured current harmonic contents and reactive power for single-phase thick-gapped units at 70.7 Volts.

a. **Red phase**
b. **White phase**
c. **Blue phase**

ac Flux	ac V	Current (A)			Current harmonics (% of fundamental current)									Reactive power
(T)	(V)	dc	total	1st	2nd	3rd	4th	5th	6th	7th	8th	9th	10th	(VAR)
0.9	70.7	0	2.49	2.47	0	2.1	0.1	0.6	0	0.5	0	0.3	0	176
0.9	70.7	0.27	2.5	2.51	0.3	1.7	0	0.6	0.1	0.4	0	0.3	0	176
0.9	70.7	0.56	2.5	2.51	0.5	2.1	0.1	0.5	0.2	0.4	0	0.3	0.1	177
0.9	70.7	0.73	2.52	2.52	0.9	2.1	0.2	0.5	0.2	0.4	0.1	0.3	0	178
0.9	70.7	1.18	2.53	2.51	1.4	1.9	0.4	0.7	0.3	0.4	0.1	0.3	0.1	178
0.9	70.7	1.48	2.56	2.56	2.2	1.2	0.8	0.9	0.4	0.3	0.2	0.4	0.1	181
0.9	70.7	1.82	2.59	2.57	4.4	0.2	1.9	1.6	1.1	0.2	0.3	0.4	0.1	180
0.9	70.7	2.3	2.83	2.85	12.8	6.7	5.3	4.6	2.9	1.5	1.2	0.8	0.7	200

ac Flux	ac V	Current (A)			Current harmonics (% of fundamental current)									Reactive power
(T)	(V)	dc	total	1st	2nd	3rd	4th	5th	6th	7th	8th	9th	10th	(VAR)
0.9	70.7	0	2.45	2.41	0.1	2.4	0	0.3	0	0.5	0	0.3	0	175
0.9	70.7	0.28	2.48	2.45	0.2	2.3	0.1	0.3	0.1	0.4	0	0.3	0	175
0.9	70.7	0.52	2.47	2.45	0.4	2.8	0.3	0.5	0.3	0.4	0	0.2	0	174
0.9	70.7	0.86	2.49	2.48	0.7	2.7	0.1	0.3	0.2	0.5	0	0.2	0.1	177
0.9	70.7	1.11	2.47	2.45	1	3.4	0.4	0.6	0.5	0.5	0.1	0.1	0.1	178
0.9	70.7	1.21	2.51	2.45	1.3	2.9	0.4	0.5	0.5	0.4	0.1	0.2	0.2	180
0.9	70.7	1.68	2.5	2.45	1.9	2.6	0.7	0.6	0.7	0.3	0.1	0.2	0.2	183
0.9	70.7	2.36	2.8	2.8	11.1	6.6	4.6	5	3.7	1.8	1.4	0.6	0.7	199

ac Flux	ac V	Current (A)			Current harmonics (% of fundamental current)									Reactive power
(T)	(V)	dc	total	1st	2nd	3rd	4th	5th	6th	7th	8th	9th	10th	(VAR)
0.9	70.7	0	2.46	2.47	0.1	2.1	0.1	0.5	0	0.4	0.1	0.3	0	173
0.9	70.7	0.28	2.45	2.41	0.4	1.9	0.1	0.7	0.2	0.5	0.1	0.3	0	173
0.9	70.7	0.54	2.45	2.42	0.6	2.2	0.3	0.7	0.2	0.5	0.1	0.2	0	174
0.9	70.7	0.8	2.47	2.41	1	2.3	0.2	0.7	0.3	0.5	0.1	0.2	0	175
0.9	70.7	1.04	2.49	2.42	1.6	2.4	0.4	0.8	0.5	0.5	0.2	0.2	0.1	176
0.9	70.7	1.26	2.51	2.44	2.2	1.8	0.4	0.8	0.5	0.4	0.1	0.3	0.1	177
0.9	70.7	1.68	2.55	2.5	4.5	0.3	1.5	1.6	1.1	0.3	0.2	0.3	0.1	181
0.9	70.7	2.07	2.81	2.83	12.1	6	4.3	4.5	2.5	1.6	1.2	1.2	0.2	200

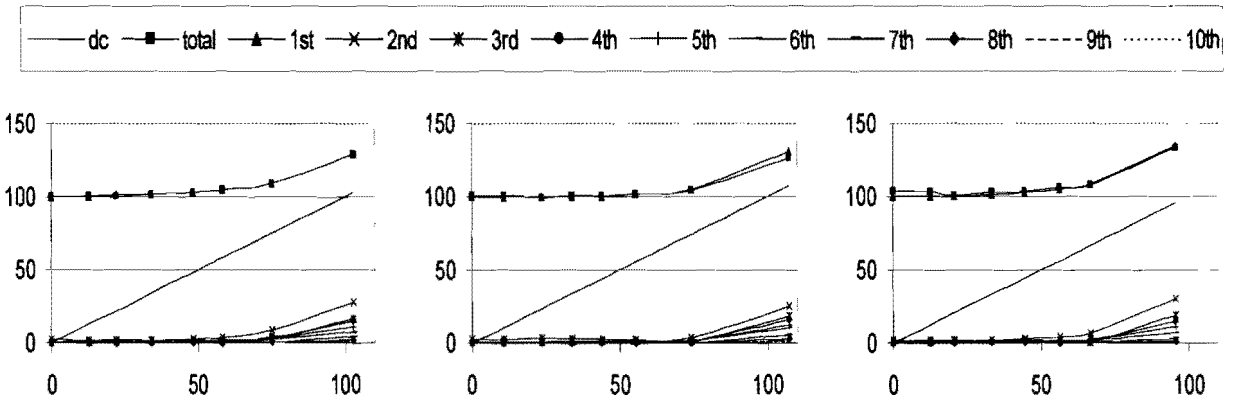

a) Red phase b) White phase c) Blue phase

Figure 4 Measured current harmonics versus dc current both taken as a percentage of fundamental current (0 dc current offset) for single-phase thin-gapped units in the phases at 70.7 Volts.

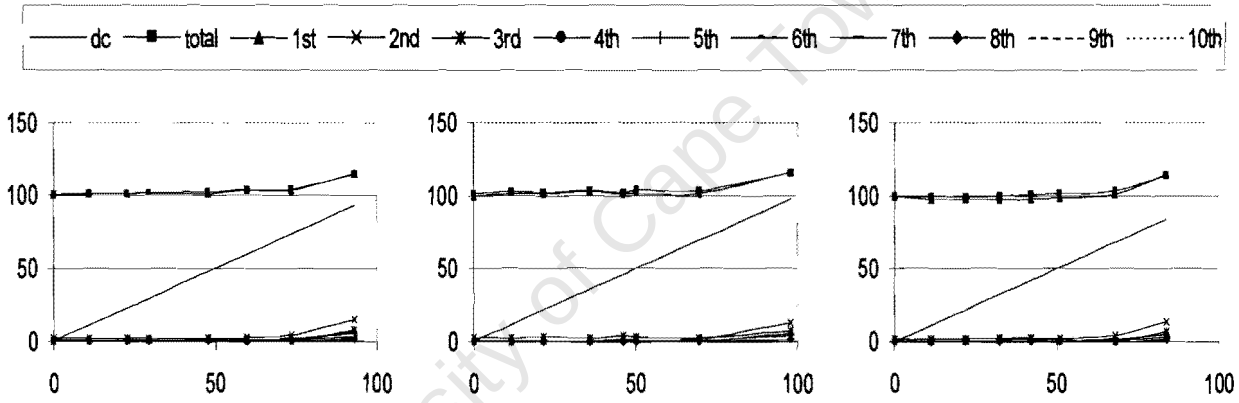

a) Red phase b) White phase c) Blue phase

Figure 5 Measured current harmonics versus dc current both taken as a percentage of fundamental current 0 dc current offset) for single-phase thick-gapped units in the phases at 70.7 Volts.

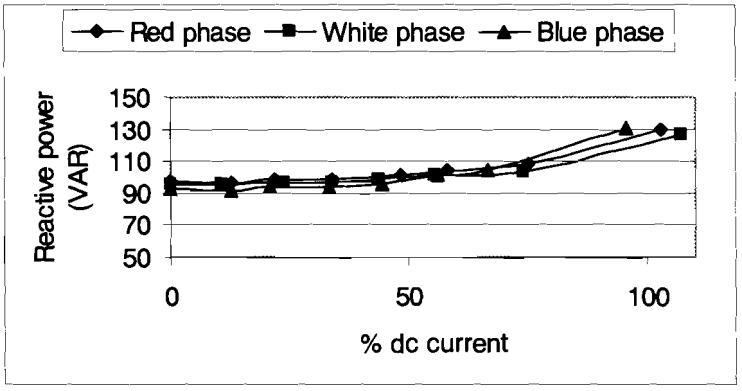

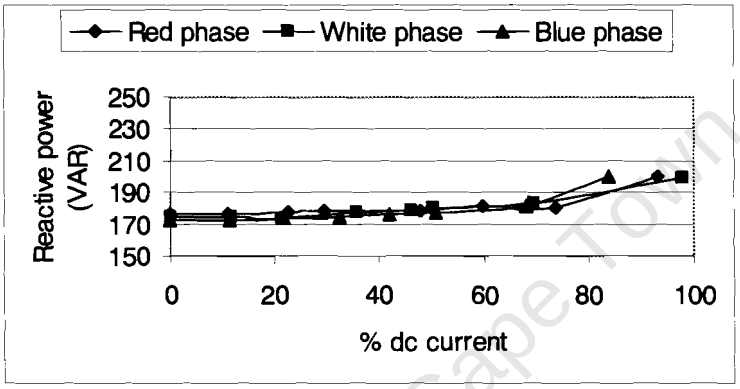

Figure 6 Measured reactive power versus dc current as a percentage of fundamental current (at 0 dc current offset) for single-phase units at 70.7 Volts.

a. **Thin-gapped**
b. **Thick-gapped**

Table 5 Measured current harmonic contents for single-phase reactors in the neutral at 70.7 Volts.

a. **Thin-gapped**
b. **Thick-gapped**

ac Flux	dc Flux	Current (A)			Current harmonics (% of fundamental current)								
(T)	(T)	dc	total	1st	2nd	3rd	4th	5th	6th	7th	8th	9th	10th
0.9	0	0	0.04	0.15	9	34	10	10	7	4	7	2	7
0.9	0.1	0.47	0.04	0.11	5	51	21	19	23	11	7	5	5
0.9	0.2	0.93	0.03	0.13	11	37	10	10	9	3	7	3	7
0.9	0.3	1.4	0.03	0.14	11	36	10	9	11	4	7	2	7
0.9	0.4	1.88	0.05	0.14	18	28	9	6	13	2	7	4	4
0.9	0.5	2.39	0.05	0.13	41	14	7	13	25	9	9	11	6
0.9	0.6	3.06	0.12	0.16	61	84	24	16	45	16	16	14	6
0.9	0.7	4.35	0.8	0.12	69	669	62	42	269	32	32	40	11

Table 4 (continued)

ac Flux	dc Flux	Current (A)			Current harmonics (% of fundamental current)								
(T)	(T)	dc	total	1st	2nd	3rd	4th	5th	6th	7th	8th	9th	10th
0.9	0	0	71.4	100	12.8	101	18.9	6.9	6.3	11.1	8.6	4.2	4.7
0.9	585.71	586	50	100	13.2	86.7	17.9	7.9	7.8	10.6	8.6	7.5	5.7
0.9	1171.4	1171	57.1	100	11.8	97.5	13.2	8.6	4.8	13.1	7.7	7.8	3
0.9	1764.3	1764	57.1	92.9	8.26	120	8.73	11.8	6.78	17.2	6.22	9.47	8.26
0.9	2357.1	2357	64.3	92.9	9.1	106	7.34	9.1	10.8	17.9	6.31	9.75	7.06
0.9	2971.4	2971	64.3	136	24.2	75.7	6.24	11.7	22.5	5.29	5.02	3.12	6.11
0.9	3707.1	3707	85.7	157	58.5	22.6	18.5	27.8	59.6	17	6.29	7.07	4.09
0.9	4878.6	4879	293	78.6	29.2	310	21.8	6.76	122	8.09	8.8	14.9	3.93

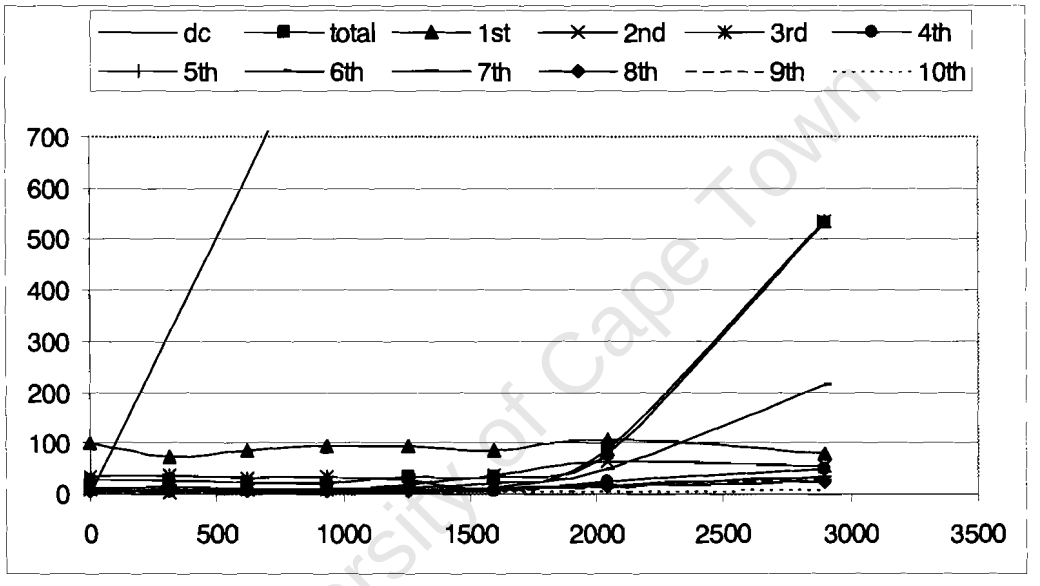

Figure 7 Measured current harmonics versus dc current both taken as a percentage of fundamental current (0 dc current offset) for single-phase units in the neutral at 70.7 Volts.

a. **Thin-gapped**
b. **Thick-gapped**

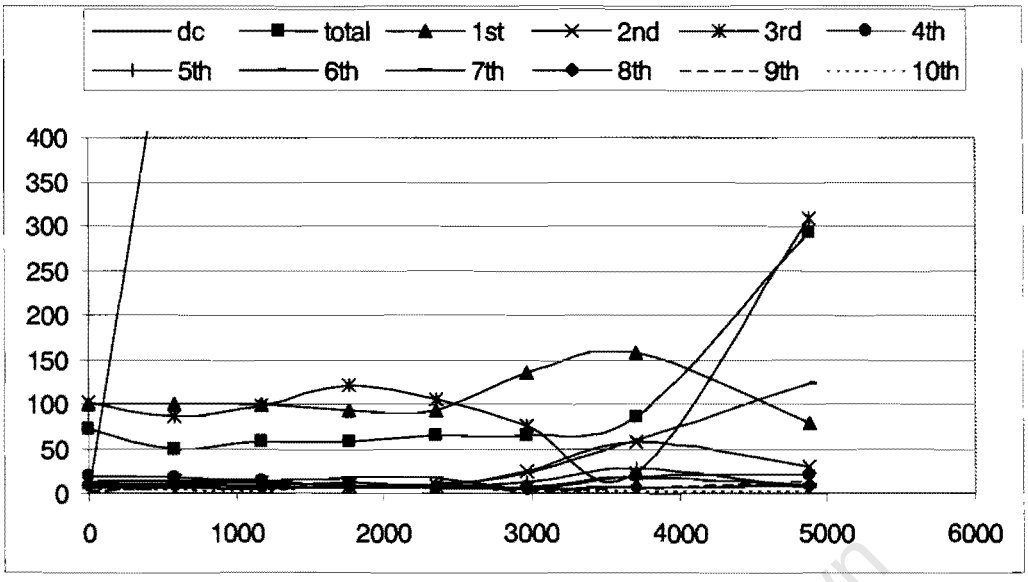

Figure 7 (continued)

Table 6 Measured current harmonic contents and reactive power for three-phase thin-gapped reactors at 70.7 Volts.

a. **Red phase**
b. **White phase**
c. **Blue phase**

ac Flux	ac V	Current (A)			Current harmonics (% of fundamental current)									Reactive Power
(T)	(V)	dc	total	fund.	2nd	3rd	4th	5th	6th	7th	8th	9th	10th	(VAR)
0.9	70.7	0	1.09	1.1	0.4	1.8	0.1	1.7	0.4	0.6	0.4	0.7	0.2	84
0.9	70.7	0.12	1.09	1.1	0.3	1.8	0.2	1.6	0.3	0.6	0.3	0.8	0.5	83
0.9	70.7	0.24	1.08	1.11	0.4	1.7	0.1	1.7	0.3	0.7	0.4	0.7	0.2	83
0.9	70.7	0.37	1.08	1.1	0.5	1.7	0.1	1.7	0.4	0.6	0.3	0.7	0.1	81
0.9	70.7	0.48	1.09	1.1	0.4	1.8	0.2	1.6	0.5	0.7	0.3	0.7	0.2	82
0.9	70.7	0.63	1.09	1.1	0.4	1.7	0.1	1.7	0.4	0.7	0.3	0.7	0.3	82
0.9	70.7	0.86	1.1	1.11	0.5	1.7	0.1	1.7	0.4	0.7	0.4	0.8	0.3	83
0.9	70.7	1.52	1.1	1.11	0.6	1.8	0.1	1.7	0.5	0.8	0.3	0.8	0.3	85

ac Flux	ac V	Current (A)			Current harmonics (% of fundamental current)									Reactive Power
(T)	(V)	dc	total	fund.	2nd	3rd	4th	5th	6th	7th	8th	9th	10th	(VAR)
0.9	70.7	0	1	0.99	0.3	2.7	0.4	0.9	0.3	0.9	0.3	1.1	0.3	77
0.9	70.7	0.11	1.01	1	0.4	2.9	0.3	1.2	0.3	0.8	0.2	1.2	0.4	77
0.9	70.7	0.23	1	0.99	0.3	2.8	0.4	1.1	0.4	0.8	0.2	1.1	0.3	77
0.9	70.7	0.35	1	0.99	0.3	2.7	0.3	1.2	0.4	0.8	0.2	1	0.6	75
0.9	70.7	0.46	1.01	0.99	0.3	2.8	0.3	1	0.3	0.8	0.3	1.1	0.4	76
0.9	70.7	0.62	1	1	0.3	2.8	0.4	1.2	0.4	0.8	0.1	1.1	0.3	75
0.9	70.7	0.85	1	1	0.4	2.9	0.3	1.1	0.4	0.9	0.3	1	0.3	75
0.9	70.7	1.38	1.01	1.01	0.3	2.7	0.4	1.1	0.3	0.9	0.2	0.9	0.3	78

Table 6 (continued)

ac Flux	ac V	Current (A)			Current harmonics (% of fundamental current)									Reactive Power
(T)	(V)	dc	total	fund.	2nd	3rd	4th	5th	6th	7th	8th	9th	10th	(VAR)
0.9	70.7	0	1.18	1.17	0.1	1	0.2	1	0.3	1	0.3	0.6	0.2	91
0.9	70.7	0.11	1.18	1.17	0.2	1	0.3	1.3	0.3	0.9	0.3	0.6	0.2	90
0.9	70.7	0.22	1.18	1.17	0.3	1.1	0.2	1.1	0.4	0.9	0.3	0.6	0.3	91
0.9	70.7	0.34	1.18	1.18	0.5	1.1	0.3	1.3	0.4	0.8	0.3	0.5	0.3	89
0.9	70.7	0.47	1.18	1.17	0.4	1	0.2	1.2	0.5	0.8	0.3	0.6	0.2	89
0.9	70.7	0.61	1.19	1.18	0.3	1.1	0.3	1.2	0.6	0.8	0.4	0.4	0.3	90
0.9	70.7	0.86	1.19	1.2	0.5	1.1	0.3	1.1	0.4	0.8	0.3	0.5	0.3	90
0.9	70.7	1.38	1.2	1.22	0.5	1	0.2	0.9	0.4	0.9	0.2	0.4	0.2	93

Table 7 Measured current harmonic contents and reactive power for three-phase thick-gapped reactors at 70.7 Volts.

a. **Red phase**
b. **White phase**
c. **Blue phase**

ac Flux	ac V	Current (A)			Current harmonics (% of fundamental current)									Reactive Power
(T)	(V)	dc	total	(VAR)	2nd	3rd	4th	5th	6th	7th	8th	9th	10th	(VAR)
0.9	70.7	0	1.83	1.78	0.2	1.2	0.1	0.9	0.1	0.4	0.1	0.6	0.1	137
0.9	70.7	0.22	1.82	1.79	0.2	1.3	0.1	0.8	0.1	0.5	0.2	0.5	0.1	138
0.9	70.7	0.43	1.83	1.78	0.3	1.3	0.1	0.8	0.2	0.4	0.1	0.5	0.2	138
0.9	70.7	0.62	1.82	1.79	0.3	1.4	0.1	0.8	0.2	0.4	0.2	0.4	0	138
0.9	70.7	0.85	1.83	1.79	0.3	1.3	0.2	0.9	0.1	0.5	0.1	0.5	0.1	137
0.9	70.7	1.08	1.83	1.79	0.2	1.4	0.1	0.8	0.1	0.5	0.2	0.4	0.1	138
0.9	70.7	1.4	1.83	1.8	0.3	1.4	0.1	0.8	0.2	0.4	0.1	0.5	0.2	140
0.9	70.7	2.08	1.84	1.81	0.3	1.3	0.1	0.8	0.1	0.4	0.1	0.4	0.2	142

ac Flux	ac V	Current (A)			Current harmonics (% of fundamental current)									Reactive Power
(T)	(V)	dc	total	(VAR)	2nd	3rd	4th	5th	6th	7th	8th	9th	10th	(VAR)
0.9	70.7	0	1.78	1.74	0.1	1.3	0.1	0.7	0.1	0.4	0	0.6	0.1	137
0.9	70.7	0.19	1.77	1.73	0.2	1.4	0.2	0.7	0.2	0.5	0.1	0.5	0.2	138
0.9	70.7	0.41	1.78	1.72	0.1	1.3	0.1	0.6	0.1	0.4	0	0.6	0.2	138
0.9	70.7	0.61	1.76	1.72	0.2	1.4	0.1	0.6	0.1	0.6	0.1	0.4	0.3	138
0.9	70.7	0.82	1.78	1.73	0.2	1.4	0.1	0.7	0.1	0.5	0.1	0.5	0.2	137
0.9	70.7	1.02	1.79	1.76	0.1	1.4	0.2	0.7	0.2	0.5	0.1	0.6	0.2	138
0.9	70.7	1.4	1.79	1.75	0.1	1.3	0.2	0.7	0.2	0.4	0.2	0.4	0.3	140
0.9	70.7	2	1.8	1.76	0.2	1.4	0.1	0.8	0.1	0.4	0.1	0.5	0.2	142

Table 7 (continued)

ac Flux	ac V	Current (A)			Current harmonics (% of fundamental current)									Reactive Power
(T)	(V)	dc	total	fund.	2nd	3rd	4th	5th	6th	7th	8th	9th	10th	(VAR)
0.9	70.7	0	1.97	1.97	0.1	0.7	0.2	0.6	0	0.4	0.3	0.6	0	137
0.9	70.7	0.16	1.95	1.96	0.2	0.8	0.3	0.7	0.2	0.4	0.2	0.6	0	138
0.9	70.7	0.36	1.95	1.95	0.1	0.7	0.1	0.6	0.1	0.5	0.3	0.5	0.1	138
0.9	70.7	0.58	1.94	1.95	0.2	0.8	0.2	0.6	0.2	0.5	0.4	0.4	0.1	138
0.9	70.7	0.82	1.95	1.96	0.2	0.8	0.2	0.8	0.2	0.4	0.3	0.6	0.1	137
0.9	70.7	1.1	1.95	1.96	0.2	0.7	0.3	0.6	0.1	0.4	0.3	0.5	0	138
0.9	70.7	1.34	1.97	1.97	0.1	0.7	0.2	0.7	0.1	0.3	0.3	0.5	0.1	140
0.9	70.7	2.11	2	2	0.2	0.6	0.1	0.8	0.2	0.2	0.1	0.6	0.1	142

Table 8 Measured current harmonic contents for three-phase reactors in the neutral at 70.7 Volts.

a. **Thin-gapped**
b. **Thick-gapped**

ac Flux	dc Flux	Current (A)			Current harmonics (% of fundamental current)								
(T)	(T)	dc	total	fund.	2nd	3rd	4th	5th	6th	7th	8th	9th	10th
0.9	0	0	0.19	0.25	5	10	5	4	4	2	4	2	4
0.9	0.1	0.35	0	0.01	38	59	3	24	16	10	16	7	12
0.9	0.2	0.7											
0.9	0.3	1.06											
0.9	0.4	1.42											
0.9	0.5	1.85	0.02	0.09	50	37	11	10	14	12	13	3	1
0.9	0.6	2.55											
0.9	0.7	4.34	0	0.10	45	26	1	11	15	4	2	9	5

ac Flux	dc Flux	Current (A)			Current harmonics (% of fundamental current)								
(T)	(T)	dc	total	fund.	2nd	3rd	4th	5th	6th	7th	8th	9th	10th
0.9	0	0	0.2	0.26	5	10	4	4	4	2	4	2	4
0.9	0.1	0.61											
0.9	0.2	1.22											
0.9	0.3	1.84	0.02	0.10	42	16	10	16	14	2	8	9	4
0.9	0.4	2.47											
0.9	0.5	3.16	0	0.09	49	27	4	15	16	10	2	9	7
0.9	0.6	4.12											
0.9	0.7	6.18	0	0.13	26	2	15	10	7	10	4	5	7

Table 9 Measured current harmonic contents and reactive power for three-phase thin-gapped reactors at 74.6 Volts without the cancelling effect.

a. **Red phase**
b. **White phase**
c. **Blue phase**

ac Flux	dc Flux	Current (A)			Current harmonics (% of fundamental current)									Reactive power
(T)	(T)	dc	total	fund.	2nd	3rd	4th	5th	6th	7th	8th	9th	10th	(VAR)
0.95	0	-0	1.03	1.03	0.00	0.04	0.00	0.18	0.00	0.02	0.00	0.03	0.00	76.62
0.95	0.1	0.11	1.03	1.03	0.19	0.12	0.17	0.22	0.02	0.01	0.04	0.04	0.00	77.56
0.95	0.2	0.22	1.05	1.03	0.53	0.36	0.40	0.29	0.07	0.05	0.06	0.02	0.02	80.43
0.95	0.3	0.33	1.09	1.04	1.23	0.94	0.83	0.52	0.22	0.16	0.12	0.04	0.02	85.51
0.95	0.4	0.46	1.16	1.07	3.48	2.87	2.37	1.65	1.11	0.85	0.61	0.41	0.32	94.31
0.95	0.5	0.66	1.39	1.20	13.0	11.2	9.23	7.07	5.26	3.86	2.65	1.74	1.1	117.45
0.95	0.6	1.15	2.33	1.72	37.0	32.3	26.7	21.0	15.7	11.3	7.59	4.83	2.9	205.99
0.95	0.65	1.71	3.68	2.41	52.9	46.1	38.2	29.9	22.3	15.8	10.6	6.67	4.0	332.33

ac Flux	dc Flux	Current (A)			Current harmonics (% of fundamental current)									Reactive power
(T)	(T)	dc	total	fund.	2nd	3rd	4th	5th	6th	7th	8th	9th	10th	(VAR)
0.95	0	0	1.04	1.04	0.00	0.02	0.00	0.08	0.00	0.01	0.00	0.01	0.00	77.29
0.95	0.1	0.11	1.04	1.04	0.09	0.06	0.08	0.10	0.01	0.00	0.02	0.02	0.00	78.19
0.95	0.2	0.22	1.06	1.04	0.25	0.17	0.19	0.14	0.03	0.02	0.03	0.01	0.01	80.91
0.95	0.3	0.33	1.09	1.04	0.58	0.44	0.39	0.25	0.11	0.08	0.06	0.02	0.01	85.58
0.95	0.4	0.45	1.15	1.06	1.66	1.37	1.13	0.79	0.53	0.40	0.29	0.20	0.15	92.89
0.95	0.5	0.6	1.27	1.12	6.55	5.65	4.66	3.57	2.66	1.95	1.34	0.88	0.57	107.45
0.95	0.6	0.89	1.7	1.36	22.0	19.2	15.9	12.5	9.36	6.70	4.51	2.87	1.72	150.45
0.95	0.65	1.18	2.3	1.69	35.6	31.1	25.7	20.1	15.0	10.6	7.11	4.49	2.67	208.37

ac Flux	dc Flux	Current (A)			Current harmonics (% of fundamental current)									Reactive power
(T)	(T)	dc	total	fund.	2nd	3rd	4th	5th	6th	7th	8th	9th	10th	(VAR)
0.95	0	0	1.24	1.24	0.00	0.03	0.00	0.15	0.00	0.02	0.00	0.02	0.00	92.25
0.95	0.1	0.13	1.24	1.24	0.16	0.10	0.14	0.18	0.02	0.01	0.03	0.03	0.00	93.36
0.95	0.2	0.26	1.27	1.24	0.44	0.30	0.33	0.24	0.06	0.04	0.05	0.01	0.01	96.75
0.95	0.3	0.4	1.31	1.25	1.02	0.78	0.69	0.44	0.19	0.13	0.10	0.03	0.01	102.69
0.95	0.4	0.55	1.39	1.28	2.91	2.40	1.98	1.38	0.92	0.71	0.51	0.35	0.27	112.68
0.95	0.5	0.77	1.63	1.41	11.0	9.51	7.85	6.02	4.48	3.28	2.26	1.48	0.95	137.09
0.95	0.6	1.28	2.56	1.93	32.9	28.7	23.8	18.7	14.0	10.0	6.77	4.31	2.58	225.55
0.95	0.65	1.85	3.88	2.62	48.6	42.5	35.1	27.5	20.5	14.6	9.72	6.14	3.65	351.04

Table 10 Measured current harmonic contents and reactive power for three-phase thick-gapped reactors at 74.6 Volts without the cancelling effect.

a. **Red phase**
b. **White phase**
c. **Blue phase**

ac Flux	dc Flux	Current (A)			Current harmonics (% of fundamental current)									Reactive power
(T)	(T)	dc	total	fund.	2nd	3rd	4th	5th	6th	7th	8th	9th	10th	(VAR)
0.95	0	-0	1.87	1.87	0.00	0.02	0.00	0.10	0.00	0.01	0.00	0.01	0.00	139.18
0.95	0.1	0.2	1.88	1.87	0.11	0.07	0.09	0.12	0.01	0.00	0.02	0.02	0.00	140.81
0.95	0.2	0.4	1.91	1.87	0.29	0.20	0.22	0.16	0.04	0.03	0.03	0.01	0.01	145.76
0.95	0.3	0.6	1.97	1.88	0.68	0.52	0.46	0.29	0.12	0.09	0.07	0.02	0.01	154.29
0.95	0.4	0.82	2.07	1.91	1.95	1.61	1.33	0.93	0.62	0.47	0.34	0.23	0.18	167.90
0.95	0.5	1.1	2.33	2.03	7.62	6.57	5.43	4.16	3.09	2.27	1.56	1.03	0.66	196.47
0.95	0.6	1.68	3.24	2.55	24.8	21.7	18.0	14.1	10.6	7.57	5.10	3.25	1.94	286.30
0.95	0.65	2.28	4.53	3.25	39.2	34.2	28.3	22.2	16.6	11.7	7.84	4.95	2.95	409.83

ac Flux	dc Flux	Current (A)			Current harmonics (% of fundamental current)									Reactive power
(T)	(T)	dc	total	fund.	2nd	3rd	4th	5th	6th	7th	8th	9th	10th	(VAR)
0.95	0	0	1.87	1.87	0.00	0.01	0.00	0.05	0.00	0.01	0.00	0.01	0.00	139.48
0.95	0.1	0.2	1.88	1.87	0.05	0.03	0.04	0.06	0.01	0.00	0.01	0.01	0.00	141.07
0.95	0.2	0.4	1.91	1.87	0.14	0.09	0.10	0.08	0.02	0.01	0.02	0.00	0.00	145.85
0.95	0.3	0.6	1.97	1.88	0.32	0.24	0.22	0.14	0.06	0.04	0.03	0.01	0.00	153.97
0.95	0.4	0.8	2.05	1.89	0.93	0.76	0.63	0.44	0.29	0.23	0.16	0.11	0.09	166.09
0.95	0.5	1.04	2.21	1.95	3.75	3.23	2.67	2.05	1.52	1.12	0.77	0.50	0.32	186.64
0.95	0.6	1.42	2.66	2.19	13.6	11.9	9.86	7.73	5.80	4.15	2.80	1.78	1.07	234.86
0.95	0.65	1.75	3.24	2.52	23.8	20.8	17.2	13.5	10.1	7.13	4.76	3.01	1.79	292.90

ac Flux	dc Flux	Current (A)			Current harmonics (% of fundamental current)									Reactive power
(T)	(T)	dc	total	fund.	2nd	3rd	4th	5th	6th	7th	8th	9th	10th	(VAR)
0.95	0	0	2.05	2.05	0.00	0.02	0.00	0.09	0.00	0.01	0.00	0.01	0.00	153.22
0.95	0.1	0.22	2.07	2.05	0.10	0.06	0.08	0.11	0.01	0.00	0.02	0.02	0.00	155.01
0.95	0.2	0.44	2.1	2.06	0.26	0.18	0.20	0.15	0.04	0.02	0.03	0.01	0.01	160.43
0.95	0.3	0.66	2.17	2.07	0.62	0.47	0.42	0.26	0.11	0.08	0.06	0.02	0.01	169.74
0.95	0.4	0.89	2.28	2.09	1.78	1.46	1.21	0.84	0.56	0.43	0.31	0.21	0.16	184.43
0.95	0.5	1.2	2.54	2.22	6.98	6.02	4.97	3.80	2.83	2.07	1.43	0.94	0.60	214.30
0.95	0.6	1.8	3.45	2.74	23.1	20.2	16.7	13.1	9.85	7.05	4.75	3.02	1.81	304.88
0.95	0.65	2.41	4.73	3.44	37.1	32.4	26.8	21.0	15.7	11.1	7.41	4.68	2.78	428.01

Table 11 Measured current harmonic contents for three-phase reactors in the neutral at 74.6 Volts without the cancelling effect.

a. **Thin-gapped**
b. **Thick-gapped**

ac Flux	dc Flux	Current (A)			Current harmonics (% of fundamental current)								
(T)	(T)	dc	total	fund.	2nd	3rd	4th	5th	6th	7th	8th	9th	10th
0.95	0	0	0.21	0.21	0.00	0.47	0.00	0.48	0.00	0.06	0.00	0.32	0.00
0.95	0.1	0.35	0.41	0.21	0.51	1.46	0.44	0.57	0.28	0.02	0.09	0.45	0.01
0.95	0.2	0.7	0.73	0.21	1.39	4.46	1.05	0.78	0.89	0.12	0.15	0.21	0.04
0.95	0.3	1.07	1.09	0.21	3.2	11.6	2.2	1.4	2.8	0.4	0.3	0.5	0.0
0.95	0.4	1.46	1.48	0.22	9.1	35.1	6.2	4.3	13.5	2.2	1.6	5.1	0.8
0.95	0.5	2.04	2.09	0.26	31.6	127	22.5	17.2	60	9.4	6.3	19.9	2.7
0.95	0.6	3.32	3.72	0.49	67.8	277	49.1	38.5	135	20.7	13.6	41.5	5.3
0.95	0.65	4.74	5.8	0.85	79.5	324	57.4	45.0	157	23.8	15.5	46.9	6.0

ac Flux	dc Flux	Current (A)			Current harmonics (% of fundamental current)								
(T)	(T)	dc	total	fund.	2nd	3rd	4th	5th	6th	7th	8th	9th	10th
0.95	0	0	0.19	0.19	0.00	0.52	0.00	0.52	0.00	0.07	0.00	0.36	0.00
0.95	0.1	0.61	0.64	0.19	0.56	1.61	0.48	0.63	0.31	0.02	0.10	0.50	0.01
0.95	0.2	1.23	1.24	0.19	1.5	4.9	1.2	0.9	1.0	0.1	0.2	0.2	0.0
0.95	0.3	1.85	1.86	0.19	3.6	13	2.4	1.5	3.0	0.5	0.3	0.5	0.0
0.95	0.4	2.51	2.52	0.20	10.0	38	6.8	4.7	14.8	2.4	1.7	5.5	0.9
0.95	0.5	3.35	3.38	0.24	33.8	136	24.1	18.4	64	10.1	6.8	21.3	2.9
0.95	0.6	4.89	5.17	0.48	69.5	283	50.3	39.4	138	21.2	14.0	42.5	5.4
0.95	0.65	6.45	7.26	0.84	80.4	328	58.1	45.5	159	24.1	15.7	47.4	6.0

Appendix D: Measured currents, current harmonics and reactive power versus respective modelled currents, current harmonics and reactive power.

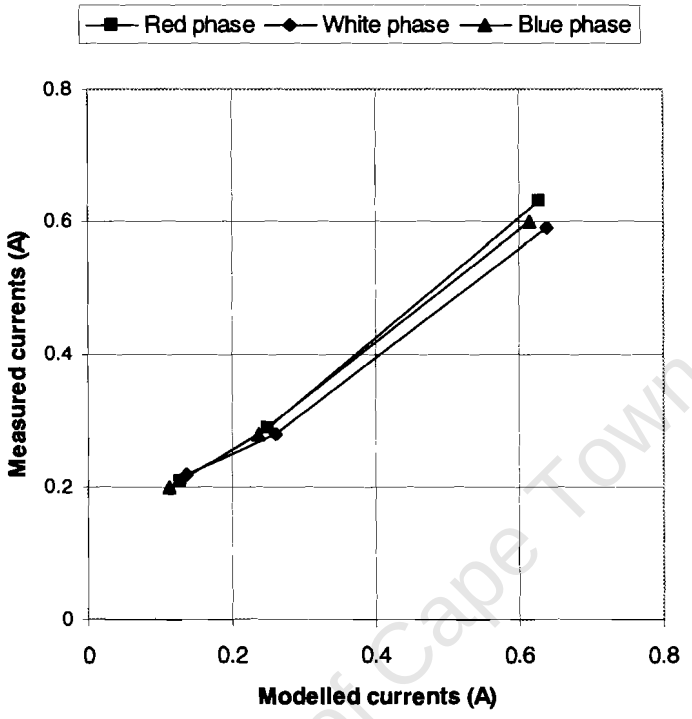

Figure 1 Measured fundamental currents versus modelled fundamental currents at 70.7 Volts over a range of varying dc currents for single-phase reactors in the phases.

a. **Non-gapped**
b. **Thin-gapped**
c. **Thick-gapped**

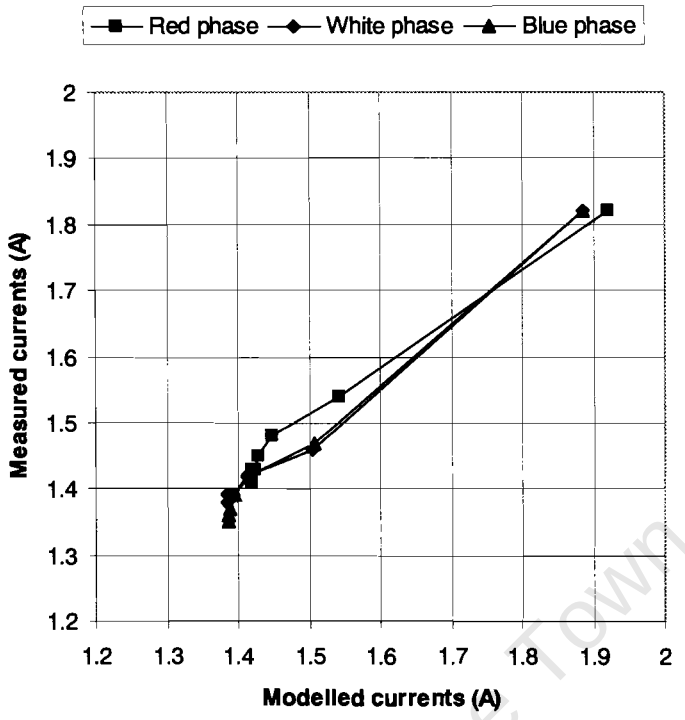

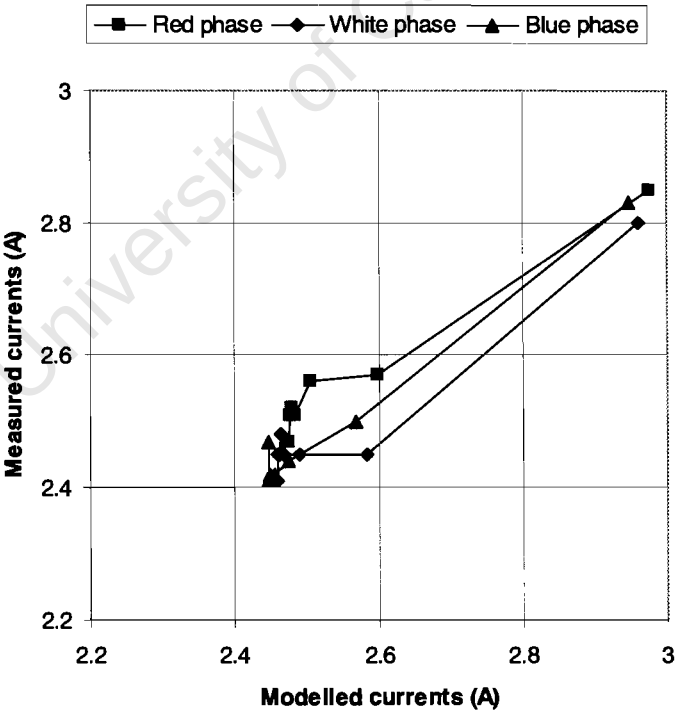

Figure 1 (continued)

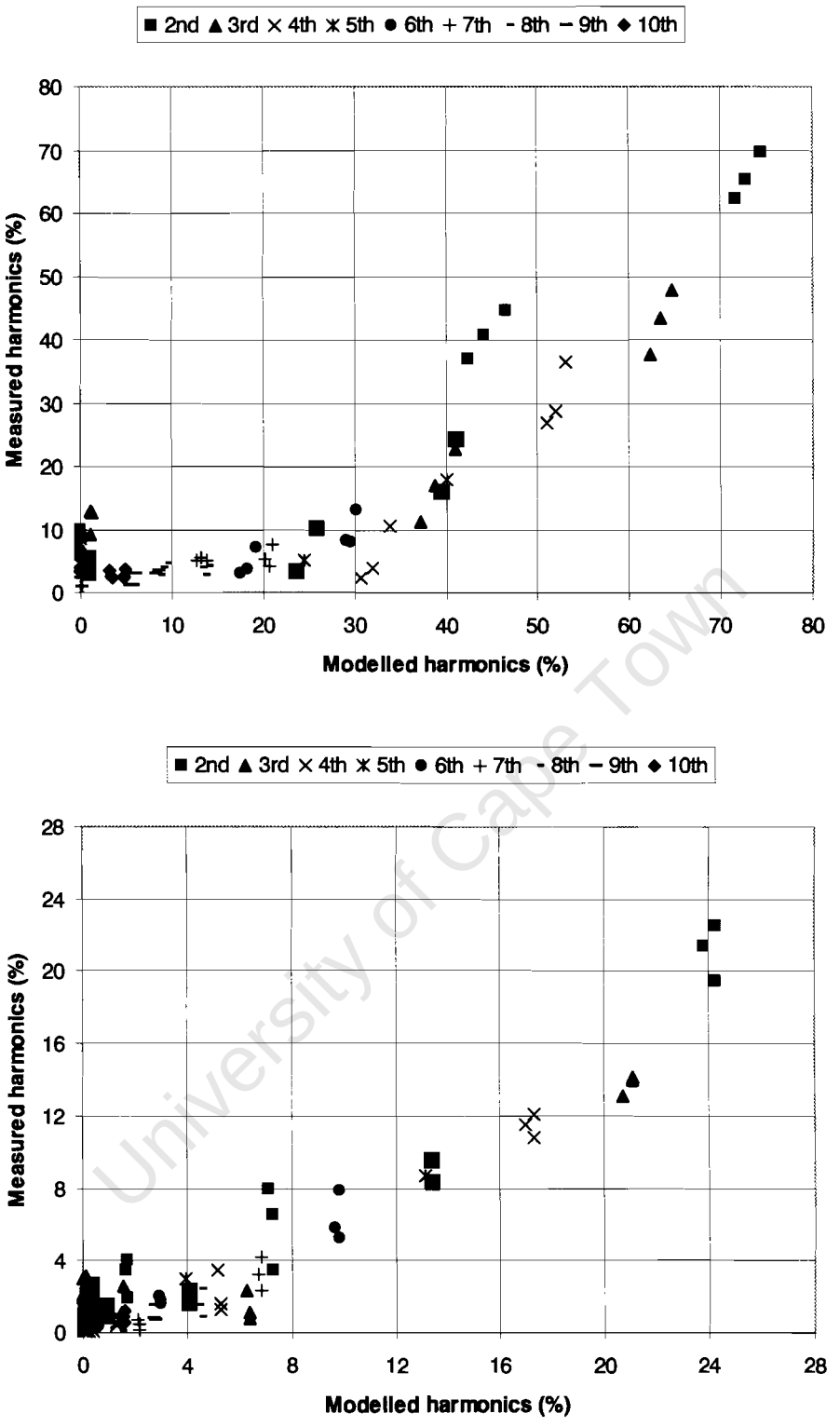

Figure 2 Measured current harmonics versus modelled current harmonics at 70.7 Volts over a range of varying dc currents for single-phase reactors in the phases.

a. **Non-gapped**
b. **Thin-gapped**
c. **Thick-gapped**

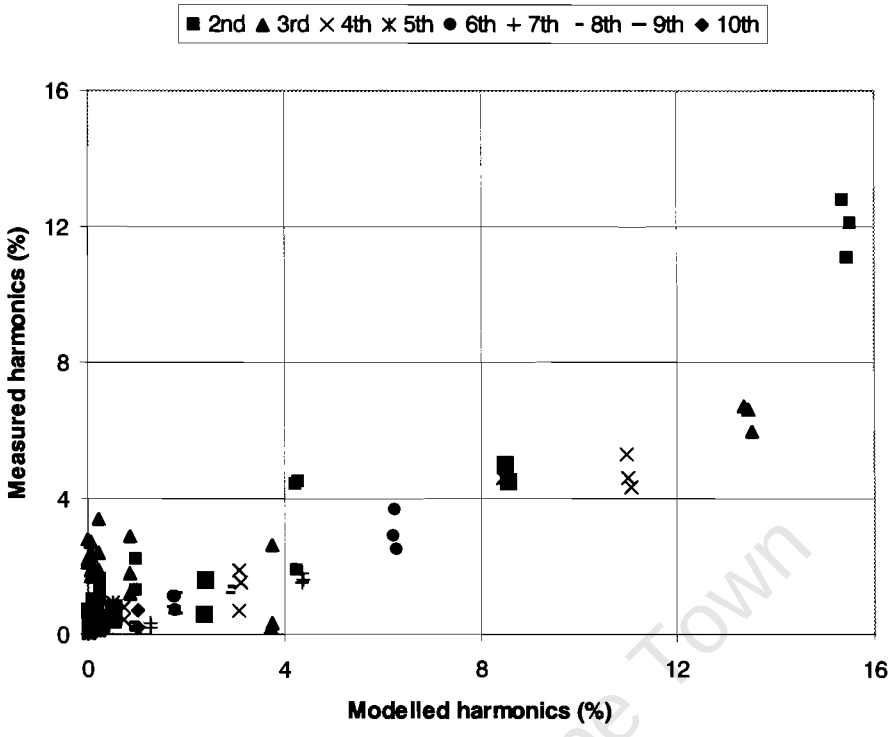

Figure 2 (continued)

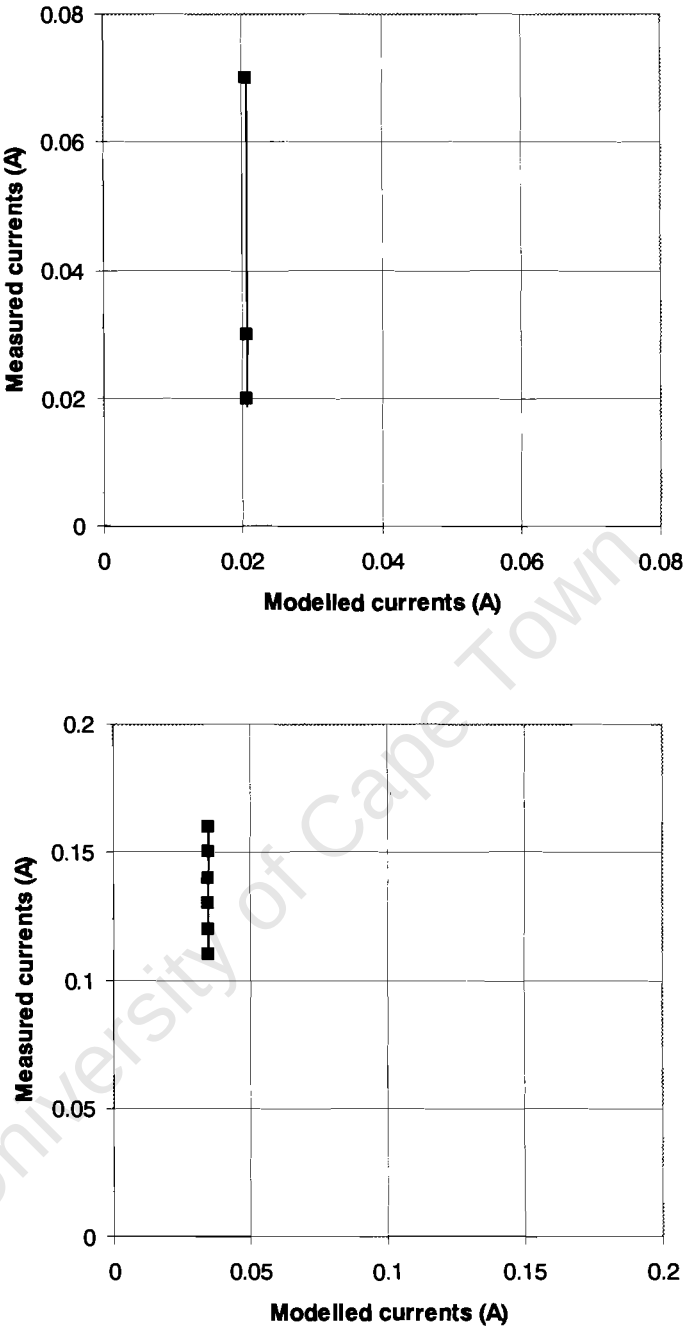

Figure 3 Measured fundamental current versus modelled fundamental current at 70.7 Volts over a range of varying dc currents for single-phase reactors in the neutral.

a. **Non-gapped**
b. **Thin-gapped**
c. **Thick-gapped**

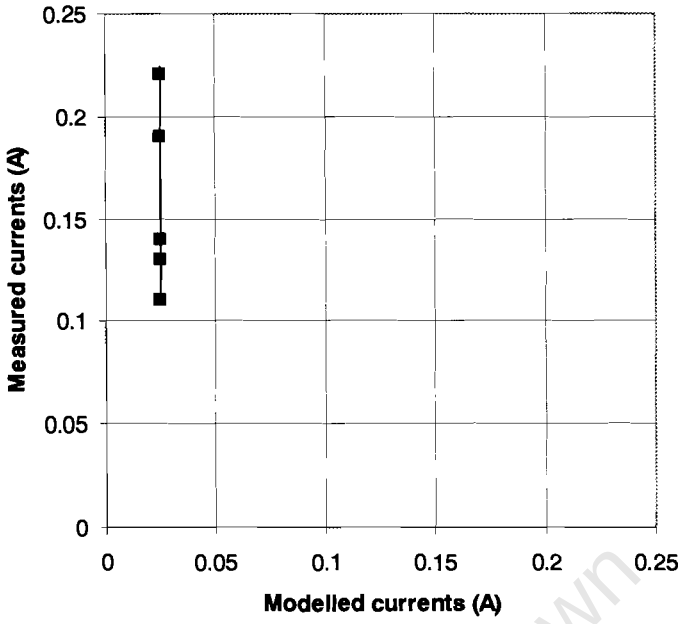

Figure 3 (continued)

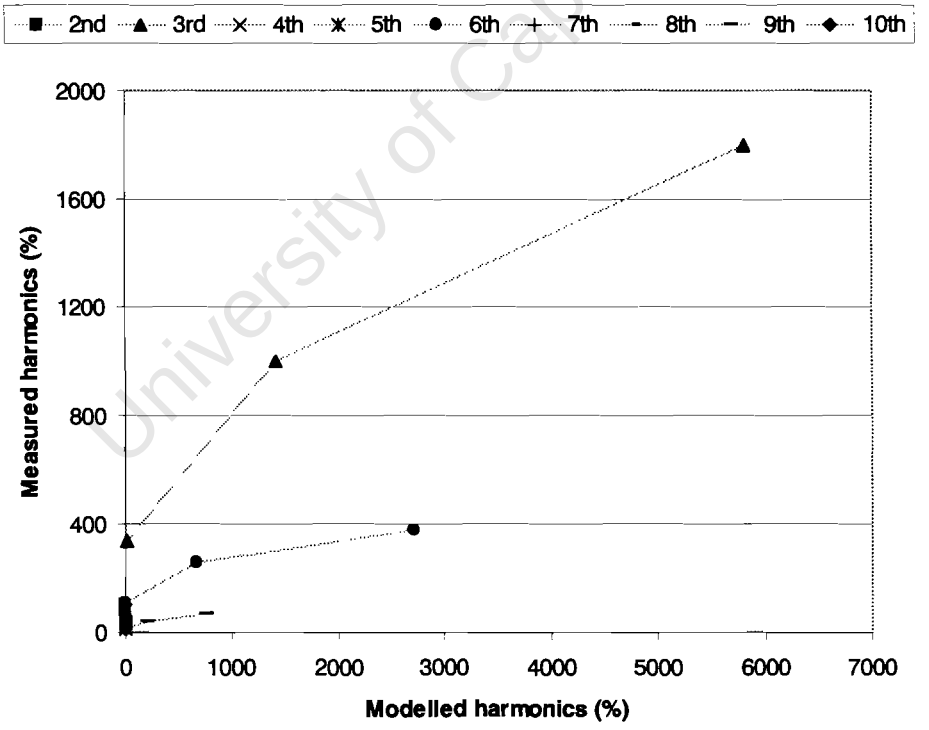

Figure 4 Measured current harmonics versus modelled current harmonics at 70.7 Volts over a range of varying dc currents for single-phase reactors in the neutral.

a. **Non-gapped**
b. **Thin-gapped**
c. **Thick-gapped**

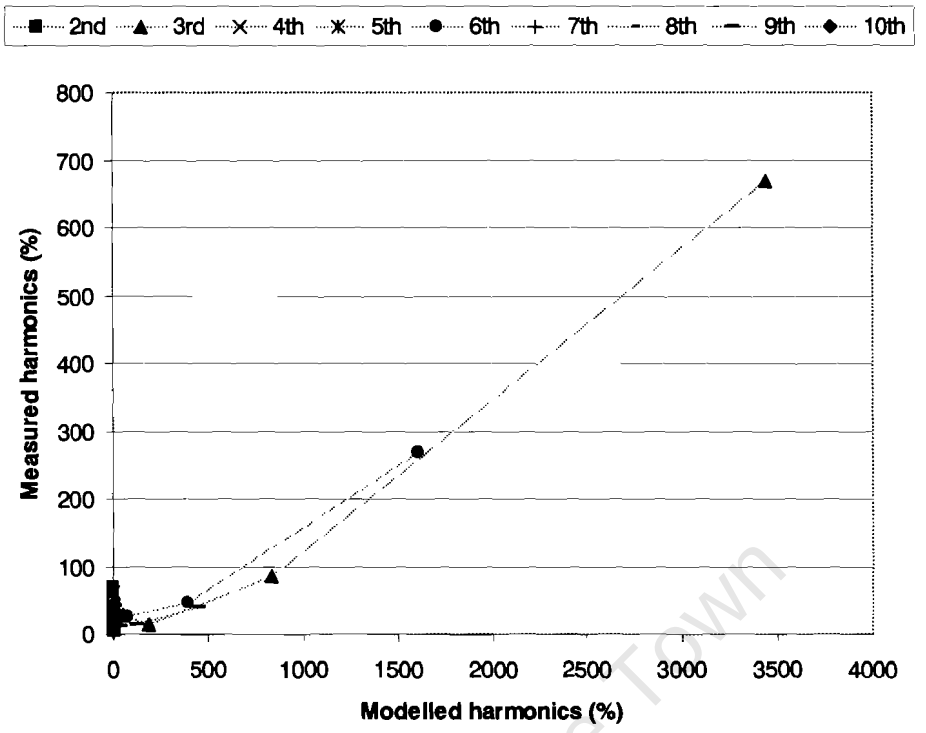

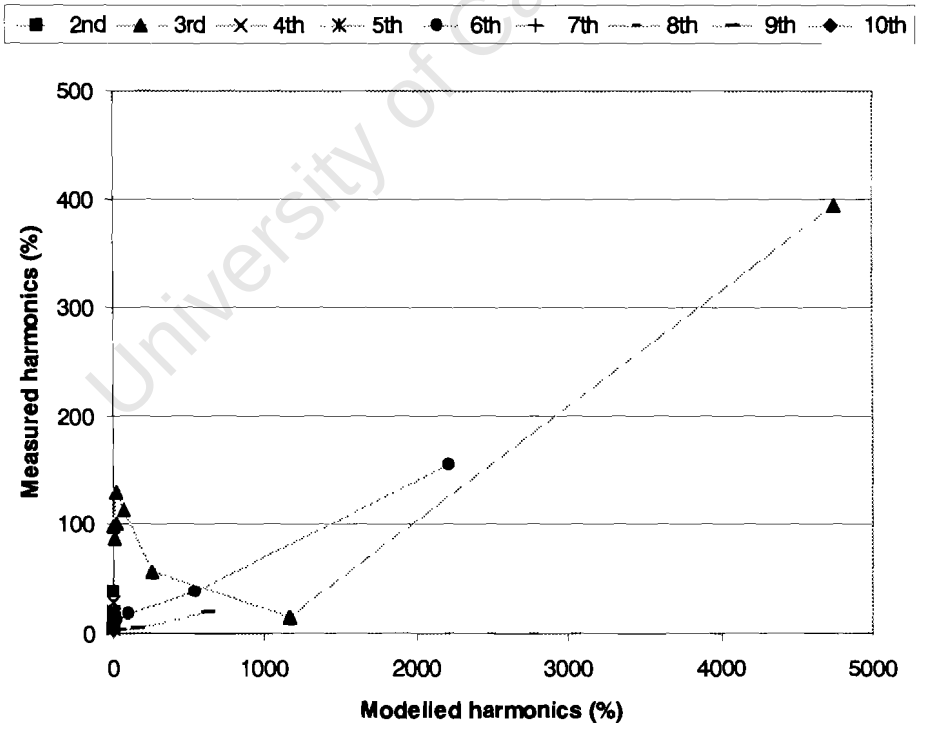

Figure 4 (continued)

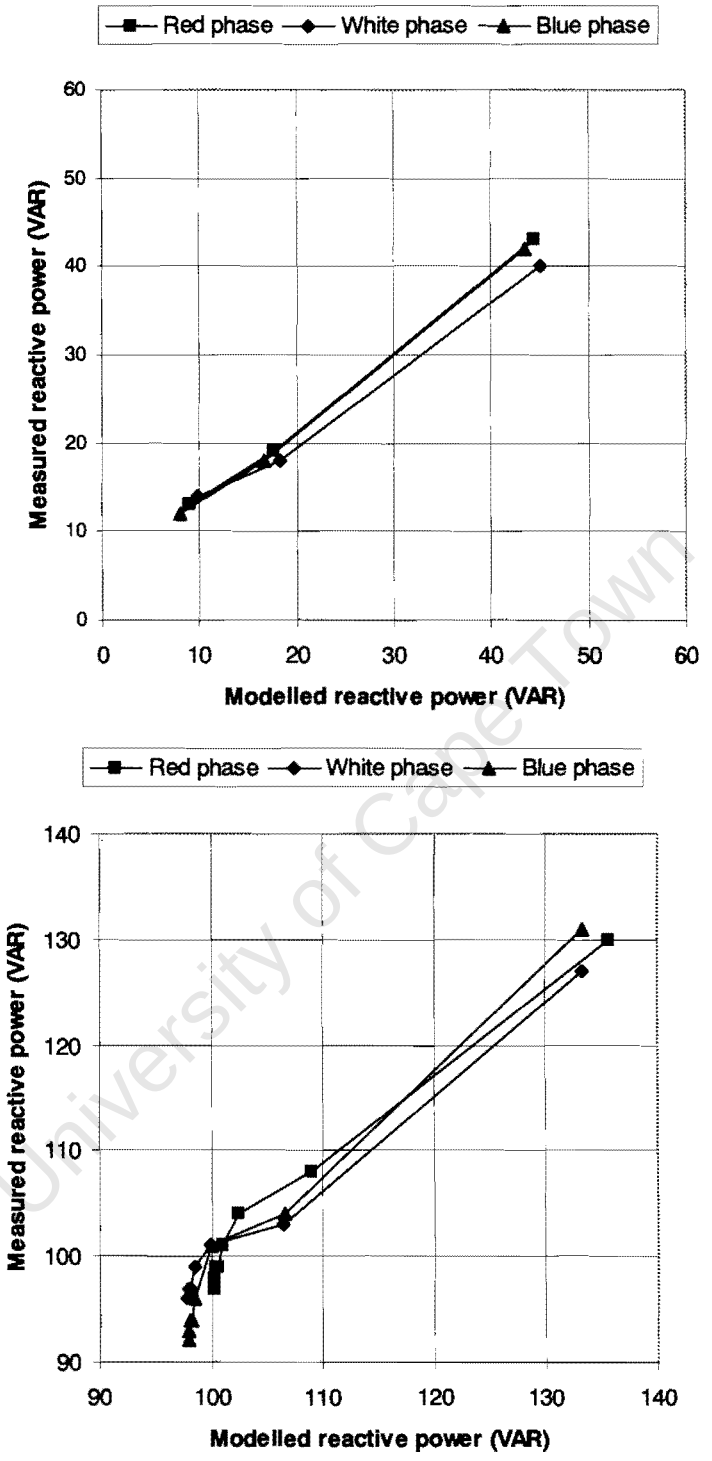

Figure 5 Measured reactive power versus modelled reactive power at 70.7 Volts over a range of varying dc currents for single-phase reactors.

a. **Non-gapped**
b. **Thin-gapped**
c. **Thick-gapped**

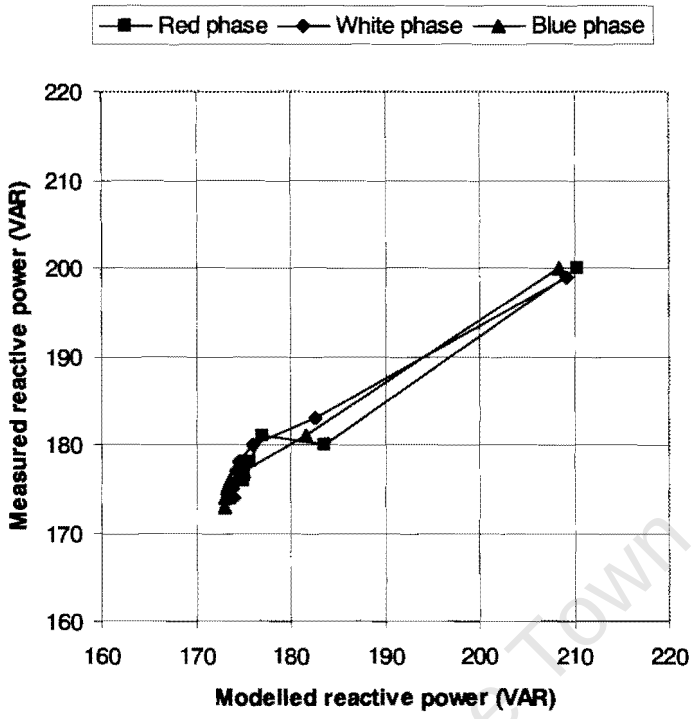

Figure 5 (continued)

Table 1 Summary of current harmonic contents and reactive power for three-phase thin-gapped units at 70.7 Volts.

a. **Modelled**
b. **Measured**

Phase	Current (A)			Current harmonics (% of fundamental current)									Reactive power
	dc	total	fund.	2nd	3rd	4th	5th	6th	7th	8th	9th	10th	(VAR)
Red	-0	0.97	0.97	0	0.04	0	0.15	0	0.03	0	0.03	0	69
White	0	0.98	0.98	0	0.02	0	0.07	0	0.01	0	0.01	0	69
Blue	0	1.17	1.17	0	0.04	0	0.13	0	0.02	0	0.02	0	83

Phase	Current (A)			Current harmonics (% of fundamental current)									Reactive power
	dc	total	fund.	2nd	3rd	4th	5th	6th	7th	8th	9th	10th	(VAR)
Red	0	1.09	1.1	0.44	1.75	0.13	1.68	0.4	0.68	0.34	0.74	0.26	84
White	0	1	0.99	0.33	2.79	0.35	1.1	0.35	0.84	0.23	1.06	0.36	77
Blue	0	1.18	1.17	0.35	1.05	0.25	1.14	0.41	0.86	0.3	0.53	0.25	91

Table 2 Summary of current harmonic contents and reactive power for three-phase thick-gapped units at 70.7 Volts.

a. **Modelled**
b. **Measured**

	Current (A)			Current harmonics (% of fundamental current)									Reactive power
Phase	dc	total	fund.	2nd	3rd	4th	5th	6th	7th	8th	9th	10th	(VAR)
Red	-0	1.77	1.77	0	0.02	0	0.08	0	0.02	0	0.01	0	125
White	0	1.77	1.77	0	0.01	0	0.04	0	0.01	0	0.01	0	125
Blue	0	1.94	1.94	0	0.02	0	0.08	0	0.01	0	0.01	0	137

	Current (A)			Current harmonics (% of fundamental current)									Reactive power
Phase	dc	total	fund.	2nd	3rd	4th	5th	6th	7th	8th	9th	10th	(VAR)
Red	0	1.83	1.78	0.26	1.33	0.11	0.83	0.14	0.44	0.14	0.48	0.13	137
White	0	1.78	1.74	0.15	1.36	0.14	0.69	0.14	0.46	0.09	0.51	0.21	137
Blue	0	1.97	1.97	0.16	0.73	0.2	0.68	0.14	0.39	0.28	0.54	0.06	137

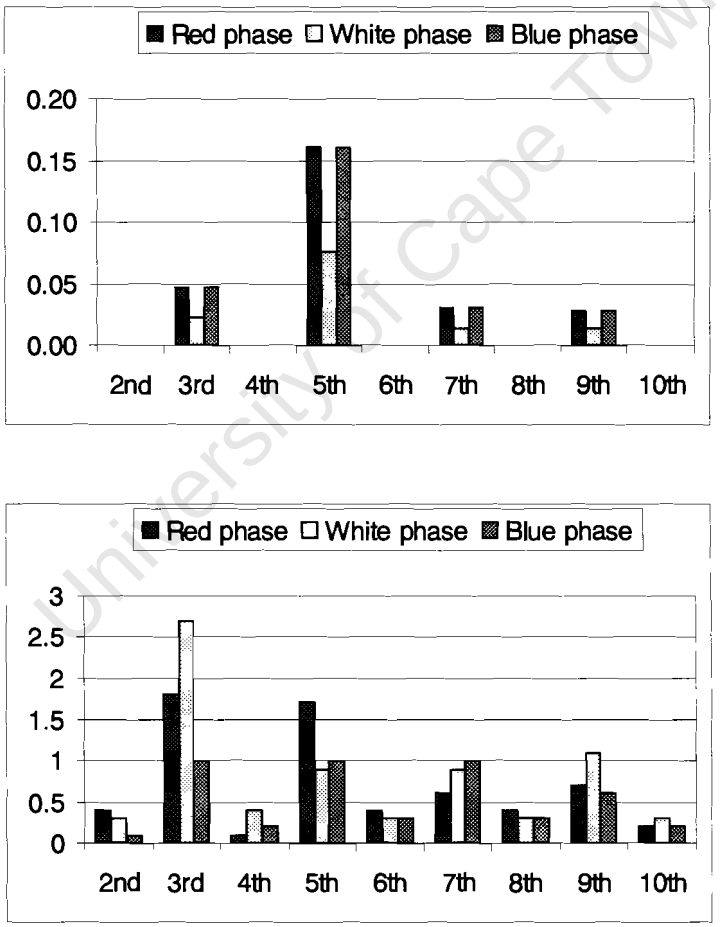

Figure 6 Current harmonic contents for three-phase thick-gapped units at 70.7 Volts.

a. **Modelled**
b. **Measured**

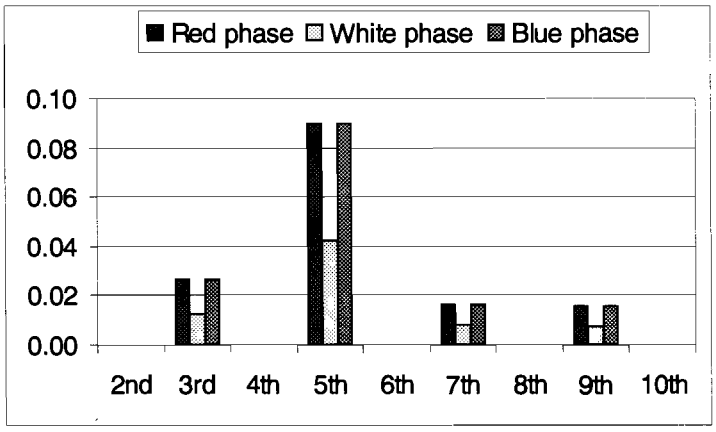

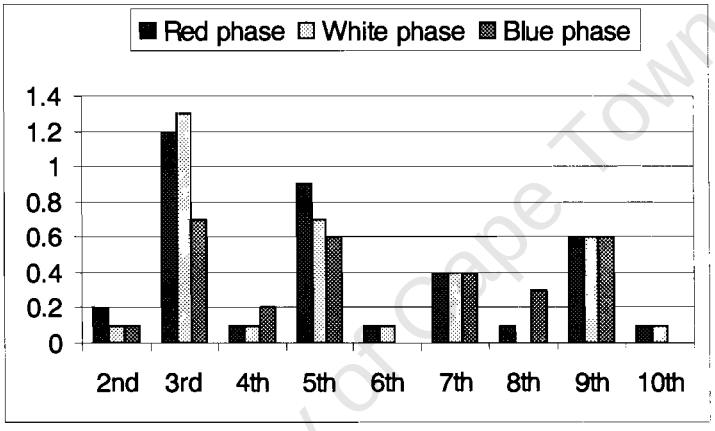

Figure 7 Current harmonic contents for three-phase thin-gapped units at 70.7 Volts.

a. Modelled

b. Measured